THERMODYNAMIC ANALYSIS OF VAPOUR ABSORPTION HALF EFFECT SOLAR DRIVEN WATER LITHIUM BROMIDE SYSTEM FOR SPACE COOLING

A Major Thesis Submitted in Partial Fulfilment of the requirements for the award of the degree of

MASTER OF TECHNOLOGY

IN

RENEWABLE ENERGY TECHNOLOGY

Submitted by

ABHISHEK VERMA

ROLL NO. 2K14/RET/03

SESSION 2014-16

Under the Guidance of

PROF. R. S. MISHRA **DR. AKHILESH ARORA**

DEPARTMENT OF MECHANICAL, PRODUCTION & INDUSTRIAL AND AUTOMOBILE ENGINEERING
DELHI TECHNOLOGICAL UNIVERSITY, DELHI-110042

DECLARATION

I hereby declare that the work which being presented in the major thesis entitled **"Thermodynamic Analysis of Vapour Absorption Half Effect Solar Driven Water Lithium Bromide System for Space Cooling"** in the partial fulfilment for the award of the degree of Master of Technology in **"Renewable Energy Technology"** submitted to Delhi Technological University (Formerly Delhi College of Engineering), is an authentic record of my own work carried out under the supervision of **PROF. R. S. MISHRA & DR. AKHILESH ARORA,** Department of Mechanical Engineering, Delhi Technological University (Formerly Delhi College of Engineering). I have not submitted the matter of this dissertation for the award of any other Degree or Diploma or any other purpose what so ever. I confirm that I have read and understood 'Plagiarism policy of DTU'. I have not committed plagiarism while completing the attached piece of work, similarity found after checking is ___ which is below the permitted limit of 20%.

Place: Delhi **ABHISHEK VERMA**

Date**:** **Roll No. 2K14/RET/03**

CERTIFICATE

This is to certify that ABHISHEK VERMA, (Roll no. 2K14/RET/03), student of M.Tech, Renewable Energy Technology, Delhi Technological University, has submitted the dissertation titled **"Thermodynamic Analysis of Vapour Absorption Half Effect Solar Driven Water Lithium Bromide System for Space Cooling"** under our guidance towards the partial fulfilment of the requirements for the award of the degree of Master of Technology under our guidance and supervision.

PROF. R. S. MISHRA
Professor & HOD
Department of Mechanical Engineering
Delhi Technological University
(Formerly Delhi College of Engineering)
Delhi-110042

DR. AKHILESH ARORA
Assistant Professor
Department of Mechanical Engineering
Delhi Technological University
(Formerly Delhi College of Engineering)
Delhi-110042

ACKNOWLEDGMENT

It is said that gratitude is a virtue. This part is dedicated to special thanks that I would like to deliver to the people who helped me in making the fulfilment of this thesis project possible.

I take great pride in expressing my unfeigned appreciation and gratitude to my learned mentors **PROF. R.S. MISHRA AND DR. AKHILESH ARORA,** and Department of Mechanical Engineering, Delhi Technological University (Formerly Delhi College of Engineering), for their invaluable inspiration, guidance and continuous encouragement throughout this project work. Their critics and suggestions on my work have always guided me towards perfection. This work is simply the reflection of their thoughts, ideas, concepts and above all his efforts. Working under their guidance has been a privilege and an excellent learning experience that I will cherish for a long time.

I express my deepest gratitude to PROF. R.S. MISHRA**,** Head of Department Mechanical Engineering Delhi Technological University (Formerly Delhi College of Engineering). He always encouraged us and advised us to keep in constant touch with our mentors. He is a source of great knowledge and he is always working hard to do the best for his students.

ABHISHEK VERMA
(2K14/RET/03)

ABSTRACT

Nowadays Solar Cooling systems are becoming popular to reduce the carbon footprint of air conditioning. The use of an absorption unit connected to solar thermal panels is increasing.
The need and importance of solar based cooling system can play a very prominent role in attenuating energy crisis by the use of solar energy. Two types of the absorption systems, the single and half effect cycles, can operate using low temperature hot water. The unique characteristic of the half-effect absorption cycle is that its running capability at lower temperatures in comparison to the single effect vapour absorption system. The COP of half effect system is almost half to that of the single-effect cycle but it is operated at lower temperature to that of single effect. The system functions with the principle of absorption refrigeration cycle having water as a refrigerant and Lithium Bromide as an absorbent.

In the present work, thermodynamic analysis and simulation of vapour absorption half effect cooling system using flat plate solar collectors as source of energy, for an office space has been done and the system performances were analyzed parametrically by using EES. The cooling load calculation of an office space was carried out on 21st of June located at Dehradoon, Uttarakhand India (Latitude 30°N). The estimated capacity of the office space (Q_e), comes out to be 25 kW (approx). The evaporator temperature is maintained constant at 7°C and condenser temperature is varied from 30°C and 46°C and generators temperatures are varied from 65 to 85 °C. For a given condenser temperature (say 38°C) there is an optimum generator temperature for which the total area flat plate collector is minimum. This optimum generator temperature comes out to be 80°C. This generator temperature gives the maximum COP and exergetic efficiency of the absorption cooling system. There exists an optimum intermediate pressure corresponding to which COP and exergetic efficiency are maximum. The optimum intermediate pressure comes out to be 4.935 kPa. (for TC = Tal =Tah = 38°C, TE = 7°C and Tgh = Tgl = 80°C). For the same input parameters the maximum COP obtained is 0.4158 and the maximum exergetic efficiency is about 7.36%.

The ultimate goal in the long term would ideally be to reduce the consumption of electricity used for refrigeration and air conditioning, hence saving money and reducing the stress on our electricity generation and distribution networks. The cost analysis of the half effect system is done by comparing it with the conventional vapour compression refrigeration system (VCRS). Based on the cost calculation of two systems, the payback period of the half effect system is calculated and it comes out to be 2.8 years.

TABLE OF CONTENTS

LIST OF FIGURES

LIST OF TABLES

LIST OF ABBREVIATIONS USED

COP	Coefficient of Performance
VARS	Vapour Absorption Refrigeration System
VCRS	Vapour compression refrigeration system
HEX	Solution Heat Exchanger
HVARS	Vapour Absorption half effect solar driven water lithium bromide system
HFC	Hydro Flouro Carbons
EES	Engineering Equation Solver
NH3	Ammonia
$LiBr_2$	Lithium Bromide
H_2O	Water
LiNO3	Lithium Nitrate
NLP	Non-linear programming
LCA	Life cycle assessment
FNP	Fraction of total load met by non-purchased energy
LPG	Low pressure generator
HPG	High pressure generator
DBT	Dry Bulb Temperature
WBT	Wet Bulb Temperature
RH	Relative Humidity
ASHRAE	American Society of Heating, Refrigerating, and Air-Conditioning Engineers
PBP	Pay-back period
LPG	Low pressure generator
HPG	High pressure generator
TFM	Transfer Function Method
CLTD	Cooling Load Temperature Differential
CLF	Cooling Load Factors

TA	Time-Averaging
TETD	Total Equivalent Temperature Differential
ED	Exergy Destruction
EDR	Exergy Destruction Ratio
EP	Exergy of Product
EHXh	Effectiveness of high pressure side solution heat exchanger
EHXl	Effectiveness of low pressure side solution heat exchanger
SCR	Solution circulation ratio

LIST OF SYMBOLS

kW	Kilowatt
TR	Tons of Refrigeration
Btu/h	British Thermal Units per hour
W_P	Pump work
W_c	Compressor work
U	Overall heat Transfer Coefficient
Po	atmospheric pressure
h	Specific Enthalpy
s	Specific Entropy
m	Mass flow rate
P	Pressure
T	Temperature
Q	Heat Exchange per unit mass
W	Specific Work
ɳ	Isentropic Efficiency
ɳex	Exergetic Efficiency
TG	Generator Temperature
TC	Condenser Temperature
TE	Evaporator Temperature
Tgh	High Pressure side Generator Temperature
Tgl	Low Pressure side Generator Temperature
Tah	High Pressure side Absorber Temperature
Tah	High Pressure side Absorber Temperature
Qe	Refrigeration Capacity

Pi	Intermediate Pressure
P	Power consumed in by compressor in VCRS
E_d	Energy consumption per day
E	Energy consumption per year
C	Cost of Flat Plate Collectors
f	solution circulation rates
K	Kelvin temperature
km	Kilometer
PE	Evaporator Pressure
PC	Condenser Pressure
X_{Sl}	Equilibrium strong solution LP side
X_{Wl}	Equilibrium weak solution LP side
X_{Sh}	Equilibrium strong solution HP side
X_{Wh}	Equilibrium weak solution HP side
h	Enthalpy
HP	High pressure
LP	Low pressure
X	LiBr mass fraction

Subscripts

a	Absorber
c	Condenser
e	Evaporator
ex	Exergetic
g	Generator
h	High Temperature stage
l	Low temperature stage
max	Maximum
opt	Optimum
p	Pump
r	Refrigerant/room
rtv	Refrigerant throttle valve
s	Strong
she	Solution heat exchanger
t	Total
w	Weak
0	Dead

CHAPTER 1

INTRODUCTION

1.1 Motivation

At present, the conventional sources of energy are depleting day by day led to the researchers to identify the systems which use renewable sources of energy. The depletion of conventional sources of energy not only increasing the cost of energy production but also polluting the environment in a severe manner.

The refrigeration and air conditioning systems have a major demand of the total energy consumption of the world. The harmful emissions of fossil fuels and chlorine based refrigerants used are responsible for the global warming and the ozone layer depletion. All these problems have led the scientists to develop a refrigeration system which uses renewable sources of energy.

The energy of the sun may be harnessed to produce the refrigerating effect which reduces the dependency on high-grade energy and do not pollute the environment.

1.2 Solar Cooling

Use of solar energy for cooling is an interesting idea as cooling loads and availability of solar radiation are approximately in phase. Solar cooling utilizes solar thermal energy to operate a refrigerator. Ammonia-water vapour absorption refrigeration systems are commonly preferred for low-temperature usages. The heat input for these type of system is required at high temperatures i,e more than 90°C. Therefore, high-performance solar collectors are needed to supply a sufficient solar energy input to run the system.

The solar cooling system is commonly consists of three sub-systems: refrigeration system, the solar energy conversion system, and the cooling load. The relevant cycle for each system depends on cooling demand, the temperature levels of the refrigerated space and the surroundings. A numeral of likely paths for cooling applications from the solar energy. The solar energy has two important paths: solar thermal collectors for solar heating and PV cells to produce electricity. For solar thermal collectors, distinct collector types exhibit distinct temperature levels. This designate that the temperature level can be equal to various cycle demands. For example, the Rankine cycle, need a rather high impelling temperature whereas the desiccant cycle need at a lower temperature of heat furnish.

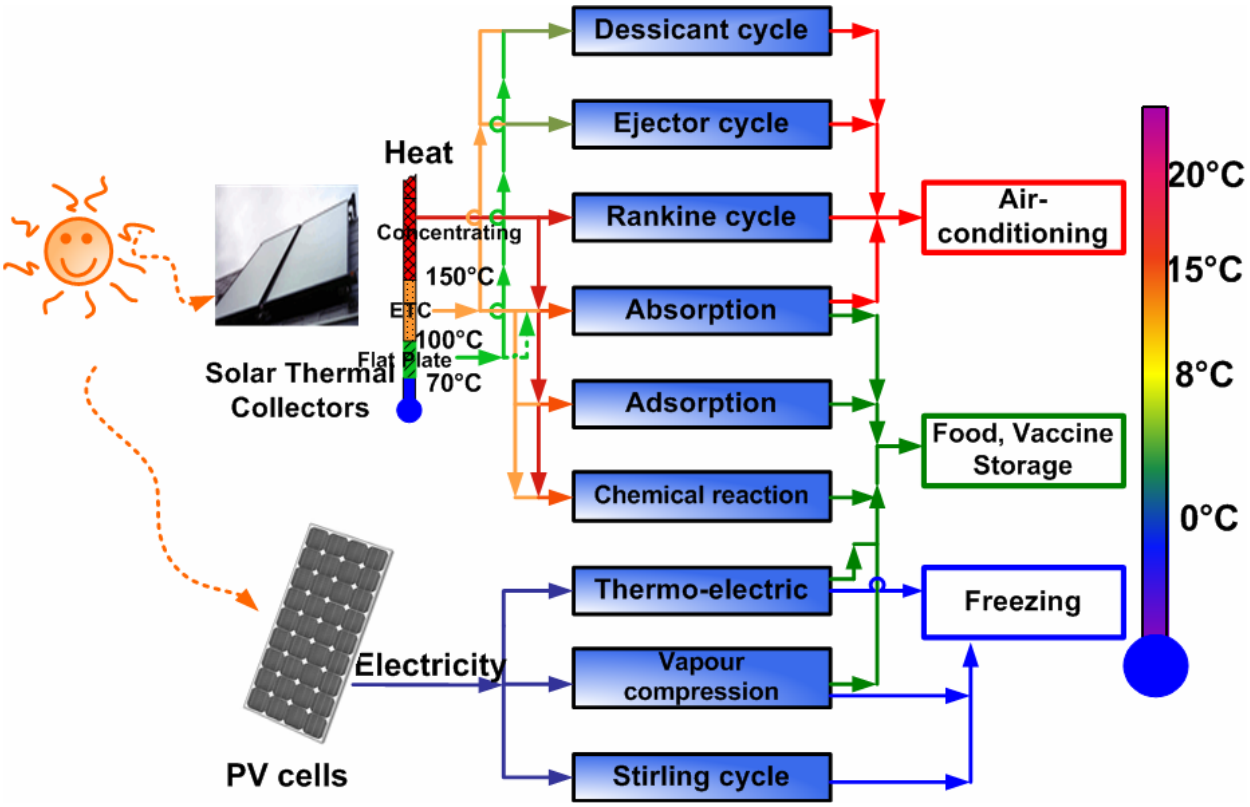

Figure 1.1- Solar Cooling Path [1]

The same type of temperature is essential for the cold end. Since several cycles typically cause with water as a working fluid, it is impracticable to achieve temperatures below 0°C for few cycles. The air conditioning cycles driven by solar thermal can be based on absorption cycles, double rankine cycle, adsorption cycles, desiccant cooling cycle, or ejector refrigeration cycle. When using low temperature applications for food storing at 0 to -8°C, different cycles can be appropriate, that is , thermoelectric cycle (Peltier effect),adsorption cycle, the vapour compression cycle, absorption cycle, and a chemical reaction cycle. For the applications need temperatures less than 0°C commonly require small storing volumes e.g., freezing case. A suitable cycle for this application has proved to be the vapour compression cycle driven by solar PV, or a Stirling cycle driven by the same. The adsorption cycle, double effect absorption cycle and chemical reaction cycle can also be used, particularly for larger storing volumes, i.e. ice production. Typically for the cycles in Figure is that, the efficiency of the electricity- driven refrigeration cycles are quite high but they need photovoltaic panels and batteries, which are costly. Heat driven cycles on the other side, are less effective, but the thermal solar collectors may gain much higher conversion efficiencies than the PV's, even though the product is heat, not electricity. Therefore, the overall efficiency is high in which route. One example: System 1, a heat driven cycle with a cycle COP of 0.7 accept its heat from a solar collector with 80% effectiveness. System 2, a vapour compression refrigeration cycle with a COP of 4 accepts its electricity from a PV array with an efficiency of 15%.[1]

1.3 Solar Cooling Technologies

The main components of solar air conditioning systems are the thermal driven refrigerating subsystem and the solar collector subsystem.

Solar energy can be converted into cooling by using two leading principles:

- Electricity generated with the help of photovoltaic modules may be converted into cooling by the use of the refrigeration technologies that are chiefly supported on vapour compression cycles.

    - Heat generated with solar thermal collectors can be converted into cooling using thermally driven air conditioning technologies or refrigeration. Most of these systems apply the physical phenomena of sorption in either a closed or an open thermodynamic cycle. Other technologies, such as steam jet cycles or other cycles using a converting heat into mechanical energy and mechanical energy to the cooling system are less important.

- Techniques which assign the use of solar thermal collectors for the air-conditioning of buildings utilizing the thermal energy to drive the chillers can be noted as in two main types:

    - A closed cycle where thermally driven chillers are a utility to exhibit chilled water which can be used for any style of air-conditioning equipment.

    - An open cycle, also assign to as desiccant cooling systems, are interesting for the straight management of air in a ventilation system.

1.4 A Brief Introduction for Refrigeration

Refrigeration is the process by which heat energy is transferred from a lower temperature room to a higher temperature room. The fundamentals of the refrigeration phenomenon are governed by the second law of thermodynamics.

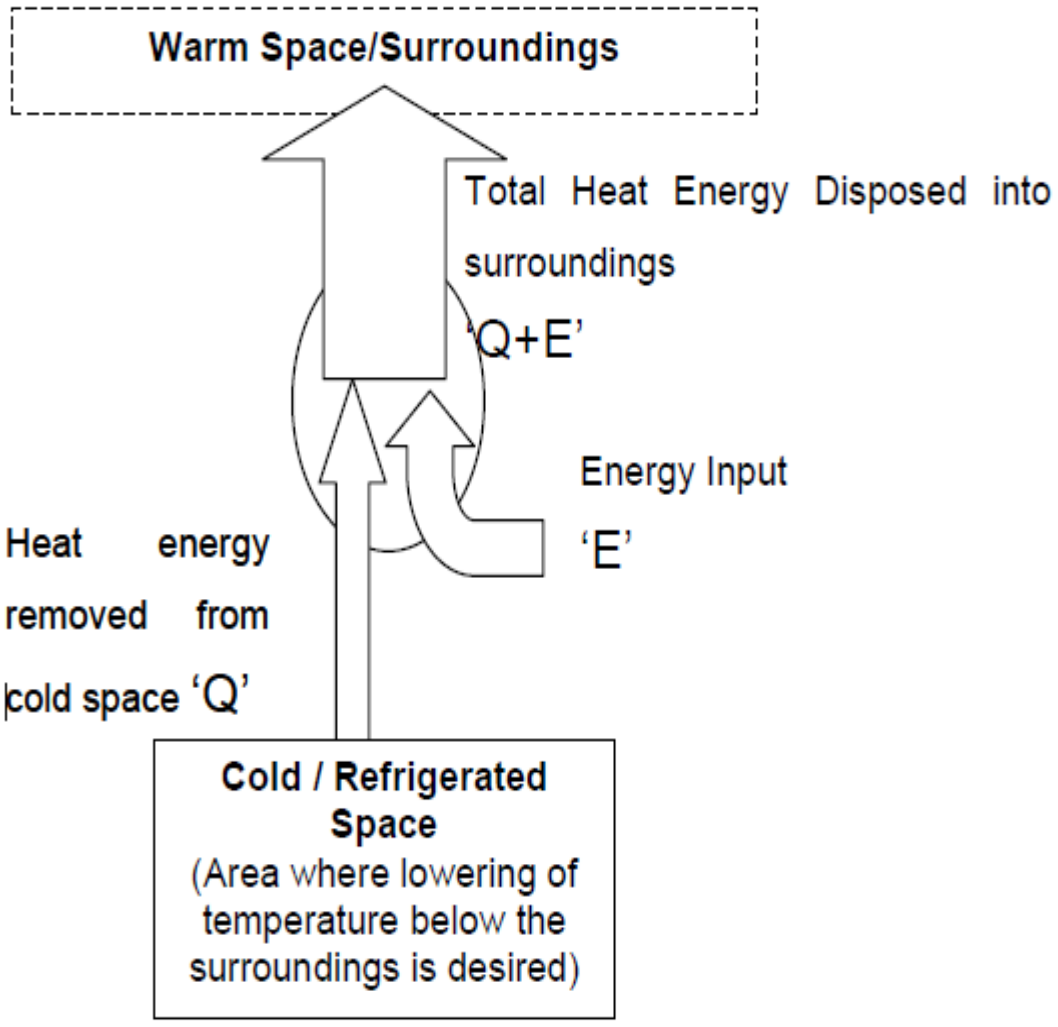

Figure 1.2-Refrigeration Process

- Basic standard units used in the refrigeration system

The capacity of the refrigeration system is measured in terms of power. This is usually expressed in Wattage (kW), Tons of Refrigeration (TR) or British Thermal Units per hour (Btu/h)

1 TR = 12000 Btu / hr = 3.517 kW

A ton of refrigeration refers to heat removal rate that will freeze a short ton of water (2000 lb or 907 kg) at 0 ° C (32 ° F) by removing the latent heat of fusion (333.55 KJ/kg or 144 btu/lb) in one day(24 hours).[2]

1.5 Coefficient of the Performance for the Refrigeration System (COP)

The coefficient of performance (COP) of the system is defined to the ratio of the desired effect derived to the input given. The efficiency of refrigeration system is compared on the basis of the COP.

For a refrigeration system, this is the ratio of heat removed to the energy supplied:

COP = (Net Heat Removed / Net Energy Input) = Qremoved / Einput

In order to examine cyclic refrigeration, it is provident to start at an ideal refrigeration cycle which works on the reverse Carnot cycle.

1.6 Vapour Absorption Refrigeration Systems (VARS)

The Vapour Absorption Refrigeration System (VARS) pertain to the set of vapour cycles resembling to vapour compression refrigeration systems. However, unlikely vapour compression refrigeration systems, the direct input to absorption systems is in the form of heat. Hence the systems are also called as heat driven or thermal energy operated systems. Since the conventional vapour absorption systems use liquids for absorption of refrigerant, these are also called as wet absorption refrigeration systems.

Similar to vapour compression refrigeration systems, vapour absorption refrigeration systems have also been commercialized and are extensively usage in different refrigeration and air conditioning applications. Since these systems are operated on low-grade thermal energy, they are used only when low-grade energy likes the energy from sun i.e, the solar energy or waste heat. Since the conventional absorption systems use native refrigerants like ammonia or water as they are environment favorable.

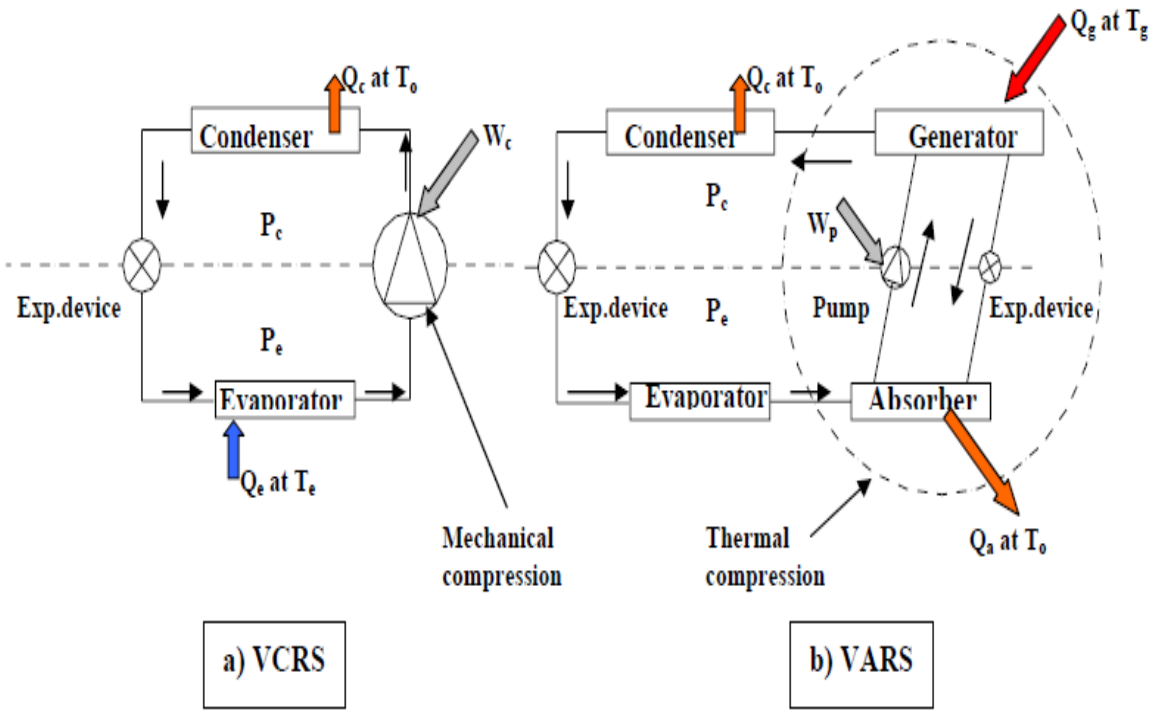

Figure 1.3- a) Vapour compression refrigeration system (VCRS)
b) Vapour Absorption Refrigeration System (VARS) [3]

Figure 1.3 (a) and (b) show an uninterrupted output vapour compression refrigeration system and an uninterrupted output vapour absorption system. In an uninterrupted absorption refrigeration system, low pressure and low-temperature refrigerant with low quality enters the evaporator and evaporate by exhibit useful refrigeration Qe. From the evaporator, the low pressure, low temperature refrigerant vapour enters the absorber where it comes in contact to a solution which is weak solution of the refrigerant. The weak solution absorbs the refrigerant and becomes strong solution. The heat of absorption is rejected to the exterior heat sink at To. The solution that is now becomes rich in refrigerant is pumped to the high pressure by the use of a solution pump and feed to the generator. Heat at high temperature Tg is supplied in the generator, as a result refrigerant vapour is generated at high pressure.

This vapour at high pressure is now condensed in the condenser by rejection of heat of condensation to the exterior heat sink at To. This condensed refrigerant in liquid form is now throttled in the expansion device and is then fed to the evaporator to conclude the refrigerant cycle. On the solution side, the hot solution at high-pressure which is weak in refrigerant is throttled to the pressure of absorber in the solution expansion valve and fed to the absorber where it comes in contact to the refrigerant vapour coming from evaporator. Thus continual refrigeration is produced at evaporator, and the heat at high temperature is provided to the

generator. Heat rejection to the exterior heat sink taken place at absorber and condenser. A small amount of mechanical energy is need to run the solution pump. On neglecting the pressure drops, the absorption system works between the condenser and evaporator pressures. The pressure in the absorber is equal to that in evaporator and pressure in generator is equal to that in the condenser.

It may be seen from the Figure.1.3, that components like the condenser, expansion valve and evaporators are concerned both absorption and the compression systems are similar. The dissimilarity lies in the way the refrigerant is compressed to pressure of condenser. In vapour compression refrigeration system (VCRS) the vapour is compressed mechanically by using the compressor, while in vapour absorption refrigeration system (VARS) the vapour is first converted into a liquid and then the liquid is pumped to condenser pressure with the help of solution pump. For the same pressure difference, the work input need to pump a liquid (solution) is much less than the work need to compress a vapour due to very small specific volume of liquid, the mechanical energy need to cause vapour absorption refrigeration system is much less than that need to cause a compression system.

However, the absorption system needs a relatively huge amount of low-grade thermal energy at generator temperature to generate the vapour of refrigerant from the solution available in the generator. The energy input in the vapour compression refrigeration systems is in the form of mechanical energy, while it is in the form of thermal energy in case of the vapour absorption refrigeration systems. The solution pump work is nearly negligible as compared to the heat energy given to the generator. Thus the COP for the vapour absorption and vapour compression systems are given by:

$$COP_{(VCRS)} = \frac{Q_e}{W_c}$$

$$COP_{(VARS)} = \frac{Q_e}{(Q_g + W_p)} \Rightarrow \frac{Q_e}{Q_g}$$

Thus absorption systems are beneficial where a large amount of low-grade thermal energy is available readily at required temperature. However, it is seen that for the same refrigeration and heat rejection temperatures, the COP of VCRS is much higher than that of the vapour absorption refrigeration system. The high grade mechanical energy is used in the VCRS, while a low-grade thermal energy is used in vars. However, the comparison of these two systems based on COP is not fully satisfactory, as the mechanical energy is more costly than the thermal energy which is readily available. Hence, the second law (or exergetic) efficiency is used to compare the two refrigeration systems. It is seen that the second law (or exergetic) efficiency of the absorption system is of the same fashion as that of the compression system.

1.7 Various Designs of Vapour absorption System

Absorption chillers are commonly categorized as direct- or indirect-fired, and as half effect, single effect, double effect - or triple-effect vapour absorption systems. In direct-fired units, the heat origin can be gas or some other fuel that is burned within the system. The Indirect-fired systems use steam or some other fluid which can carry in heat from an isolated origin, such as the heat coming from a boiler or the heat that is retrieved from the industrial process. The hybrid systems, which are relatively habitual with absorption chillers, combine gas systems and electrifying systems for load optimization and flexibleness.

1.7.1 The half-effect system

The primitive characteristic of the half-effect absorption cycle is the running capableness at lower temperatures compared to others. The name "half-effect" rising from the COP, which is almost half that of the single-effect cycle It must be eminent that, any absorption refrigeration system can be work only when the solution in the absorber is rich in concentration in refrigerant as compared to that in the generator. If the temperature increases or the pressure reduces, the portion of refrigerant hold in the solution is reduced, and vice versa. When the generator temperature is reduced, the circulation rate of the solution will be increased which cause the COP to decrease. If it is too low, the system can be no longer work.

The half effect vapour absorption refrigeration system was presented for an uniqueness that it works on a relatively low-temperature heat origin. The system construction is accurately the same as the double-effect absorption system using water and NH3 with the difference is that the heat flow directions are distinct. It must be eminent that COP of the half-effect vapour absorption system is comparatively less as it discard more heat than a single-effect absorption cycle around 50%. However, it can be work with the relatively low temperature heat origin.[1].

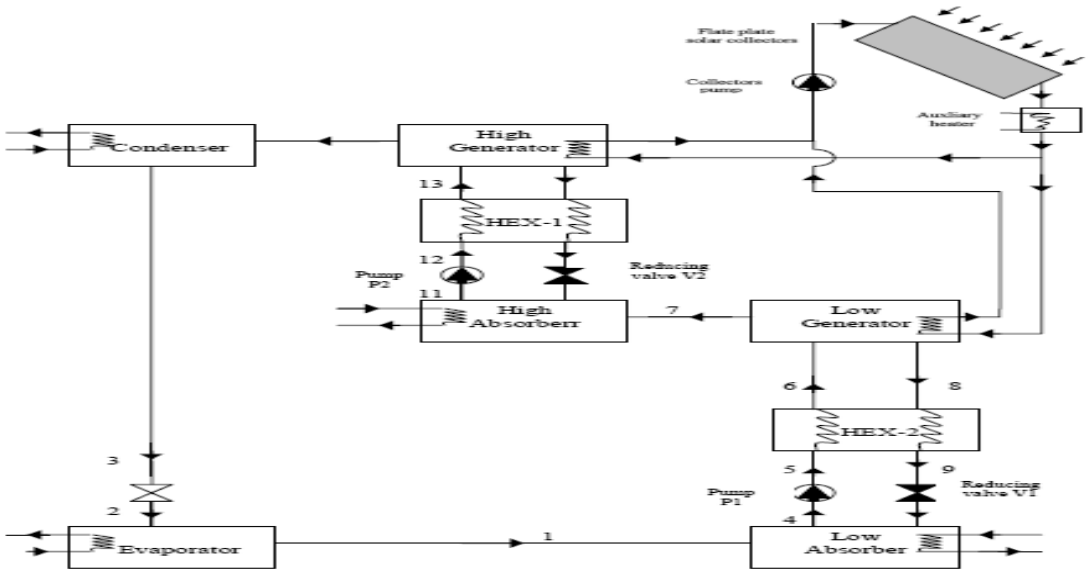

Figure 1.4 Half effect absorption system [1]

1.7.2 Single-effect system

The single-effect vapour absorption system is the simplest and most generally custom design. There are two design configurations impend on the working fluids used. High temperature heat provide to the generator is utility to evaporate refrigerant out from the solution (discard out to the surroundings at the condenser) and is utility to heat the solution from the absorber temperature (discard out to the surroundings at the absorber). Thus, irreversibleness is caused as high temperature heat at the generator is stripped out at the absorber and the condenser. The heat exchanger concede the solution that is passing through the absorber is to be preheated before it enters to the generator by using the heat that is coming from the hot solution that is leaving the generator of the unit. Therefore, the COP is increased when the heat input to the generator is diminished. Also, the dimensions of the absorber component can be diminished as less heat given is reduced.[4]

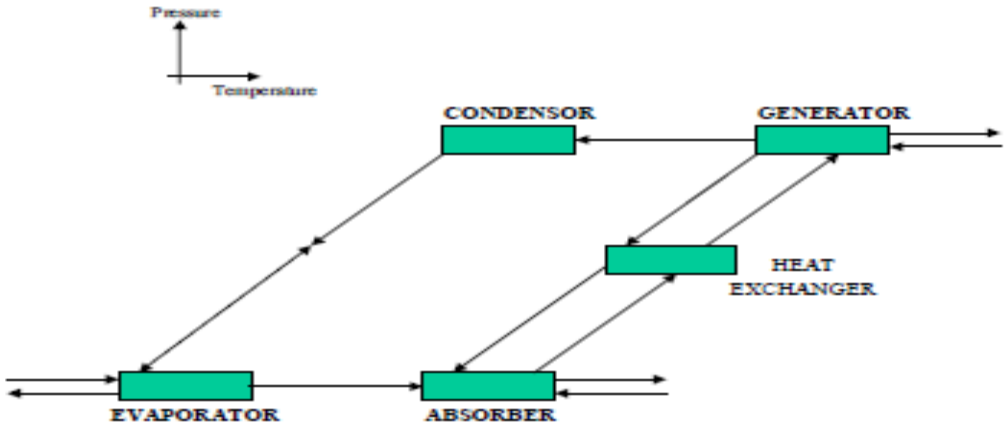

Figure 1.5 Single-effect absorption system [4]

1.7.3 Double Effect system

The wish for higher efficiencies in absorption chillers led to the inducement of double-effect LiBr/H2O systems. The double-effect chiller vary from the single-effect vapour absorption system is that there are two generators and two condensers, which permits more refrigerant to boil-off from the absorbent solution within the cycle. The Figure 3 reveal the double effect vapour absorption cycle on a Pressure-Temperature diagram with respective concentrations. The generator at higher temperature uses the steam which is externally furnished to boil the refrigerant from the weak absorbent of the cycle. The refrigerant vapour that is coming from the high temperature generator is condensed and the heat generated in the process is used to supply heat to the generator which is at low temperature.[4]

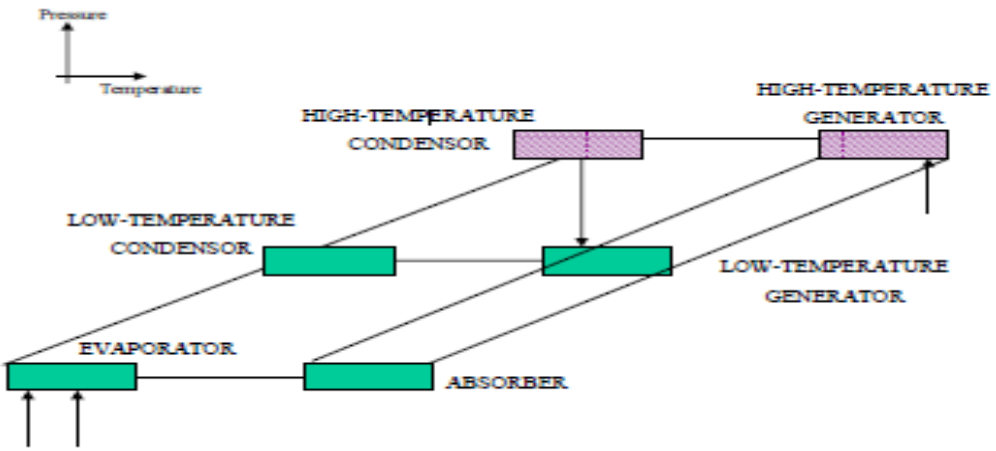

Figure 1.6 Double effect absorption system [4]

1.7.4 Triple Effect system

The triple-effect cycles are the next sound increase over the double-effect system. The refrigerant vapour that is coming from the generator which are at high and medium temperatures is condensed and the generated heat is supplied to the next generator which is at lower temperature. The refrigerant that is coming from all three condensers proceed to an evaporator where it draw more heat to work the cycle.[4]

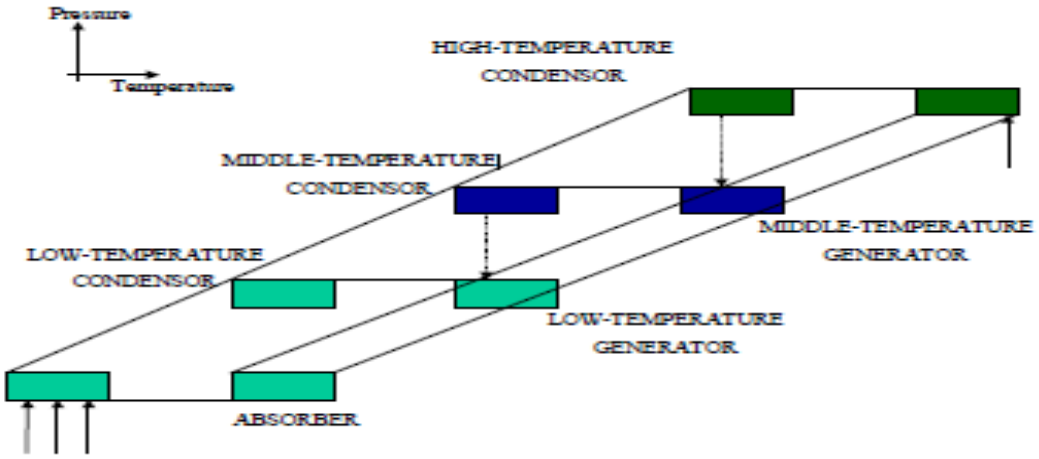

Figure 1.7 Triple effect absorption system [4]

1.8 Scope of the Thesis

The Thesis mainly deals with the Half effect Solar driven Vapour absorption System as we are using the low temperature available from flat plate collectors.

CHAPTER 2

LITERATURE REVIEW

2.1 Literature:

Gomri [5] simulated the operation of a half-effect absorption refrigeration system of 10 kW. The energy from the sun is utilized to run the flat plate collector, which are used as the source of heat generation for the vapour absorption refrigeration system. The system has two units, one unit is for the generation of heat which would be utilized to run the second unit i.e. the absorption cooling unit. The two units were simulated by developing a computer program. The exergetic and energy analysis is done for all components of the two units. The calculation of energy destruction in all the components is done. The minimum value of hot water temperature is calculated. The optimum operations were seen when the temperature of condenser was defined at 28°C, 32°C and 36°C.
The computer program was developed to calculate the thermodynamic property at each point. The atmospheric conditions, flat plate collector parameters, effectiveness of solution heat exchangers, solution pump efficiencies, temperature of components and the load on evaporator were the inputs given to the program.

- When the temperature of evaporator is fixed to 5°C and the temperature of condenser is changed from 28°C and 36°C, the temperature of generators is changed from 42°C to 62°C; the maximum value of COP was 0.44 and the maximum value of exergy efficiency was around 21%.

- For a defined temperature of condenser there was an optimum temperature of generator for which there exits the maximum value COP and exergy efficiency.

- The maximum efficiency of flat plate collector was 0.6.

- The thermal efficiency of the whole system was decreased with an increased temperature of generator and condenser.

Arora et al. [6] carried out the analysis of exergy and energy of half effect lithium bromide water vapor absorption refrigeration system. The optimum intermediate pressure is evaluated to maximize the exergetic efficiency and COP under different conditions. The optimum pressure for both maximum COP and exergy is same.
The calculation of optimum pressure involves the effect of high and low pressure temperatures of generator, evaporator, difference of high and low pressure of generator and evaporator, effectiveness of heat exchangers carrying strong and weak solution of Lithium bromide and water. The maximum COP obtained in the range of 0.415 to 0.438, and the value of maximum efficiency is varied from 6.96 to 13.74%.

The following results were obtained:

- The half effect system will stop working below a specific generator temperature, at this point the COP and exergy efficiency will be zero.
- At the optimum value of intermediate pressure, the exergetic efficiency and COP were maximum. The optimum value of intermediate pressure was increased with the increase of low pressure or high pressure generator temperature and the evaporator temperature, and decreased with the increase in absorber temperature.

- The change of maximum COP (at optimum intermediate pressure) is negligible with increase in generator temperature while the maximum value of exergy efficiency decreased under same conditions. The maximum value of COP and exergy efficiency was decreased with the increase in absorber temperature.

- There was negligible increase in maximum COP with the increase in temperature of evaporator while the maximum exergy efficiency was decreased under same conditions.

- The maximum values of COP and exergy efficiency, the optimum intermediate temperature were increased with the increase in effectiveness of the heat exchangers carrying strong and weak solution. The effectiveness of low pressure heat exchanger is dominating than that of high pressure heat exchanger.

- The maximum values of COP and exergy efficiency were higher when low pressure generator temperature is higher as compared to high pressure generator temperature.

Arivazhagan et al. [7] carried out an experiment to investigate the performance of a half effect vapour absorption refrigeration system. They designed a prototype of 1 kW cooling load, by the use of HFC based working fluids (R134a was refrigerant and DMAC was absorber). The generator temperature range, COP, and the second law efficiency was calculated as performance parameters. The system produces the lowest evaporator temperature as -7°C, the temperature of generator ranges from 55 to 75°C. The range of degassing was 40% more in high absorber than that in low absorber as the former is at optimum intermediate pressure. The optimum range of generator temperature was 65 to 70°C at which the COP was 0.36.

- The second law efficiency was decreased as the temperature of absorber and generator was increased.

- The COP of the system was decreased with an increase in temperature of absorber, due to low degassing range at high absorber temperature.

- The COP was not significantly changed with the generator temperature as the cooling load and heat input increases proportionately with the increased temperature of generator.

Arivazhagan et al. [8] simulated the half effect vapour absorption system having R134a as refrigerant and DMAC as the absorbent, for cold storage, using low temperature heat source as solar energy. The optimum intermediate pressure was calculated to maximize the COP. The COP of the system was on the basis of temperatures of condenser, generator and evaporator. The temperature of low absorber is more dominant as compared to that of high absorber. The COP of the system was varied from 0.35 corresponding to the low evaporator temperature and high condensing temperature and 0.46 corresponding to high evaporator temperature and low condenser temperature. The COP of the system was improved 5 to 15 % by using the condensate pre cooler.

- The COP of the cycle was changed from 0.35 to 0.46 corresponding to the evaporator temperature range of -5 to 5°C with generator temperature at 70°C, condenser temperature as 20 to 30°C and absorber temperature at 25°C. R134a-DMAC gives a marginal high COP as compared to that of ammonia water combination for the half effect vapour absorption system operated at low temperature.

Gomri [9] investigated the half effect va[pour absorption refrigeration system. The major components of the system consists of the evaporator, the condenser, low pressure generator, low pressure absorber, high pressure generator, , high pressure absorber etc. The low pressure absorber and the evaporator operated at low pressure i.e, evaporator pressure (Pev). The low pressure generator and the high pressure absorber operate at the intermediate pressure (Pi). The condenser and the high pressure generator operates at high pressure of the cycle i.e, the condenser pressure (Pcd).The maximum COP and the exergetic efficiency are evaluated at the optimum intermediate pressure for a given set of evaporator, generator, absorber and condenser temperatures. The intermediate pressure is directly calculated by developing a new correlation. The developed correlation was valid for the absorption system having the chilled water temperature in the range of 7 to 12°C, when the generator temperature was ranged from 40 to 80°C, the evaporator temperature was 4°C, the absorber and condenser temperature were varied from 28 to 38°C.

- The COP of the system increases on increasing the generator temperature but when the condenser temperature increases, the COP of the system was decreased.

- The value of the intermediate pressure was obtained by the simulation model technique in order to obtain the following relation; the use of least squares method has been done.
  .

$$P_i = \left(a_1 . e^{a_2 . t_{cd}}\right) t_g^2 + \left(a_3 . t_{cd} + a_4\right) t_g + a_5 . t_{cd}^{a_6}$$

Where,

tcd : condenser temperature (°C) , tg: generator temperature (°C)

a1=3.0917, a2=0.0087, a3=-17.3190, a4=141.2300, a5=6.9464, a6=2.1608.

- There was an optimum generator temperature for each evaporator and condenser temperature value to minimize the total exergy destruction, at this point the COP and exergetic efficiency obtained were maximum.

- The maximum COP of the half-effect absorption system were in the range of 0.408 – 0.435. The maximum exergetic efficiency of the half-effect absorption systems were in the range of 14.7%– 22.6%.

Jianzhao Wang et al. [10] analyzed the performance of single effect, half effect and double effect lithium bromide-water absorption system. The blank for the minimum generator temperature of the single effect and the double effect was noticed, and found that the gap can be perfectly filled up by the one and a half effect (1.5 effect). The analysis of the 1.5 effect system was done and two new configuration of 1.5 effect system were found. The optimum range for the 1.5 effect system was found to be 110 to 140°C, for the condenser temperature 42°C, evaporator temperature 5°Cand absorber temperature 37°C. The COP of the 1.5 effect system was found to be 1.0., which was 30% more than that of single effect system under same conditions. The performance of the effectiveness of solution heat exchanger, the absorption temperature (or the condensation temperature), the temperature of evaporator and the generator temperature on the performances of the different configurations of 1.5-effect cycle were analyzed. It was seen that one configuration, which is composed of a low-temperature half-effect sub-cycle and a single effect sub-cycle operating at high-temperature, has the maximum coefficient of performance and the most functional flexibility. Among the different parameters analyzed, the performances of 1.5-effect cycles are the most sensitive to the change in absorption temperature (or condensation temperature), and then to the change of generation temperature.

Bajpai [11] designed and pondered an environment favorable vapour absorption refrigeration system having one TR capacity by the use of water and R 717 (NH_3) as the working fluids. His system is designed and trialed for different operant conditions using hot water as source of heat. He evaluated the performance of the invented system with regard to different operant conditions related to condenser, heat source, evaporator and absorber temperatures.

The heat input needed to run the 1 TR vapour absorption refrigeration system, for the operant state designed, is around 304.2 KJ/min. The heat in the generator is provided by the hot water that is coming from the solar flat plate collector,. the practicability of the solar driven vapour absorption system has been moderately proved.

Domínguez-Inzunza et al. [12] has done the modeling of a progressive absorption cooling systems operating with NH_3-$LiNO_3$. The evaporator temperature as low as 60^{o}C may be obtained with half-effect systems at low generator temperature and COP is around 0.3. With double-effect systems it is likely to get COP as high as 1.12. The maximum COP can be obtain with triple-effect systems but at generator temperature above 150 ^{o}C.

The coefficient of performance for a half-effect system with the evaporator temperature for distinct generator temperatures and condenser temperatures of 30^{o}C 40 ^{o}C, and 50 ^{o}C. It can be accomplished that the coefficient of performance increases with an increase in the temperature of generator and the temperature of evaporator and decreases with an increase in the temperatures of absorber and condenser. The COP of the half-effect systems operating with H2O-LiBr deviate between 0.42 and 0.46 for generator temperature between 50 ^{o}C and 70 ^{o}C, while with NH3-LiNO3 the COP values were close to 0.30.

Saeed. Sedigh et al. [13] analyzed the performances of half-effect, single-effect and double-effect H2O/LiBr absorption cooling cycles, and found that there is an evident void for generator temperature between the minimum generator temperatures of the double-effect cycle, and the maximum generator temperature of the single-effect cycle and the energy analysis of half effect and the single effect water– lithium bromide vapour absorption systems is completed. A computational model has been developed for the parametric examination of the two systems. For this intention, the prevalent equations of the two cycles were given and the two cycles are examined by considering some parameters fixed. Then, the coefficients of performances of the two systems and the exchanged heat in distinct components are obtained. It was seen that an increase in the temperature of generator the COP increases in both half effect and the single systems up to an optimal generator temperature. It was seen that increasing the temperature of absorber lessen the system performance adversely as compared to the increase in the condenser temperature. A computer program has been developed to foretell the performance of half effect and the single effect systems by using energy analysis.

The one of a kind characteristic of the half-effect machine is that the demanded heat input temperature is lower than that is needed for the single-effect machine with the same cold water and heat rejection temperatures. Unfortunately, there is a thermodynamic fine that must be contented to permit the cycle to be fired at this lower temperature. It is noticed that the half-effect system cycle rejects almost 50% more heat than that in single effect cycle. This is uniform with the deed that the COP of the half effect is 0.42 for some operation condition and single-effect COP of 0.83 under the same operating conditions. This increased heat rejection is the thermodynamic fine combined with using low-grade input energy.

Adhikari et al. [14] examined and evaluated the practicability of a vapour absorption refrigeration unit work on solar Energy. The system was designed with the postulate of vapour absorption refrigeration cycle with Lithium Bromide as an absorbing medium and water as a refrigerant. The cooling load for the office building is 5 kW. The designed absorption refrigeration system has COP equitable to 0.77. The COP of the absorption system has opposite relation to the heat added to the system. Thus for the fixed evaporator load, there is no importance of higher heat added to the generator.

The performances of the system were analyzed parametrically by using EES software. It proved that the best performance in terms of COP would be succeeded when operated at low generator temperature and the low generator heat. Solar collector area to conduct system is 8 m^{2}. On the increase of mass flow rate of the refrigerant, the overall cooling effect increases, but the COP

decreases. The absorption cooling system is an alternative to the conventional vapour compression system. Here, Lithium bromide has been chosen as absorbent for cooling intention and water as refrigerant.

Sharma et al. [15] carried out the modeling and design for 10.5 kW of solar sustain vapour absorption air conditioning system using water-Lithium Bromide as the working fluid. Water acts as the refrigerant and the LiBr2 as the absorbent. The parametric study has been carried out to ponder the effect of evaporator temperature, generator temperature, absorber temperature and the condenser temperature, on coefficient of performance (COP) and effect of the generator temperature on the particular solution circulation rates (f).On the basis of the parametric study the distinct components of vapour absorption refrigeration system i.e. absorber, evaporator, condenser, and solution heat exchanger has been designed. Also the availableness of solar energy for running the absorption refrigeration system for 09 hours i.e. 09:00 hrs to 18:00 hrs (office hours) for April, May and June in Dehradun, Uttarakhand has been studied.

Based upon the study stated conclusions have been made :

1. A design has been developed which can foretell the COP of the system. Each constituent of the absorption system i.e. absorber, generator, evaporator and the condenser, has been designed.

2. Higher the generator and the evaporator temperature, results in high coefficient of performance (COP) of the system due to the deed that as the temperature of generator increases, the heat transfer to the solution in the generator increases, which results in the increase in the mass flow rate of the system, which in turn increases the COP of the system.

3. Lower temperature of condenser results in higher COP due to the deed that as Tcd increases, the condensing temperature increased and hence purposed the less heat transfer in the condensing component, which results in an increase in enthalpy and the temperature of the refrigerant at the exit of the condenser. As a result, the cooling capacity decreases as does the COP.

4. For the range of generator temperature from 65°C to 80°C, the absorption refrigeration system work effectively.

Ullah et al. [16] carried out a review on solar thermal cooling technologies, all over the globe for industrial and home cooling intention. These cooling systems are more applicable in distant areas or islands where conventional cooling is painful and solar energy is always profitable. These systems are also more becoming than conventional refrigeration systems because pollution-free working fluids (in lieu of of chloro- fluorocarbons) are used as refrigerants.

Study also sum up the different practical fluids of solar absorption cooling systems and adsorption cooling systems, providing different results with their benefit and limitations. Though the coefficient of performance (COP) of the absorption refrigeration system is better than that of adsorption refrigeration systems, the higher temperature issues can be readily handled with solar adsorption system. In addition to that, the solar hybrid cooling systems can afford higher capacity and better coefficients of performance (COP) by the elimination of some of the problems which occurs with the single working pairs.

Gebreslassie et al. [17] developed a systematic method for reducing the life cycle environmental impact of absorption cooling cycles is developed. The system formularizes a bi-criteria non-linear programming (NLP) proposition which recognizes the designs that diminish the entire chiller area and the environmental stroke of the absorption system. The environmental impact of the absorption system was evaluated in accordance with the principles of life cycle assessment (LCA). The methodology bestowed in this work is purposed to forward a more sustainable design of the absorption cooling systems, towards the adoption of alternatives which results in the lower environmental impact.

The consequence of the cooling water, generator, and chilled water temperatures on the minimum world-wide warming potential and lessen chiller area designs are search using the model developed. The results show that an increase in the generator temperature improves the performance parameters of the chiller at low temperature of generator and hence improves the environmental impact performance and reduces the area of chiller. As the temperature of generator further increases, the performance of the system ceases due to the increase in exergy destruction in the absorber, generator and condenser of the system.

Gebreslassie, et al. [18] carried out an exergy analysis, which only estimates the inevitable exergy destruction, is conducted for the single, double, triple and half effect Water–Lithium bromide absorption systems. Thus, the obtained performances depict the highest achievable performance under the granted operation conditions.

The exergetic efficiency, the coefficient of performance (COP) and the exergy destruction rates are possessed and the effect of the temperature of the heat source is calculated. As expectation, the COP increases significantly from double lift to triple effect cycles. The exergetic efficiency deviate less among the different configurations. In all cycles the manifestation of the temperature of heat source on the destruction rates of exergy is uniform for the same type of components, but the quantitative contributions impend on cycle type and flow configuration. Largest destruction of exergy appears in the generators and the absorbers, peculiarly at high temperatures of heat source.

Li, et al. [19] reviewed the elapsed efforts in the address of solar powered air-conditioning systems with the absorption pair of lithium bromide and water. A numeral of effort has been made by researchers to rectify the performance of the solar incline air-conditioning (chiller) subsystems. It is accomplished that the generator inlet temperature of the chiller is the most essential feature in the design and construction of a solar powered air-conditioning system.

While collector selection, system design and arrangement are the other impingement factors for the system operation.

Mittal et al. [20] has done the modeling of a solar-powered, single stage, vapour absorption cooling system, by using a flat plate collector which is used as a heat source and the solution of water–lithium bromide. A computer program has been developed for the vapour absorption cooling system to simulate different configurations of the cycle with the support of diverse weather data available for the village of District Bhiwani, named Bahal. in Haryana, India.

The effects of hot water entrance temperatures on the surface area of the absorption cooling component and the coefficient of performance (COP) are studied. The hot water entrance temperature is found to affect the surface area of some of the components.

He studied the following results:

1. The hot water entrance temperature is found to influence the surface area of some of the system components. With the Increase this hot water temperature the surface area of the solution heat exchanger and the absorber decreases, and the dimensions of the other components stay unchanged.

2. The high reference temperature increases the system COP and decreases the surface area of the components of the system, but the lower reference temperature gives better results for FNP (fraction of total load met by non-purchased energy) than that of the high reference temperatures do. For this study, a 353 K is taken as the reference temperature is the best option.

Sumathy et al. [21] proposed an unworn model of two-stage water lithium bromide absorption chiller. Test results have verified that the two-stage water lithium bromide chiller would be driven by the low temperature hot water that is ranging from 60 to 75 C, which can be smoothly provided by conventional solar flat plate collector systems. Relying on the successes of the proposed system, an integrated system consists of solar heating and solar cooling systems, having two-stage absorption chiller were erected (having cooling capacity of 5100 kW). Preliminary operant data of the system has denoted that such type of system could be the efficient and expense effective systems. Compared to the stipulated cooling system, the intended system with a two-stage chiller could obtain approximately the same total COP as of the stipulated system with a reduction of expense around 50%.

Florides et al. [22] presented a methodology to appraise the characteristics and performance of a single effect water-lithium bromide (LiBr2) absorption machine. The important heat transfer and mass transfer equations and necessary equations depicts the properties of the working fluids were indicated. The equations specified are applied in a computer based program, and the sensitivity analysis is performed. The variation between the absorber LiBr entrance and exit percentage ratio, the efficiency of the system in relation to the solution strength effectiveness and the solution heat exchanger area in relation to the absorber solution outlet temperature and the

coefficient of performance of the unit in relation to the temperature of generator were discussed. The adapted theoretical values were compared to experimental results deduced for a small unit with a nominal capacity of 1 kW. At the end, the cost analysis for a residential size absorber cooling system is bestowed.

Singh et al. [23] load calculation is done for the library located at Sharda University in Greater Noida, is chosen. Sharda University is located at a distance of 42 Km from New Delhi at a Latitude 28.35 0N.. Through the calculation it is possess that entire heat gain in the library is around 165880.977 Btu/hr (48614.91 W). There are two distinct types of heat gain in the library i.e. internal heat gain (lights, fan, people etc) and external heat gain (conduction, convection and radiation). The sensible heat load, latent heat load and total heat gain of the library is 155109.6855 Btu/hr (45458.15 W), 10771.29 Btu/hr (3156.75 W) and 165880.977 Btu/hr (48614.91 W) regardfully. So there is demand of 13.83 TR (or 14 TR) air conditioner is need for Sharda University library which provide comfort cooling for occupancy of 30 people.

Ma and Deng, [24] carried out theoretical analysis of low temperature hot source driven two-stage half effect water lithium bromide absorption refrigeration system. The effects of varying hot water and chilled water temperatures on COP of the system have been investigated. He had reported preparatory results of an experimental research on a 6 kW vapour absorption system working on the half-effect absorption system with Water-LiBr2 as the working fluids. With hot water requirement of temperature was about 85°C, and a chilled water temperature of around 7°C has been reached in his experiment. His results showed that the COP of half effect cycle is lower than that of single effect Vapour absorption refrigeration system using water lithium bromide.

Crepinsek et al. [25] compared the performance of absorption refrigeration systems which are used for refrigeration temperatures below 0°C. Since ammonia-water solution is the most common vapour absorption refrigeration systems with water as the absorbent and ammonia as the refrigerant, research has been done for the improvement of the performance of ammonia-water absorption systems in recent years. The performances of the ammonia-water and possible alternative systems such as ammonia sodium thiocyanate, ammonia-lithium nitrate, monomethylamine-water, R32-DMEU, R22-DMEU, R152a-DMEU, R124-DMEU, R134a-DMEU, R125- DMEU, methanol- TEGDME, trifluoroethanol (TFE)-tetraethylenglycol dimethylether (TEGDME), and R134a-DMAC were compared with respect of the circulation ratio (f) and the coefficient of performance (COP). The highest COP and the lowest f, were found as a function of the temperatures of the generator, absorber, condenser, and evaporating, etc.

Henning et al. [26] discussed the principle ways of covering part of the demand for heating, cooling and domestic hot water by using solar technologies and a design study of a solar thermally driven heating and cooling system for a virtual space is presented. The model of the same space has been examined under various climatic conditions in order to study the impact of

sizing of forelock components on the overall performance. In addition an analysis of economic performance is presented for the case of the location Malta in Mediterranean Sea.

Gebreslassiea et al. [27] presented a multi-objective and a multi-period optimization based on mathematical programming of solar driven absorption cooling systems. Seven solar collector models were combined with a gas fired heater and an absorption cooling system. The optimization of the task was formulated using the non-linear programming (MINLP) problem which is responsible for the minimization of the total cost of the system which avoids the adverse impact on the environment. The environmental performance was measured by following the principles of the Life Cycle Assessment (LCA).

Gomri, [28] presents the simulation results and an overview of the performance of low capacity single stage and half-effect absorption cooling systems, becoming for residing and small construction applications. The primitive heat source was the heat solar energy provided from flat plate collectors. The complete system (i.e., the solar collectors and absorption system) were simulated with the help of a developed software program. The exergy and energy analysis was carried out for different components of the complete system. When temperature of the evaporator was fixed at 5°C and the temperature of condenser was fixed at 28°C, 32°C and 36°C respectfully.

2.2 Conclusions from Literature Review

The following conclusions are drawn from the literature review:

- Solar powered absorption cooling systems can serve both heating and cooling requirements in the building. The availableness of solar energy for running the absorption refrigeration system for 09 hours i.e. 09:00 hrs to 18:00 hrs (office hours). These systems are also more becoming than conventional refrigeration systems because pollution-free working fluids (in lieu of of chloro- fluorocarbons) are used as refrigerants.

- The energy from the sun is utilized to run the flat plate collector, which are used as the source of heat generation for the vapour absorption refrigeration system. The Single flat plate water heating system can be used for heating purpose in winter and rainy seasons and cooling effect during summer. The hot water entrance temperature is found to affect the surface area of some of the components. Increase this hot water temperature the surface area of the solution heat exchanger and the absorber decreases.

- The search for new systems is directed to higher efficiency systems such as double effect or even triple effect systems and in the other hand the use of half effect and single stage systems can operate at even lower firing temperatures. . If the low temperature heat source is used the half-effect absorption cycle gives the best performance.

- The COP increases significantly from double lift to triple effect cycles.

- The half-effect machine is that the demanded heat input temperature is lower than that is needed for the single-effect machine with the same cold water and heat rejection temperatures. The half effect system will stop working below a specific generator temperature; at this point the COP and exergy efficiency will be zero. It is noticed that the half-effect system cycle rejects almost 50% more heat than that in single effect cycle. This increased heat rejection is the thermodynamic fine combined with using low-grade input energy.

- The optimum value of intermediate pressure was increased with the increase of low pressure or high pressure generator temperature and the evaporator temperature, and decreased with the increase in absorber temperature. The optimum pressure for both maximum COP and exergy is same. The maximum values of COP and exergy efficiency, the optimum intermediate temperature were increased with the increase in effectiveness of the heat exchangers carrying strong and weak solution.

- Coefficient of performance of absorption cooling systems is better than that of adsorption systems using solar energy. COP of this type refrigeration system increases as sunlight becomes intense. The coefficient of performance increases with an increase in the temperature of generator and the temperature of evaporator and decreases with an increase in the temperatures of absorber and condenser. Theoretical study show that coefficient of performance (COP) value can be improved by elevating generator

temperature up to certain level and lowering absorber temperature. Lower temperature of condenser results in higher COP. On the increase of mass flow rate of the refrigerant, the overall cooling effect increases, but the COP decreases. The COP of the system was improved 5 to 15 % by using the condensate pre cooler..

- For the range of generator temperature from 65°C to 80°C, the absorption refrigeration system work effectively. Increase in the generator temperature improves the performance parameters of the chiller at low temperature of generator and hence improves the environmental impact performance and reduces the area of chiller. The thermal efficiency of the whole system was decreased with an increased temperature of generator and condenser. . Largest destruction of exergy appear in the generators and the absorbers, peculiarly at high temperatures of heat source.

2.3 Research Gaps

From the literature review, it can be concluded that many of the researchers have gone through detailed investigation on the COP of the system by the use of first law analysis and also investigated the exergetic efficiency by the use of second law analysis of half effect water lithium bromide solar driven vapour absorption system for the given cooling load capacity. The following research gaps are identified from the literature review:

- The analysis of half effect system preceded by the cooling load capacity calculation has not been carried out.

- Also the optimization of input parameters for the minimization of area of flat plate collector and maximization of COP and exergertic efficiency has not been noticed.

- The cost analysis of half effect system in comparison to the conventional vapour compression system and the calculation of payback period have not been carried out.

2.4 Objectives

The following objectives will be achieved:

- Thermodynamic analysis of Vapour Absorption half effect solar driven water lithium bromide system (HVARS) for space cooling, using a flat plate collector is to be done.

- Numerical and Mathematical modeling of the system is to be done.

- A computer program will be developed for the absorption system to simulate various cycle configurations. The simulation of the system will be carried out using Engineering Equations Solver.

- The cooling load calculation of an office space is to be carried out to find out the capacity of the system which is to be cooled by the half effect solar driven vapour absorption system (HVARS).

- Calculation of area and cost of Flat plate collector and its economic survey is done for HVARS.

- Optimization of the intermediate pressure for the given generator, evaporator and absorber temperature, in HVARS using EES.

- Payback period of the HVARS is calculated in comparison with the Vapour compression refrigeration system (VCRS) with the same input parameters.

CHAPTER 3

METHODOLOGY

The following methodology is adopted to achieve the objectives of the Thesis:

3.1 Cooling Load Estimation:

3.1.1 Components of Cooling Load:

The entire building cooling load comprise of heat transferred through the building encasement (roof, walls, windows, floor, doors etc.) and the heat produce by occupants, light and equipments The load due to heat transfer through the enclosure is named as external load, while all other loads are known as internal loads. The percentage of exterior versus interior load diversifies with construction type, construction design and site climate. The entire cooling load on any building insists of both sensible as well as latent load components. The sensible load influence the dry bulb temperature, while the latent load influences the moisture content of the conditioned room.

Buildings can be categorized as outside loaded and inwardly loaded. In outside loaded buildings the cooling load on the building is chiefly due to heat transfer between the surroundings and the interior conditioned room. Since the surrounded conditions are highly changing in any assumed day, the cooling load of an outside loaded building deviate extensively.

In inwardly loaded buildings the cooling load is chiefly due to interior heat produce origin such as occupants, lights or appliances. In common the heat formation due to interior heat origin may continue clearly invariable, and since the heat transfer from the changing surroundings is much less comparison to the interior heat origin, the cooling load of an inwardly loaded construction continue fairly fixed. Obviously from energy effectiveness and economic point of opinion, the system design tactics for an outside loaded construction should be distinct from an inwardly loaded construction. Hence, preceding instruction of whether the building is outside loaded or inwardly loaded is necessary for effectual system design.

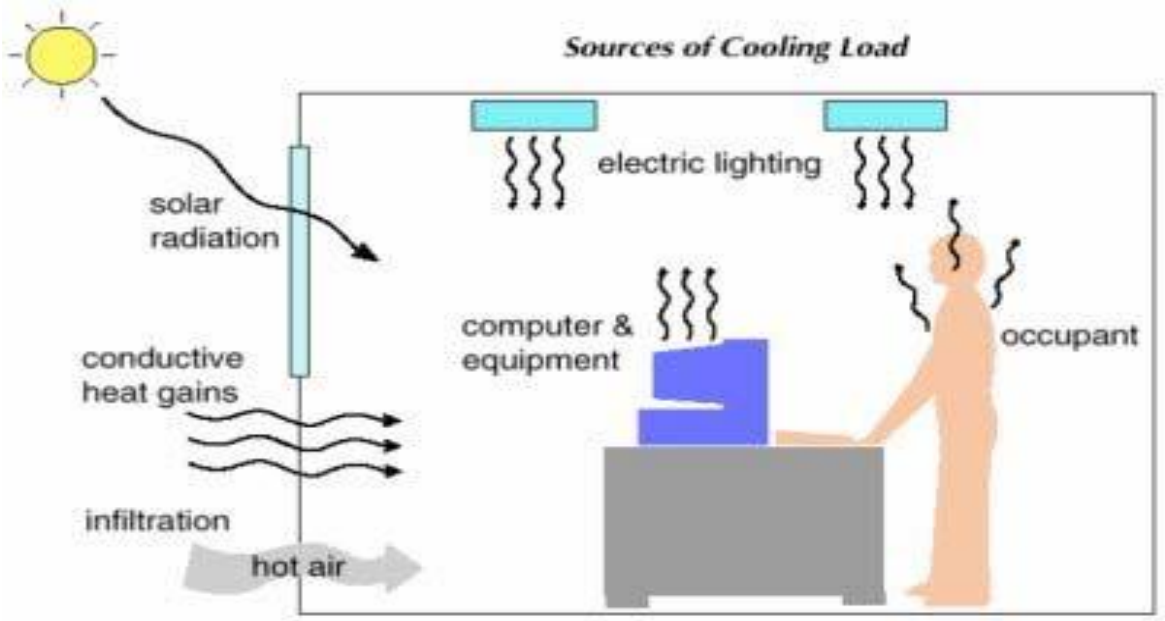

Figure 3.1.1-Components of cooling load

3.1.2 Cooling Load Calculation Method

For a perfect estimate of the zones and whole-building loads, one of the succeeding three methods should be engrossed:

a. **Transfer Function Method (TFM):** This is the most complicated of the methods intend by ASHRAE and need the utility of a computer program or sophisticated spreadsheet.[30]

b. **Cooling Load Temperature Differential/Cooling Load Factors (CLTD/CLF):** This method is deduce from the TFM process and uses schematize data to abbreviate the computation process. The method can be clearly readily carry over into simple spreadsheet programs but has some limitations due to the application of schematize data.[30]

c. **Time-Averaging/Total Equivalent Temperature Differential (TA/TETD):** This was the elect method for hand or simple spreadsheet computation before the preliminary of the CLTD/CLF method.[30]

These three above given methods are well documented in the ASHRAE Handbook Fundamentals, 2001.

In this Thesis, for the cooling load calculation of the assumed office space, CLTD method is used.

3.2 The Half-Effect System:

The fundamental characteristic of the half-effect absorption cycle is that its running capableness at lower temperatures in comparison to the others. The name "half-effect" objected from the COP, that is almost half to that of the single-effect cycle It must be noticed that, any absorption refrigeration system can only be when the solution in the absorber of the system is richer in the quantity of refrigerant than that in the generator. When the pressure reduces or the temperature increases, the fraction of refrigerant quantity contained in the solution is decreased, and vice versa. When the generator temperature is decreased, the solution circulation rate in the cycle will be increased which object the COP to drop. If the generator temperature is too low, the system will cease to work.

The half-effect absorption systems were induced for an epithet with a relatively low-temperature heat origin. It must be noticed that COP of the half-effect absorption system is relatively low in comparison to the single-effect absorption system as it rejects more heat than a single-effect absorption refrigeration cycle around 50%. However, the half effect absorption system can work at relatively low temperature heat source. The half-effect absorption refrigeration system, comprises of evaporator, condenser, two absorbers, two generators, two solution heat exchangers, two pumps, two solution reducing valves and one refrigerant expansion valve. In the system functionality, the low pressure absorber and the evaporator function at low pressure (evaporation pressure Pe).

The high absorber and the low pressure generator (LPG) work at intermediate pressure (Pi) in the system while the condenser and the high pressure generator (HPG) works at high pressure (i.e, at the condenser pressure, Pc). Both the generators (HPG and LPG) can be accommodate with heat at the same temperature. The refrigerant vapour coming out from the evaporator is absorbed by the strong solution in the low absorber to function the cycle.

The weak solution coming from the low absorber in the low pressure circuit is pumped to the low generator by the low solution heat exchanger within the circuit. The strong solution in the low generator is reverting to the low absorber by the low solution heat exchanger. The refrigerant vapour in the low generator is absorbed through the strong solution in the high absorber in the high pressure circuit. The weak solution in the high absorber is pumped to the high generator by the high solution heat exchanger. The strong solution in the high generator is reverting to the high absorber by the high solution heat exchanger. In both the heat exchangers, the weak solution coming from the absorber is heated by the strong solution coming from the generator. The refrigerant gets heat and boiled out of the solution in the high generator and propagates to the condenser. The liquid refrigerant from the condenser is reverting to the evaporator with the help of an expansion valve.

The half effect system has three levels of pressure condenser pressure (Pc), intermediate pressure (Pi) and the evaporator pressure (Pe) and four levels of temperature [29]. Though the half effect systems have lower COP, as compared to the single effect refrigeration systems, but this can work at lower temperature of generator.

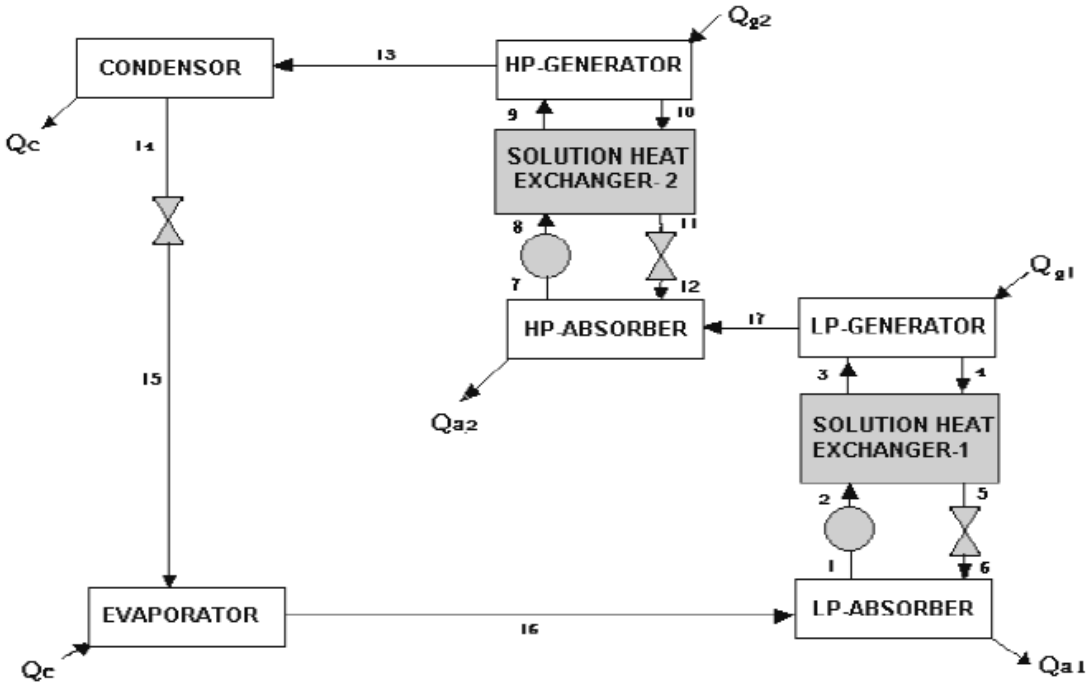

Figure 3.2.1-Schematic diagram of the Half-effect Vapour Absorption Refrigeration System (HVARS)

The one of a kind feature of the Half-effect refrigeration systems is that it need heat input at low temperature than that required in Single-effect refrigeration system keeping the same condenser and evaporator temperature The diagram scheme of the Half-effect vapour absorption refrigeration system (HVARS) is shown in Figure 3.2.1 and the analogous p-t-x diagram is shown in Figure 3.2.2.

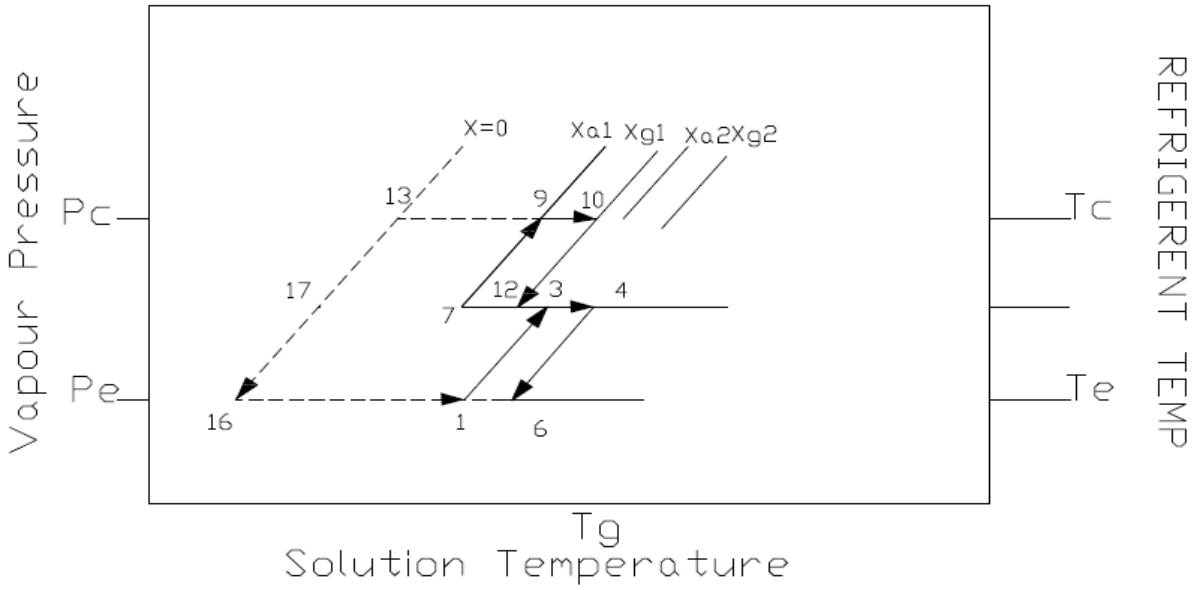

Figure 3.2.2-The p-t-x diagram for the half effect vapour absorption refrigeration system (HVARS)

3.2.1 Thermodynamic Analysis of Half Effect System:

3.2.1.1 Description of the Half effect Vapour Absorption System:

The half effect water lithium bromide absorption refrigeration system shown consists of an condenser, evaporator, LP & HP generators, LP & HP absorbers, LP and HP solution heat exchangers, , solution pumps and solution and refrigerant throttle valves. The condenser and HP generator work at same pressure which is the maximum pressure of the system. The LP generator and HP absorber work at the same intermediate pressure whereas the evaporator and the LP absorber work at same lowermost pressure of the system. Following relationship exists among the pressures in these components:

$$(P_{gh} = P_c) > (P_{gl} = P_{ah}) > (P_{al} = P_e)$$

The refrigerant (i.e., water) is circulated through the condenser, evaporator, LP absorber, LP generator, HP absorber, HP generator. When the water vapour has condensed in the condenser, it revert to the evaporator through an expansion valve. However, the absorbent that is the lithium bromide aqueous solution is circulated within two distinct stages i.e. the LP stage between the LP generator and the LP absorber, and the HP stage between the HP generator and the HP absorber. Compared to a single-stage vapour absorption refrigeration system, there are two additional components namely LP generator and HP absorber, in a half effect system. These are utilized to concentrate the lithium bromide aqueous solution in the LP stage cycle. [6]

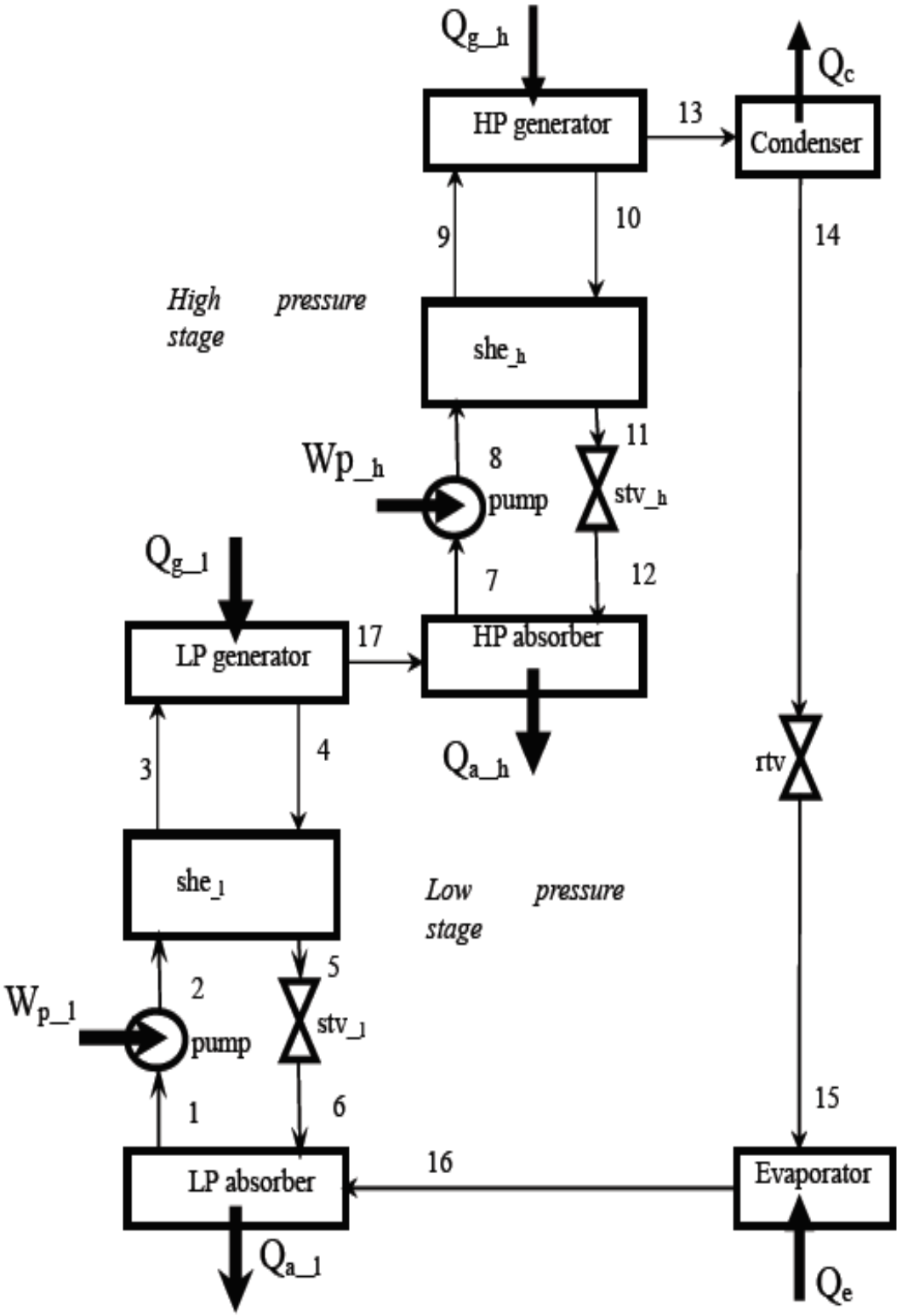

Figure 3.2.2.1-Schematic diagram of the half effect water $LiBr_2$ vapour absorption Refrigeration System [6]

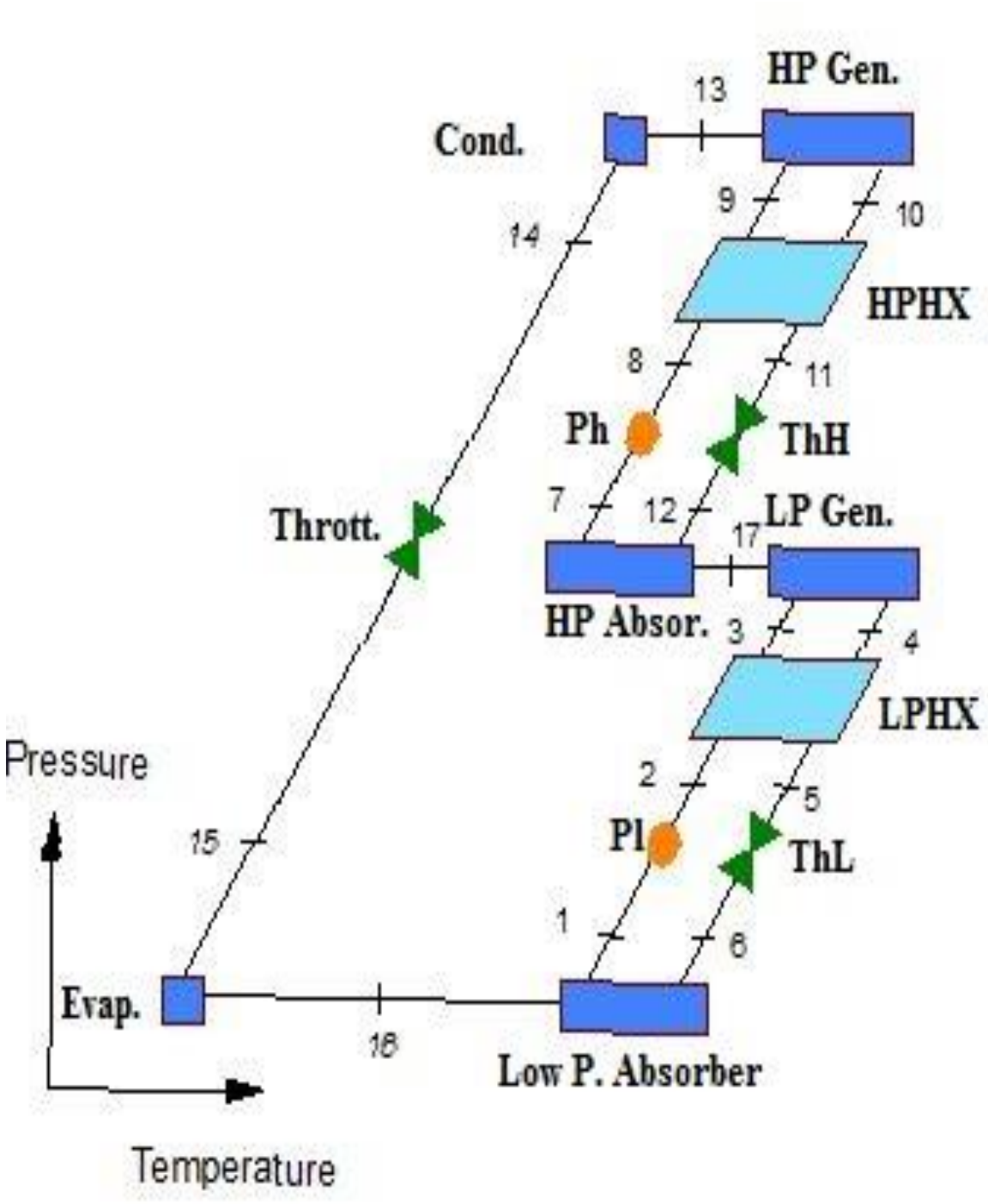

Figure 3.2.2.2-Block diagram of Half Effect Vapour Absorption Refrigeration System

Table 3.2.1.1: p-t-x data for Half effect vapour absorption system

State point	P	T	X	Working fluid state
1.	PE	TAL	X_{Sl}	Equilibrium strong solution LP side
2.	PI	TAL	X_{Sl}	Strong solution
3.	PI	T3	X_{Sl}	Pre heated strong solution
4.	PI	TGL	X_{Wl}	Equilibrium weak solution LP side
5.	PI	T5	X_{Wl}	Sub cooled weak solution
6.	PE	T6	X_{Wl}	Sub cooled weak solution
7.	PI	TAH	X_{Sh}	Equilibrium strong solution HP side
8.	PC	TAH	X_{Sh}	Strong solution
9.	PC	T9	X_{Sh}	Pre heated strong solution
10.	PC	TGH	X_{Wh}	Equilibrium weak solution HP side
11.	PC	T11	X_{Wh}	Sub cooled weak solution
12.	PI	T12	X_{Wh}	Sub cooled weak solution
13.	PC	T13	0	Superheated refrigerant vapour
14.	PC	TC	0	Saturated refrigerant liquid
15.	PE	TE	0	Two phase refrigerant
16.	PE	TE	0	Saturated vapour refrigerant
17.	PI	T17	0	Superheated refrigerant vapour

3.2.1.2 Thermodynamic Analysis:

The base of thermodynamics is established in the first and second laws. The first law of thermodynamics characterizes the conservation of energy, while the second law of thermodynamics is utilized to describe the quality of energy and material used. For doing the thermodynamic analysis of the vapour absorption refrigeration system the principles of conservation of mass, first law and second law of thermodynamics are applied particularly to each component of the system.

3.2.1.2.1 Assumptions:

In direction to simulate these absorption refrigeration systems, several assumptions are made, comprehend the succeeding:

- The analysis of the system is prevailed under steady state conditions.
- The refrigerant (i.e., water) at the exit of the condenser is assumed to be the saturated liquid.
- The refrigerant (i.e., water) at the exit of the evaporator is assumed to be the saturated vapour.
- The Lithium bromide solution at the exit of the absorber is a strong solution and it is at the absorber temperature.
- The exit temperatures from the generator and the absorber from corresponding to equilibrium conditions of the separation and mixing particularly.
- The pressure losses in the pipelines and all the heat exchangers are assumed to be negligible.
- Heat exchange between the surroundings and the system, other than in that is prescribed by heat transfer at the absorber, generator, condenser, evaporator, do not appear.
- The reference environmental state for the system is water at an environment temperature To of 25°C and 1 atmospheric pressure (Po).
- The system exhibit chilled water.
- The system rejects heat to cooling water at the absorber and the condenser.

Mass conservation

The mass conservation law applied for each component is written as:

$$\sum m_i = \sum m_e$$

This law applied for each component of the cycle is written as:

.$m_1 = m_2 = m_3$

$m_4 = m_5 = m_6$

$m_7 = m_8 = m_9$

$m_{10} = m_{11} = m_{12}$

$m_{13} = m_{14} = m_{15} = m_{16} = m_{17}$

LP generator or LP absorber

. $m_3 = m_4 + m_{17}$

HP generator or HP absorber

. $m_9 = m_{10} + m_{13}$

Conservation of concentration

The law of concentration conservation for each component is written as:

$$\sum m_i X_i = \sum m_e X_e$$

Where m is the mass flow rate in the system and X the is mass concentration of lithium bromide in the solution.

The law is applied for each component of the cycle is written as:

LP generator or LP absorber

$m_3X_3 = m_4X_4$

HP generator or HP absorber

$m_9X_9 = m_{10}X_{10}$

$X_1 = X_2 = X_3$

$X_4 = X_5 = X_6$

$X_7 = X_8 = X_9$

$X_{10} = X_{11} = X_{12}$

$X_{13} = X_{14} = X_{15} = X_{16} = X_{17} = 0$

3.2.1.2.2 Energy Balance:

The first law of thermodynamics permits the energy balance of each component (each component may be treated as a control volume with entrance and exit streams, work interactions and heat transfer) of the absorption system as follows:

$$\sum(m_e h_e) - \sum(m_i h_i) + \sum Q_i = W$$

Where the 'Q' is the heat transfer rates between the environment and its control volume, and W denotes the positive work, when it is performed on the system. The energy balance equations applied for some of the components of the system are expressed as follows:

Low absorber:

$$QA_l = ms_l \cdot h_1 - (mw_l \cdot h_6 + mr \cdot h_{16})$$

High absorber:

$$QA_h = ms_h \cdot h_7 - (mw_h \cdot h_{12} + mr \cdot h_{17})$$

Low generator

$$QG_l + ms_l \cdot h_3 = mr \cdot h_{17} + mw_l \cdot h_4$$

High generator:

$$QG_h + ms_h \cdot h_9 = mr \cdot h_{13} + mw_h \cdot h_{10}$$

Low heat exchanger:

$$e_{SHE,l} = \frac{h_4 - h_5}{h_4 - h2_4}$$

$$QSHE_l = ms_l \cdot h_3 - ms_l \cdot h_2$$

High heat exchanger

$$e_{SHE,h} = \frac{h_{10} - h_{11}}{h_{10} - h8_{10}}$$

$$QSHE_h = ms_h \cdot h_9 - ms_h \cdot h_8$$

Condenser:

$$QC = mr \cdot (h_{14} - h_{13})$$

Evaporator:

$$QE = mr \cdot (h_{16} - h_{15})$$

Coefficient of Performance (COP):

The overall energy performance of the half effect vapour absorption system is determined by the evaluation of its coefficient of performance (COP)

$$COP = \frac{QE}{QG_h + QG_l + Wp_h + Wp_l}$$

Circulation Ratio:

The ratio of mass flow rate of the strong solution in the respective component to the mass flow rate of the refrigerant is termed as circulation ratio. The solution circulation ratio of the high pressure and the pressure stages are given by :

$$SCR_l = \frac{ms_l}{mr}$$

$$SCR_h = \frac{ms_h}{mr}$$

Efficiency of global system:

The efficiency of global system is given as ;

$$h_{global} = COP \cdot K$$

Where K is the efficiency of flat plate collector

3.2.1.2.3 Exergy Balance

Exergy destruction in each component of the Half effect vapour absorption system is expressed as:

Low absorber:

Exergy Destruction

$$ED_{a,l} = mr \cdot (h_{16} - To \cdot S_{16}) + mw_l \cdot (h_6 - To \cdot S_6) - ms_l \cdot (h_1 - To \cdot S_1)$$

Exergy Product

$$P_{ED,a,l} = ED_{a,l} \cdot \frac{100}{ED_t}$$

High absorber:

Exergy Destruction

$$ED_{a,h} = mr \cdot (h_{17} - To \cdot S_{17}) + mw_h \cdot (h_{12} - To \cdot S_{12}) - ms_h \cdot (h_7 - To \cdot S_7)$$

Exergy Product

$$P_{ED,a,h} = ED_{a,h} \cdot \frac{100}{ED_t}$$

Low generator:

Exergy Destruction

$$ED_{g,l} = \left[1 - \left(\frac{To}{TG_l + 273.15}\right)\right] \cdot QG_l + ms_l \cdot (h_3 - To \cdot S_3) - mw_l \cdot (h_4 - To \cdot S_4) - mr \cdot (h_{17} - To \cdot S_{17})$$

Exergy Product

$$P_{ED,g,l} = ED_{g,l} \cdot \frac{100}{ED_t}$$

High generator:

Exergy Destruction

$$ED_{g,h} = \left[1 - \left(\frac{To}{TG_h + 273.15}\right)\right] \cdot QG_h + ms_h \cdot (h_9 - To \cdot S_9) - mw_h \cdot (h_{10} - To \cdot S_{10}) - mr \cdot (h_{13} - To \cdot S_{13})$$

Exergy Product

$$P_{ED,g,h} = ED_{g,h} \cdot \frac{100}{ED_t}$$

Low heat exchanger:

Exergy Destruction

$$ED_{she,l} = ms_l \cdot (h_2 - To \cdot S_2) - ms_l \cdot (h_3 - To \cdot S_3) + mw_l \cdot (h_4 - To \cdot S_4) - mw_l \cdot (h_5 - To \cdot S_5)$$

Exergy Product

$$P_{ED,she,l} = ED_{she,l} \cdot \frac{100}{ED_t}$$

High heat exchanger:

Exergy Destruction

$$ED_{she,h} = ms_h \cdot (h_8 - To \cdot S_8) - ms_h \cdot (h_9 - To \cdot S_9) + mw_h \cdot (h_{10} - To \cdot S_{10}) - mw_h \cdot (h_{11} - To \cdot S_{11})$$

Exergy Product

$$P_{ED,she,h} = ED_{she,h} \cdot \frac{100}{ED_t}$$

Condenser:

Exergy Destruction

$$ED_c = mr \cdot (h_{13} - To \cdot S_{13}) - mr \cdot (h_{14} - To \cdot S_{14})$$

Exergy Product

$$P_{ED,c} = ED_c \cdot \frac{100}{ED_t}$$

Evaporator:

Exergy Destruction

$$ED_e = \left[1 - \left(\frac{To}{Tr + 273.15}\right)\right] \cdot QE + mr \cdot (h_{15} - To \cdot S_{15}) - mr \cdot (h_{16} - To \cdot S_{16})$$

Exergy Product

$$P_{ED,e} = ED_e \cdot \frac{100}{ED_t}$$

Throttling Valve:

Exergy Destruction

$$ED_{rtv} = mr \cdot (h_{14} - To \cdot S_{14}) - mr \cdot (h_{15} - To \cdot S_{15})$$

Exergy Product

$$P_{ED,rtv} = ED_{rtv} \cdot \frac{100}{ED_t}$$

Pressure reducing valve on low pressure side cycle :

Exergy Destruction

$$ED_{stv,l} = mw_l \cdot (h_5 - To \cdot S_5) - mw_l \cdot (h_6 - To \cdot S_6)$$

Exergy Product

$$P_{ED,stv,l} = ED_{stv,l} \cdot \frac{100}{ED_t}$$

Pressure reducing valve on high pressure side cycle :

Exergy Destruction

$$ED_{stv,h} = mw_h \cdot (h_{11} - To \cdot S_{11}) - mw_h \cdot (h_{12} - To \cdot S_{12})$$

Exergy Product

$$P_{ED,stv,h} = ED_{stv,h} \cdot \frac{100}{ED_t}$$

Total Energy Destruction

$$ED_t = ED_{a,l} + ED_{a,h} + ED_{g,l} + ED_{g,h} + ED_c + ED_e + ED_{she,l} + ED_{she,h} + ED_{stv,l} + ED_{stv,h} + ED_{rtv}$$

Energy Input to the System:

$$Exergy_{input} = QG_h \cdot \left[1 - \left(\frac{To}{TG_h + 273.15}\right)\right] + QG_l \cdot \left[1 - \left(\frac{To}{TG_l + 273.15}\right)\right] + Wp_l + Wp_h$$

Exergy Product of the system

$$exergy_{product,E} = -QE \cdot \left[1 - \left(\frac{To}{Tr + 273.15}\right)\right]$$

Exergy Destruction Ratio

$$EDR = \frac{ED_t}{exergy_{product,E}}$$

The exergetic efficiency is given by :

$$h_{exergetic1} = \frac{exergy_{product,E}}{Exergy_{input}}$$

Or

$$h_{exergetic} = \frac{QE \cdot \left[1 - \left(\frac{To + 273.15}{TE + 273.15}\right)\right]}{QG_l \cdot \left[1 - \left(\frac{To + 273.15}{TG_l + 273.15}\right)\right] + QG_h \cdot \left[1 - \left(\frac{To + 273.15}{TG_h + 273.15}\right)\right] + Wp_l + Wp_h}$$

3.3. Solar Thermal Collectors:

A solar thermal collector is a device used to capture heat or thermal energy from solar radiation.

3.3.1 Type of solar collectors:

Solar thermal collectors can essentially be categorized as concentrating and non-concentrating. The collector with non-concentrating feature has the equal area for absorbing and for intercepting solar radiation, on the other hand a sun-tracking concentrating solar collector generally has concave reflecting surfaces to intercept and focus the sun's beam radiation for absorbance to a less area of receiving, which in turn increases the flux of radiation.[31]

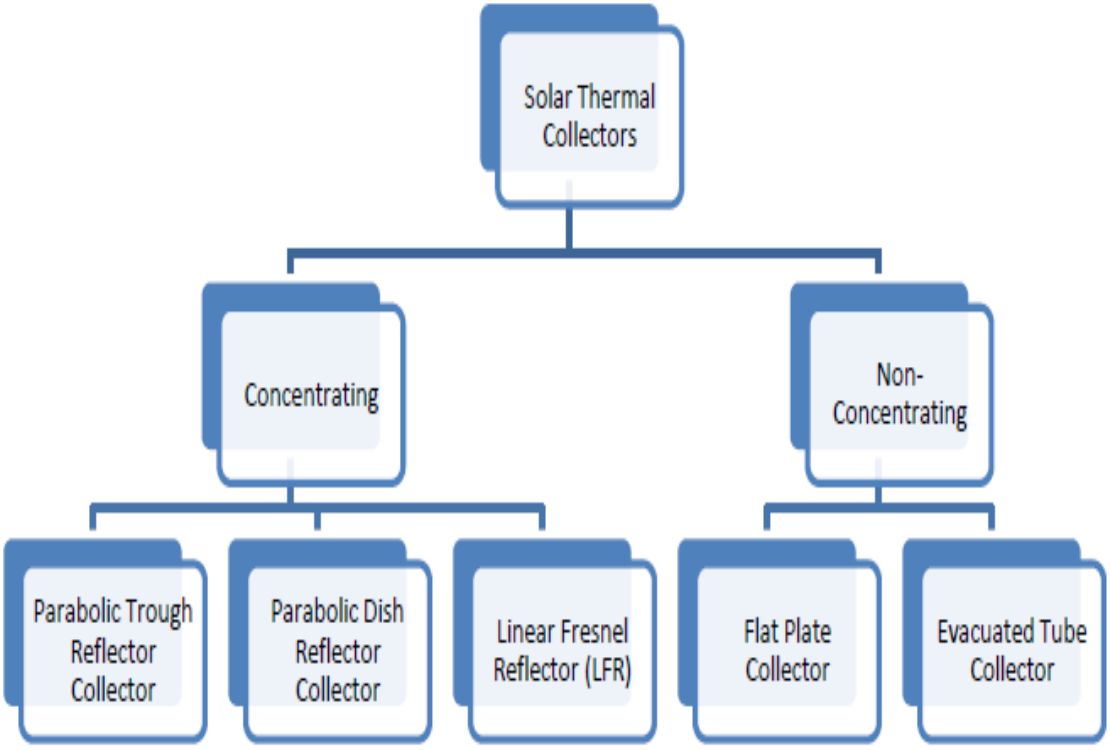

Figure 3.3.1.1-Solar Thermal Collectors Classification [32]

3.3.2 A Summary on Solar Collectors

The below table shown, give the summary of the commonly used collector types with an idea of the indicative temperature ranges and the concentration ratios which can be achieved .[31]

Table 3.3.2.1 Solar Thermal Collectors, Concentration Ratios and Indicative Output Temperatures [31]

Motion	Collector Type	Absorber Type	Concentration Ratio	Indicative Temperature range (0C)
Stationary	Flat plate collector (FPC) Evacuated tube collector (ETC) Compound parabolic collector (CPC)	Flat Flat Tubular	1 1 1-5	30-80 50-200 60-240
Single Tracking	Linear Fresnel reflector (LFR) Parabolic trough collector (PTC) Cylindrical Trough collector (CTC)	Tubular Tubular Tubular	10-40 15-45 10-50	60-250 60-300 60-300
Two-axes tracking	Parabolic dish collector (PDR) Heliostat field collector (HFC)	Point Point	100-1000 100-1500	100-500 150-200

3.3.3 The Solar Collector Subsystem

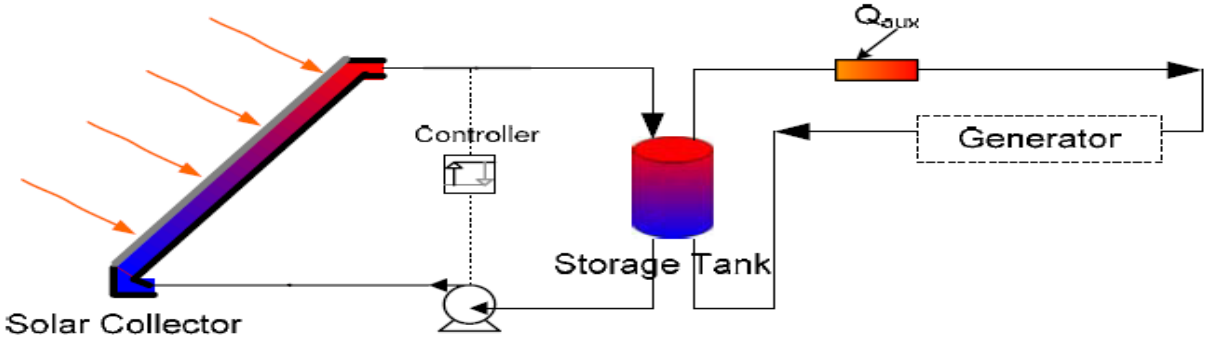

Figure 3.3.3.1 The solar collector subsystem

This subsystem consist of the solar collector, a storage tank, a controller, a pump, and an auxiliary heater. Solar radiation is converted into heat with the help of the solar collectors. The storage tank is utilized as the thermal storage when solar radiation is not adequate. The auxiliary heater is positioned between the generator and the storage tank of the refrigeration sub-system. When the temperature of the liquid that is coming from the storage tank is less than the lowest generator temperature set point, than the auxiliary heater will start to work. The noteful heat direct by the solar collector, Qu, is calculated from the heat balance equation in the solar collector derived by Hottel-Whillier-Bliss equation [33] as follows:

$$Q_u = \eta_{sc} Q_s = A_{sc} F_R \left[G(\tau\alpha)_e - U_L (T_i - T_a) \right]$$

The solar collector efficiency is determined as the ratio of the useful heat gain obtained over any time duration to the incident radiation from the sun over the same duration. The instant energy efficiency of the solar collector can also be detailed in the form of the average Bliss coefficient (FR(τα)e) and the heat loss coefficient (FRUL),[33] as shown

$$\eta_{sc} = \frac{Q_u}{A_{sc} G} = F_R (\tau\alpha)_e - \frac{F_R U_L (T_i - T_a)}{G}$$

The efficiency of global system ;

$$h_{global} = COP \cdot K$$

The following types of solar collectors are studied, a single-glazed flat plate, a double-glazed flat plate and an evacuated tube solar collector. The assumed values of FR(τα)e and FRUL for each type of solar collector used in this simulation are shown

Table 3.3.3.1 The Value of FR(τα)e and FRUL for Each Type of Solar Collector

Solar Collector Type	***FR(τα)e***	***FRUL* (Wm-2 K-1)**
Flat-plate, selective-surface, single-glass cover	0.80	5.00
Flat-plate, selective-surface, double-glass cover	0.80	3.50
Evacuated tubular collectors	0.80	1.5

3.3.4 Flat Plate Collector:

In solar cooling system widely used solar collectors are the flat plate solar collectors (FPC) and the evacuated tube collectors (ETC), are stationary type and also their range of temperature. These Collectors are capable to absorb both diffuse and beam radiation.

Flat plate collectors are an insulated box that are weather proofed, includes a dark absorber plate below one or more transparent covers.

Figure 3.3.4.1 Solar water heater

Main Parts of the Flat Plate Collector:

Cover Plate of the collector: The cover plate is made up of a tempered glass having a low content of iron and thickness is 3.2-6.4 mm. The flat plate collector has transmittance equal to 85%., when the given type of glass is utilized.

Absorber Plate of the collector: The absorber plate is made up of Copper as of its high conductivity. Also, it resists corrosion .The Copper plates of thickness 0.05 mm and 1.25 cm diameter tubes. The tubes are 15 cm spaced apart, the efficiency is 97 %.. Also, copper plate with black paint is used that has the value of emmittance between 0.08-0.12 and the value of absorptance to be 0.85-0.9 .

Enclosure/Insulation of the collector: The enclosure is made up of aluminium ,steel or fibre glass. Fibre glass is commonly used.

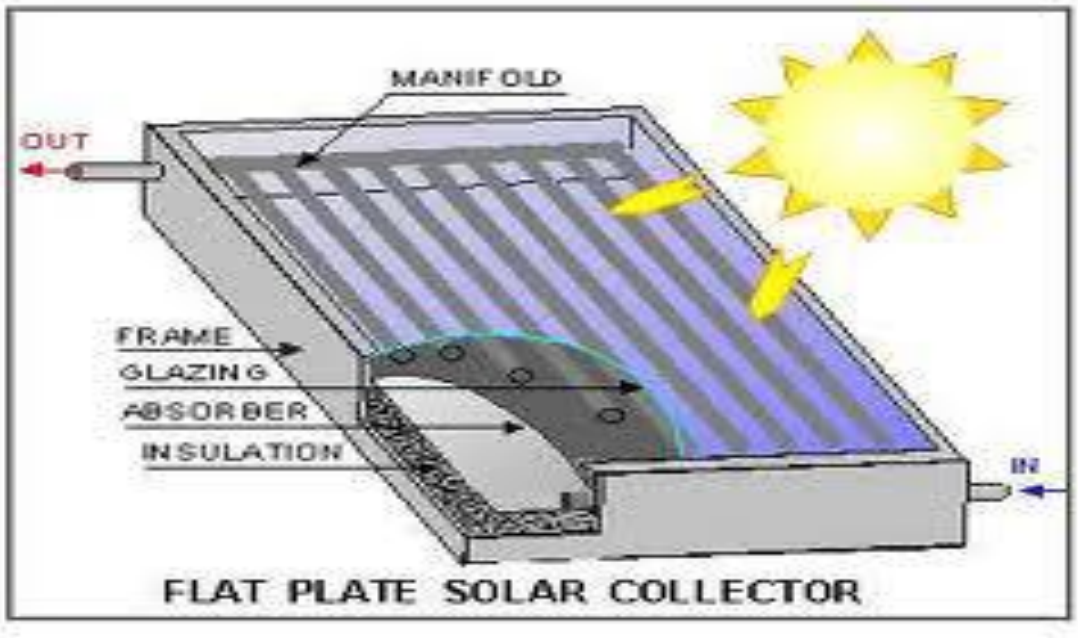

Figure 3.3.4.2 Flat Plate Solar Collector

3.3.5 Flat Plate Collector Calculation methodology:

Following steps to be followed:

- The flat plate collector of a company will be selected to run the system.
- The total area of flat plate collector required will be calculated based on the heat generated in the high pressure and low pressure generator, which is evaluated by the thermodynamic analysis of the HVARS using EES.
- Based on the specifications of the selected flat plate collector the number of flat plates required will be calculated.

3.4 Cost analysis and Payback period calculation:

The economics of solar energy systems are especially complicated with much unavoidable uncertainty due to several factors. The main argument for using solar energy for cooling or heating is to lower the energy price combined with operating buildings. Therefore, an economic analysis must be conduct out to decide whether a respective solar system is economically profitable for a specific plan.

The Pay Back Time of investment in solar cooling systems can be adapted with several approaches. On comparison, the cost difference between distinct systems, the system with the lowermost life-cycle cost can be recognized. Another way is to use the benefit –cost analysis. Generally, the pay-back period (PBP) is the numeral of years required for the net present value to reach nil, and can be characterize as the amount of period before the investment recompense for itself. The annual advantage of solar cooling system could be determined by the cost difference between conventional system and solar system. For solar cooling system, cash flows are commonly negative. The best trustworthy approach is to use the net present value benefits means. Using this approach, the cost are determine as the present value of the additional costs of wounding and maintaining a solar system and the benefits as the present value of saving in costs of energy for a solar system as compared with a conventional similar system.

The proposed solar driven half effect system is compared with the Vapour compression refrigeration system (VCRS) with the same input parameters. The cost of VCRS system is due to the cost electricity, while the cost associated with the HVARS system is only the cost of flat plate collectors. The payback period of Half-effect solar driven absorption unit (HVARS) is calculated by comparing the cost of HVARS system with the conventional VCRS system running for the same input parameters i.e., condenser temperature, evaporator temperature, cooling capacity etc. The generator of HVARS is replaced by the compressor of the conventional VCRS which runs on electricity, while rest of the components of the two system are same.

CHAPTER 4

CALCULATION

4.1 Cooling Load Calculation

Input Given

Office Location: 30^0 N Latitude

Office Plan

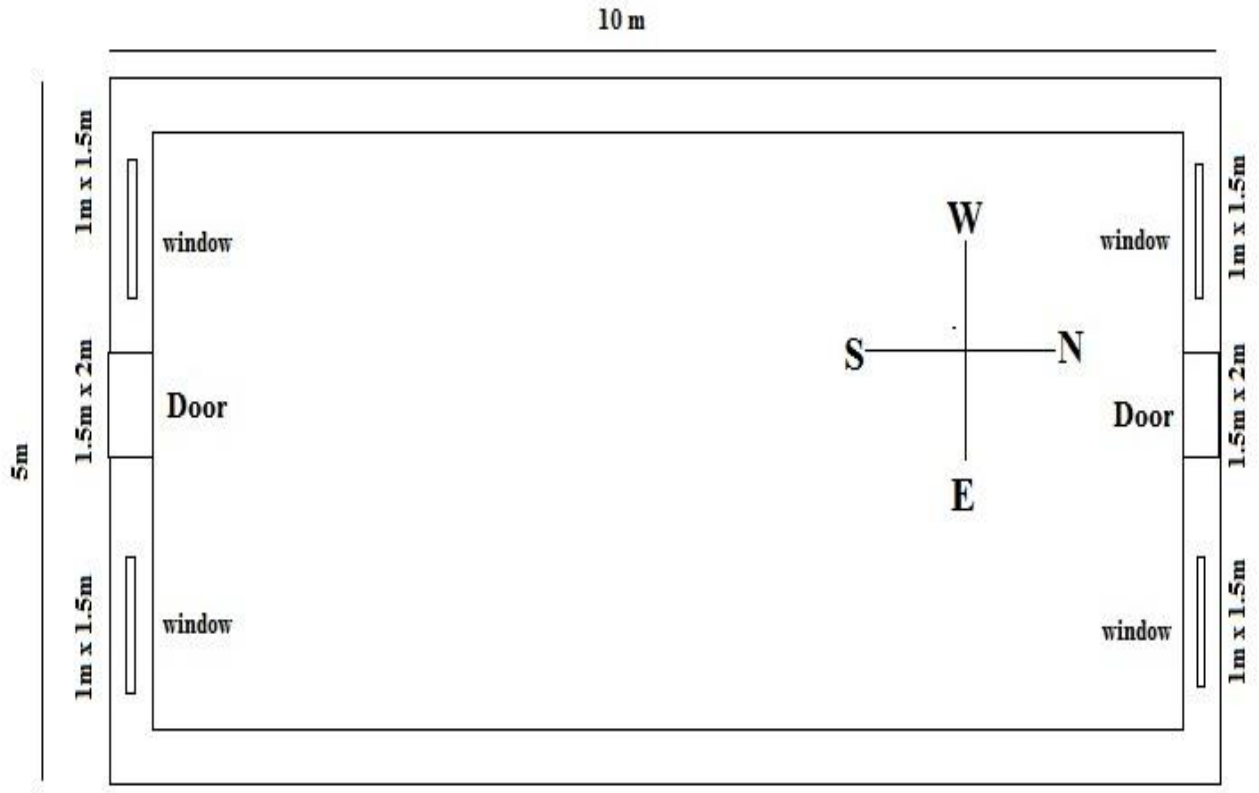

Figure 4.1.1- Plan of the office space

Office Size : 10m x 5m x 4m (l x b x h)

North side window : 2

Size of each window : 1m x 1.5 m

South side window : 2

Size of each window : 1m x 1.5 m

K_{glass} = 0.78 W/mK

$K_{concrete}$ = 1.73 W/mK

K_{brick} = 0.78 W/mK

$K_{plaster}$ = 1.32 W/mK

K_{wood} = W/mK

.h_o = 23 W/m^2K

.h_i = 7 W/m^2K

Plaster on Inside Wall : 1.25 cm = 0.0125 m

Outside wall construction : t_{brick} = 0.10 m

Roof construction : 20 cm RCC slab

Floor construction : 20 cm concrete

Densities :

Brick = 2000 kg/m^3

Concrete = 1900 kg/m^3

Plaster = 1885 kg/m^3

Fenestration { weather-stripped loose fit } :

Size : 1m x 1.5m glass

U_g = 5.9 W/m^2K

Doors : wood panels

Number of doors : 2

Size of each door : 1.5m x 2m

U_d = 0.63 W/m^2K

Outdoor design conditions : 43^o C DBT , 27^{o}C WBT

Indoor design conditions : 25^{o} C DBT , 50% RH

Daily Range : 31^{o} C to 43^{o} C = 12^{o} C

Occupancy : 10

Lights : 40 Watt Each

No. of tube lights : 6

Fans : 100 Watt each

No. of fans : 2

Machines : 300 W

Solution :

Structure Load Calculation :

Table 4.1.1 : Area consideration of different orientations of wall

	Structure Specification	Constituents of the structure	Area
1	North Wall	Plaster + 2 window Glass + Door	$A_N = A_p + A_g + A_d$
2	South Wall	Plaster + 2 window Glass+ Door	$A_S = A_p + A_g + A_d$
3	East Wall	Plaster	$A_E = A_p$
4	West Wall	Plaster	$A_E = A_p$
5	Floor	Concrete	A_F
6	Roof	RCC slab	A_R
7			

North Wall Calculation :

One Door : 1.5m x 2m

Two Window Glass : 1m x 1.5m

Plaster Wall : Rest (14 m^2)

Area of door A_d = 1.5 x 2 = 3 m^2

U value for door U_d = 0.63 W/m^2K

Area of window glass A_g = 2 x (1 x 1.5) = 3 m^2

U value of window glass U_g = 5.9 W/m^2K

Area of Plaster wall on North side A_{pN} = { 5 x 4 - (1.5 x 2) – (1 x 1.5) x 2 }

A_{pN} = 14 m^2

U value of rest Plaster Wall U_{wN} = 3.77 W/m^2K

.t_{brick} = 0.10 m

.$t_{plaster}$ = 0.0125 m

$$\frac{1}{U_{wall}} = \frac{1}{h_i} + \frac{t_{brick}}{K_{brick}} + \frac{2 \cdot t_{plaster}}{K_{plaster}} + \frac{1}{h_o}$$

$$\frac{1}{U_{wall}} = 1 / 7 + \frac{0.1}{1.32} + \frac{2 \cdot 0.0125}{8.65} + \frac{1}{23}$$

U_{wall} = 3.77 W/m^2K

Therefore,

The Net heat transfer from the North Side Wall is given by

$$Q_N = \left[\left(U_{p_N} \cdot A_{p_N} \right) + \left(U_d \cdot A_d \right) + \left(U_g \cdot A_g \right) \right] \cdot \Delta T$$

Q_N = [(3.77 x 14) + (0.63 x 3) + (5.9 x 3)] x (43 - 25)

Q_N = 1302.66 W = 1300 W

South Wall Calculation :

One Door : 1.5m x 2m

Two Window Glass : 1m x 1.5m

Plaster Wall : Rest (14 m^2)

Area of door $A_d = 1.5 \times 2 = 3\ m^2$

U value for door $U_d = 0.63\ W/m^2K$

Area of window glass $A_g = 2 \times (1 \times 1.5) = 3\ m^2$

U value of window glass $U_g = 5.9\ W/m^2K$

Area of Plaster wall on North side $A_{PS} = \{ 5 \times 4 - (1.5 \times 2) - (1 \times 1.5) \times 2 \}$

$A_{PS} = 14\ m^2$

U value of rest Plaster Wall $U_{PS} = 3.77\ W/m^2K$

$t_{brick} = 0.10\ m$

$t_{plaster} = 0.0125\ m$

$$\frac{1}{U_{wall}} = \frac{1}{h_i} + \frac{t_{brick}}{K_{brick}} + \frac{2 \cdot t_{plaster}}{K_{plaster}} + \frac{1}{h_o}$$

$$\frac{1}{U_{wall}} = 1 / 7 + \frac{0.1}{1.32} + \frac{2 \cdot 0.0125}{8.65} + \frac{1}{23}$$

$U_{wall} = 3.77\ W/m^2K$

East Wall Calculation :

Area of Wall $A_E = 10 \times 4 = 40\ m^2$

$U_{PE} = 3.77$

West Wall Calculation :

Area of Wall $A_W = 10 \times 4 = 40\ m^2$

$U_{PW} = 3.77$

Floor Calculation :

Thickness of Concrete $t_c = 0.2\ m$

$$\frac{1}{U_{floor}} = \frac{1}{h_i} + \frac{t_{concrete}}{K_{concrete}}$$

$$\frac{1}{U_{floor}} = 1 / 7 + \frac{0.2}{1.73}$$

$U_{floor} = 3.869 = 3.9\ W/m^2K$

Area of space $A_f = 10 \times 5 = 50\ m^2$

Roof Calculation:

Thickness of Concrete $t_c = 0.2$ m

$$\frac{1}{U_r} = \frac{1}{h_i} + \frac{t_{concrete}}{K_{concrete}} + \frac{t_{plaster}}{K_{plaster}} + \frac{1}{h_o}$$

$$\frac{1}{U_r} = 1 / 7 + \frac{0.2}{1.73} + \frac{0.0125}{8.65} + \frac{1}{23}$$

$U_r = 3.296 = 3.3\ W/m^2K$

Area of space $A_r = 10 \times 5 = 50\ m^2$

Table 4.1.2 : Area calculation for different wall orientation

	Structure Specification	Constituents of the structure	Area (m^2)	U Values (W/m^2K)
1	North Wall	Plaster + 2 window Glass + Door	$A_N = A_p + A_g + A_d = 14$	5.9
2	South Wall	Plaster + 2 window Glass+ Door	$A_S = A_p + A_g + A_d = 14$	5.9
3	East Wall	Plaster	$A_E = A_{pn} = 40$	3.77
4	West Wall	Plaster	$A_E = A_p = 40$	3.77
5	Floor	Concrete	$A_F = 50$	3.9
6	Roof	RCC slab	$A_R = 50$	3.3

Correction for Equivalent temperature differentials

For daily range of 12 ^{o}C = (12 – 11.1)/2 = 0.45 ^{o}C

For (t_o - t_i) of 18 ^{o}C = 18 – 8.3 = 9.7 ^{o}C

Total correction = - 0.45 + 9.7 = 9.25 ^{o}C

Equivalent temperature differentials in ^{o}C , from Tables 18.9 and 18.10 [29], and incorporating corrections :

Table 4.1.3 : Equivalent temperature differentials in ^{o}C and incorporating corrections

S. No.	Orientation	2 p.m.	3 p.m.	4 p.m.	5 p.m.	6 p.m.	7 p.m.
1	**West Wall**	14.4	14.8	15.2	16.5	17.5	_
2	**North Wall**	9.6	10.2	9.6	11.3	11.7	_
3	**South Wall**	13.1	14.7	16.0	17.4	17.8	_
4	**Roof (exposed)**	24.0	25.8	28.0	29.7	30.5	30.2

Rate of solar gains through glass on June 21 in W/m^2 form table 17.9 (d)[29]

Table 4.1.4 : Rate of solar gains through glass on June 21 in W/m^2

S. No.	Orientation	2 p.m.	3 p.m.	4 p.m.	5 p.m.
1	West Wall	309	451	508	492
2	North Wall	44	44	51	91
3	South Wall	47	44	38	32

Estimated time of maximum cooling load :

From the above table it is seen that the major components of the variable cooling loads are solar and transmission heat gains through the west wall and glass, and the roof. From these , glass and roof loads are the predominant loads. The roof load is maximum at 6 p.m., when the equivalent temperature differential is 30.5 ^{o}C. The solar gain through the west glass has a maximum value of 508 W/m^2 at 4 p.m. Thus the time of maximum load is most likely to be near 5 p.m. Heat transfer through floor :

Assuming a wind velocity of 15 kmph, we have

$$\Delta p = 0.00047\ (15)^2 = 0.11 \text{ cm } H_2O$$

Inflitration rate for windows, from table 18.11 for 0.11 cm wind pressure, [29]

$$= 2.5 \text{ m}^3\text{/h/m crack}$$

Length of crack for 4 windows = 4[2(1 +1.5)] = 20 m

Occupancy load, from table [29]

SHL = 75 W/person

LHL = 55 W/person

Ventilation rate for office

Q_v /person = 0.28 cmm (Table 16.2[29])

Q_v = 0.28 x 10 = 2.8 cmm

4.1.5 Calculation Sheet for Cooling Load Estimation: [29]

SPACE USED FOR OFFICE
SIZE 10 X 5 = 50 m^2 X 4 = 200 m^3

ESTIMATION FOR 5 P.M. LOCAL TIME
HOURS OF OPERATION DAY TIME

CONDITIONS	DB	WB	%RH	DP	H, kJ/kg	w, kg/kg
OUTDOOR	43	27	29	21.3	85.0	0.016
ROOM	25	18	50	15.7	50.85	0.01
DIFFERENCE	18				34.15	0.006

10 PEOPLE X 0.28 cmm/PERSON = 2.8 cmm
VENTILATION cmm = 2.8

DOORS 2 DOORS X 3 m^2 1.9813 cmm/m^2 = 11.88 cmm
CRACK 20 m X 2.5/60 cmm/m^2 = 0.83 cm
INFILTRATION cmm = 11.88 + 0.83 = 12.71

SENSIBLE HEAT GAIN

ORIENTATION	AREA (m^2)	SOLAR GAIN GLASS	FACTOR	W
EAST GLASS				
WEST GLASS				
NORTH GLASS	3	91		270
SOUTH GLASS	3	32		96
TOTAL Q1				**366**

LOAD CALCULATIONS				
ITEM	**AREA OR QUANTITY**	**SUN GAIN OR TEMP. DIFF. OR HUMIDITY DIFF.**	**FACTOR**	**W**
SOLAR TRANSMISSION GAIN – WALLS AND ROOF				
EAST WALL				
WEST WALL	40	16.5	3.77	2490
NORTH WALL	14	11.3	5.9	934
SOUTH WALL	14	17.4	5.9	1437
ROOF	50	29.7	3.3	4900
TOTAL Q2				**9760**
TRANSMISSION GAIN - OTHERS				
DOORS	3	18	0.63	34
ALL GLASS	6	18	5.9	637
FLOOR	50	2.5	3.9	488
INFILTRATION	12.71	18	20.4	4667
TOTAL Q3				**5826**
INTERNAL HEAT GAIN				
PEOPLE	10		140	1400
LIGHTS	6		40	240
FAN	2		100	200
MACHINES	1		340	340
ADDITIONAL				320
TOTAL Q4				**2500**

TOTAL Q	**Q = Q1 + Q2 + Q3 + Q4 = 366 + 9760 + 5826 + 2500**			**18452**
SAFETY FACTOR			5%	923
ROOM SENSIBLE HEAT (RSH)				19375
OUTDOOR AIR BYPASSED	2.8 cmm	18	20.4 x 0.15	154
EFFECTIVE ROOM SENSIBLE HEAT (ERSH)				**19530**
LATENT HEAT				
INFILTRATION	12.71	0.006	50000	3813
PEOPLE	10		55	550
STEAM				
APPLIANCE				
SUB TOTAL				4363
SAFETY FACTOR		5%		218
ROOM LATENT HEAT (RLH)				4580
OUTDOOR AIR BYPASSED	2.8 cmm	0.006	50000 X 0.15	126
EFFECTIVE ROOM LATENT HEAT (ERLH)				**4706**
GRAND TOTAL HEAT = ERSH + ERLH = 19530 + 4706 = 24236				
GRAND TOTAL HEAT = 24236/3517 = 6.89 TR = (25 kW) approx.				

4.2 Calculation for the Half-Effect System (HVARS):

The computer program is coded in Engineering Equation Solver (EES) for the thermodynamic analysis of HVARS. The coded program and its output have been attached in the Appendix [A].

In the analysis of this cycle the following assumption is considered
1. The pumping is isentropic
2. Across Solution expansion valve entropy change is neglected and temperature is also constant.

4.2.1 Input Parameters:

The following are the input parameters to half effect system:

Condenser Temperature	TC = 38^{o}C
Evaporator Temperature	TE = 7^{o}C
High Pressure side Generator Temperature	Tgh = 80^{o}C
Low Pressure side Generator Temperature	Tgl = 80^{o}C
High Pressure side Absorber Temperature	Tah = 38^{o}C
High Pressure side Absorber Temperature	Tah = 38^{o}C
Refrigeration Capacity	Qe = 25 kW
Intermediate Pressure	Pi = 4.953 kPa
Effectiveness of high pressure side solution heat exchanger	EHXh = 0.7
Effectiveness of low pressure side solution heat exchanger	EHXl = 0.7

4.3 Calculation of Flat Plate Collector:

4.3.1 Flat Plate Collector Specifications:

Dimensions = 2.005mm x 1.505mm
Gross Area (A_F) = 3 m^2
Efficiency (K) = 0.85
Cost = Rs. 6000

The specifications of flat plate collector are shown in Appendix [B].

4.3.2 Calculation of Area of Flat Plate Collector

4.3.2.1Calculation of Area of Flat Plate Collector for High pressure Generator :

Heat required in the high pressure generator of the system,

Qgh = 27.48 kW
= 27480 W

Hence, the approx. area of the flat plate collector necessary for providing this much amount of energy is given by

= 27480 / (250 × K)
= 27480 / (250 × 0.85)
= 129.32 m^2
= 130 m^2

Area of Flat Plate collector used in high pressure side (Ah)

Ah = 130 m^2

4.3.2.2 Calculation of Area of Flat Plate Collector for Low pressure Generator :

Heat required in the low pressure generator of the system,

Qgl = 32.65 kW
= 32650 W

Hence, the approx. area of the flat plate collector necessary for providing this much amount of energy is given by

$= 32650 / (250 \times K)$
$= 32650 / (250 \times .85)$
$= 153.6\ m^2$
$= 154\ m^2$

Area of Flat Plate collector used in Low pressure side (Al)

$Al = 154\ m^2$

4.3.2.3 Total Area of Flat Plate Collector (A)

$A = Ah + Al$
$A = 130 + 145$

$A = 284\ m^2$

4.3.3 Number of Flat Plate Collectors required

Number of Flat Plate Collectors required in High Pressure Side (N1)

$N1 = Ah / A_F = 130/3 = 43.33$

N1 = 44 Plates

Number of Flat Plate Collectors required in Low Pressure Side (N2)

$N2 = Al / A_F = 154/3 = 51.33$

N1 = 52 Plates

4.4 Cost analysis and Payback Period Calculation:

4.4.1 Assumptions :

- The cost of two systems is calculated on the basis that the office space required cooling for 8 hours per day.
- The cost of flat plate collector installation is the only cost considered for the calculation of payback period of HVARS.
- The costs of component of the two systems are considered to be same.
- The cost of compressor of VCRS is compensated by the cost of generator used in HVARS.
- Maintenance cost is negligible.
- The rate of electricity are taken from the Uttarakhand Electricity Regulatory Commission, shown in Appendix [C]

4.4.2 Calculation :

Step 1 : Find out the power consumption of the device in kilowatts (kW)

Power consumed in by compressor in VCRS (P) = 15.2 kW.

Step 2 : Estimate how long the device will be used for each day.

Hours used per day (h) = 8 hours

Step 3 : Multiply the power consumption by the number of hours, to get the energy use per day in kilowatt hours (kWh).

Energy consumption per day (E_d) = Power consumed x Hours used per day

$E_d = P \times h = 15.23 \times 8$

$E_d = 121.84$ kWh/day

Step 4 : Multiply this by the number of days in a year (365).

Energy consumption per year (E) = E_d x 365 (kWh/day x days in year)

$= 121.84 \times 365$

$E = 44471.6$ kWh

Step 5 : Calculate the cost of this energy,

The average cost of electricity approved by the Uttarakhand Electricity Regulatory Commission shown in Appendix [C]:

Fixed / Demand charges (per month) = Rs. 30 per kW

Cost of Fixed charges for a year (C_F) = 30 x 25 x12 = Rs. 9000

Energy charges = Rs.4.40 per kWh.

Cost of Energy charges for a year (C_E) = 44471.6 x 4.40 = Rs.195675

Expenditure per year = $C_F + C_E$ = 9000 + 195675 = Rs. 204675

This is the running cost of VCRS for a year:

(C_{VCRS}) = Rs. 204675 (Rs. 2.05 lakhs approx.)

Step 6 : Cost of HVARS

Cost of Flat Plate Collectors required in High Pressure Side (C1)

C1 = N1 x 6000
C1 = Rs. 264000

Cost of Flat Plate Collectors required in Low Pressure Side (C2)

C2 = N2 x 6000
C2 = Rs. 312000

Total Cost (C) = C1 + C2

C = Rs. 576000

Total cost of Flat Plate Collector required = Rs 5.76 Lakhs.

This is the only cost which is considered to cool the given space, thus it is considered to be the cost of cooling of HVARS and is given by C_{HVARS} .

C_{HVARS} = Rs. 576000.

Step 7 : Payback Period

Payback Period = Cost of HVARS / Expenditure per year of VCRS

Payback Period **= 576000 / 204675 = 2.8**

Payback Period = 2.8 (Years)

CHAPTER 5

RESULTS AND DISCUSSION

The energy and exergy analysis of the solar driven half effect water lithium bromide vapour absorption system (HVARS) is done. .A computer program was written for thermodynamic analysis of HVARS. The program was based on the exergy balance, energy balance, and thermodynamic properties for each reference point of the system. The mathematical model for solar driven water-lithium bromide half effect vapour absorption air conditioning system has been developed and the parametric study of system is done.

The initial conditions are granted into the program containing the ambient conditions, the solar energy collector parameter designation, the component temperatures, effectiveness of heat exchangers and evaporator load etc. With these granted parameters, the thermodynamic properties at all the respective points in the system were calculated. The results possessed from the present study may be presented as follows.

5.1 Results from cooling load calculation:

- The cooling load calculation of the office space was carried out on 21st of June in Dehradoon, Uttarakhand India (Latitude 30°N). The estimated capacity of the office space (Q_e), comes out to be 25 kW (approx), Which is one of the input parameter to the solar driven half effect water lithium bromide vapour absorption system (HVARS).

5.2 Results from parametric study of HVARS:

- **5.2.1 Effect of generator temperature (TG in °C) for different temperature of condenser (TC)** :

  - **COP:** The variation of COP with generator temperature is shown in Figure 5.1. The high values of COP are hold at high generator temperature and low condenser temperature. For a assumed condenser and evaporator temperature, there is a minimum temperature of generator, which address to the maximum COP. It should be noticed that the COP initially show the significant increase with an increase of generator temperature, and then the slope of the COP curves gets almost flat. In other words, increasing the generator temperature higher than a fixed value does not contribute to much improvement for the COP.

  - **Exergetic Efficiency:** The change of exergetic efficiency with generator temperature for a half-effect vapour absorption cooling system at distinct condenser temperatures is shown in Figure 5.2. Exergetic efficiency enhances with an increment in the generator temperature up to a certain limit of generator temperature (for a assumed

evaporator, absorber and condenser temperature, there is a minimum temperature of generator which corresponds to a maximum value of exergetic efficiency) and then it decreases.

- **Overall Efficiency of the global system :** The variation of overall efficiency with evaporator temperature is shown in Figure 5.3. The high values of overall efficiency are hold at high generator temperature and low condenser temperature. For a assumed condenser and evaporator temperature, there is a minimum temperature of generator, which address to the maximum overall efficiency. It should be noticed that the overall efficiency initially show the significant increase with an increase of generator temperature, and then the slope of the overall efficiency curves gets almost flat. In other words, increasing the generator temperature higher than a fixed value does not contribute to much improvement for the overall efficiency.

- **Total Exergy Destruction :** The change of total exergy loss with generator temperature for cooling at distinct condenser temperatures is shown in Figure 5.4. The entire exergy loss of the absorption cooling system drops keenly to a minimum value with an increase in temperature of generator and then further increases. For a given condenser temperature there is a generator temperature at which the total exergy loss of the absorption cooling system will be minimum which address to a maximum value of COP and the exergetic efficiency. In the present study, Where the evaporator temperature is maintained fixed at 7°C and condenser temperature is changed from 30°C and 46°C and generators temperatures are changed from 60°C to 80°C the maximum value of COP is 0.4157 and the maximum value of exergetic efficiency is around 7.36%.

- **Exergy Destruction Ratio :** The change of exergy destruction ratio with generator temperature for cooling at distinct condenser temperatures is shown in Figure 5.5. The entire exergy loss of the absorption cooling system drops keenly to a minimum value with an increase in temperature of generator and then further increases. For a given condenser temperature there is a generator temperature at which the exergy destruction ratio of the absorption cooling system will be minimum which address to a maximum value of COP and the exergetic efficiency.

- **Heat supplied in High pressure Generator (Q_{gh}) :** The variation of heat supplied to the high pressure generator with generator temperature is shown in Figure 5.6. As the generator temperature increases the Q_{gh} increases linearly. When the condenser temperature is increased the value of Q_{gh} also increases. . In the present study, where the evaporator temperature is maintained fixed at 7°C and condenser temperature is 38°C, generators temperature is 80°C the value of Q_{gh} is 27.48 kW.

- **Heat supplied in High pressure Generator (Q_{gl}) :** The variation of heat supplied to the low pressure generator with generator temperature is shown in Figure 5.7. The

Q_{gl} of the absorption cooling system drops keenly to a minimum value with an increase in temperature of generator and then further it approximately remains constant. In the present study, where the evaporator temperature is maintained fixed at 7°C and condenser temperature is 38°C, generators temperature is 80°C the value of Q_{gl} is 32.65 kW.

- **High Pressure side solution circulation ration (SCRh) :** The variation of (SCRh) is shown in Figure 5.5. At lower value of condenser temperature (say 38°C), the value of SCRl remains constant with the increase in generator temperature. As the value of condenser temperature increases the value of SCRh decreases slightly with the increase in generator temperature.

- **Low Pressure side solution circulation ration (SCRl) :** The variation of SCRl is shown in Figure 5.9. The SCRl of the absorption cooling system drops keenly to a minimum value with an increase in temperature of generator and then further it approximately remains constant. For a given condenser temperature there is a generator temperature at which the SCRl of the absorption cooling system will be minimum which address to a maximum value of COP and the exergetic efficiency.

- **Area of flat plate collector on High Pressure side (Ah) :** The variation of Area of flat plate collector on high pressure side is shown in Figure 5.10. As the generator temperature increases the Ah increases linearly. When the condenser temperature is increased the value of Ah also increases. In the present study, where the evaporator temperature is maintained fixed at 7°C and condenser temperature is 38°C, generators temperature is 80°C the value of Ah is 130 m^2.

- **Area of flat plate collector on Low Pressure side (Al) :** The variation of Area of flat plate collector on low pressure side is shown in Figure 5.11. The Al of the absorption cooling system drops keenly to a minimum value with an increase in temperature of generator and then further it approximately remains constant. In the present study, where the evaporator temperature is maintained fixed at 7°C and condenser temperature is 38°C, generators temperature is 80°C the value of Al is 154 m^2.

- **Total Area of flat plate collector (A) :** The variation of Total Area of flat plate collector is shown in Figure 5.12. The A of the absorption cooling system drops keenly to a minimum value with an increase in temperature of generator and then further it approximately remains constant. In the present study, where the evaporator temperature is maintained fixed at 7°C and condenser temperature is 38°C, generators temperature is 80°C the value of A is 284 m^2.

- **5.2.2 Effect of evaporator temperature (TE in °C) for different temperature of condenser (TC)** :

  - **COP :** The variation of COP with evaporator temperature is shown in Figure 5.13. With the increase in evaporator temperature , the evaporator pressure increases also the COP of the system increases due to the reduction in the solution circulation ratios in both high and low pressure stages. This tends to reduce the heat supplied in both the generators of the two stages. As the condenser temperature increases the COP of the system decreases.

  - **Exergetic Efficiency :** The variation of exergetic efficiency with evaporator temperature is shown in Figure 5.14. With the increase in evaporator temperature, the exergetic efficiency of the system decreases. As the condenser temperature increases the exergetic efficiency further decreases following the same trend.

  - **Overall Efficiency of the global system:** The variation of overall efficiency with evaporator temperature is shown in Figure 5.15. With the increase in evaporator temperature, the evaporator pressure increases also the overall efficiency of the system increases due to the reduction in the solution circulation ratios in both high and low pressure stages. This tends to reduce the heat supplied in both the generators of the two stages. As the condenser temperature increases the overall efficiency of the system decreases.

  - **Total Exergy Destruction:** The change of total exergy loss with evaporator temperature for cooling at distinct condenser temperatures is shown in Figure 5.16. The entire exergy loss of the absorption cooling system drops gradually to a minimum value with an increase in temperature of evaporator and then it further remains constant. As the condenser temperature increases the total exergy loss of the system increases.

  - **Exergy Destruction Ratio:** The variation of exergy destruction ratio with evaporator temperature for cooling at distinct condenser temperatures is shown in Figure 5.17. The exergy destruction ratio of the absorption cooling system drops keenly to a minimum value with an increase in temperature of evaporator and then it further increases. As the condenser temperature increases the exergy destruction ratio of the system increases.

  - **Heat supplied in High pressure Generator (Q_{gh}):** The variation of heat supplied to the high pressure generator is shown in Figure 5.15. As the evaporator temperature increases the Q_{gh} remains constant. When the condenser temperature is increased the value of Q_{gh} also increases.

- **Heat supplied in High pressure Generator (Q_{gl}) :** The variation of heat supplied to the low pressure generator is shown in Figure 5.19. The Q_{gl} of the absorption cooling system drops gradually with an increase in temperature of evaporator.

- **High Pressure side solution circulation ration (SCRh) :** The variation of (SCRh) is shown in Figure 5.20. The value of SCRl remains constant with the increase in generator temperature. As the condenser temperature increases the value of SCRl increases.

- **Low Pressure side solution circulation ration (SCRl) :** The variation of SCRl is shown in Figure 5.21. The SCRl of the absorption cooling system drops with an increase in temperature of evaporator. As the condenser temperature increases the value of SCRl increases.

- **Area of flat plate collector on High Pressure side (Ah) :** The variation of Area of flat plate collector on high pressure side is shown in Figure 5.22. As the evaporator temperature increases the Ah remains constant. When the condenser temperature is increased the value of Ah also increases.

- **Area of flat plate collector on Low Pressure side (Al) :** The variation of Area of flat plate collector on low pressure side is shown in Figure 5.23. The Al of the absorption cooling system drops gradually with an increase in temperature of evaporator.

- **Total Area of flat plate collector (A) :** The variation of Total Area of flat plate collector is shown in Figure 5.24. The A of the absorption cooling system drops gradually with an increase in temperature of evaporator.

➢ 5.2.3 Effect of Effectiveness of high pressure side heat exchanger (EHXh) :

- **COP**: The variation of COP with Effectiveness of high pressure side heat exchanger (EHXh) is shown in Figure 5.25. As the EHXh increases the COP of the system increases linearly. In the present study, the value of EHXh is assumed to be 0.7.

- **Exergetic Efficiency:** The variation of exergetic efficiency with evaporator temperature is shown in Figure 5.26. As the EHXh increases, the exergetic efficiency of the system increases linearly.

- **Overall Efficiency of the global system:** The variation of COP with Effectiveness of high pressure side heat exchanger (EHXh) is shown in Figure 5.27. As the EHXh increases the COP of the system increases linearly.

5.2.4 Effect of Effectiveness of low pressure side heat exchanger (EHXl) :

- **COP**: The variation of COP with Effectiveness of high pressure side heat exchanger (EHXl) is shown in Figure 5.25. As the EHXl increases the COP of the system increases linearly. In the present study, The value of EHXl is assumed to be 0.7.

- **Exergetic Efficiency:** The variation of exergetic efficiency with evaporator temperature is shown in Figure5.29. As the EHXl increases, the exergetic efficiency of the system increases linearly.

- **Overall Efficiency of the global system :** The variation of COP with Effectiveness of high pressure side heat exchanger (EHXl) is shown in Figure 5.30. As the EHXl increases the COP of the system increases linearly.

5.2.5 Effect of intermediate pressure :

- **COP** : The variation of COP with intermediate pressure is shown in Figure 5.31. As the intermediate pressure increases, the COP of the system first increases reaches to the maximum value and then starts decreasing. The intermediate pressure is optimized to maximize the COP of the system. The optimum intermediate pressure is calculated to be 4.9537 kPa.

- **Exergetic Efficiency :** The variation of exergetic efficiency with intermediate pressure is shown in Figure 5.32. As the intermediate pressure increases, the exergetic efficiency of the system first increases reaches to the maximum value and then starts decreasing.

- **Overall Efficiency of the global system :** The variation of overall efficiency with intermediate pressure is shown in Figure 5.33. As the intermediate pressure increases, the overall efficiency of the system first increases, reaches to the maximum value and then starts decreasing.

5.2.6 Effect of intermediate pressure :

The Intermediate pressure is optimized for the given input parameters by using the Golden section approach in EES. The optimum Intermediate pressure comes out to be 4.953 kPa

5.2.7 Thermodynamic state at each point :

The Table 5.1. shows the thermodynamic state of each point of the solar driven half effect water lithium bromide vapour absorption system (HVARS).

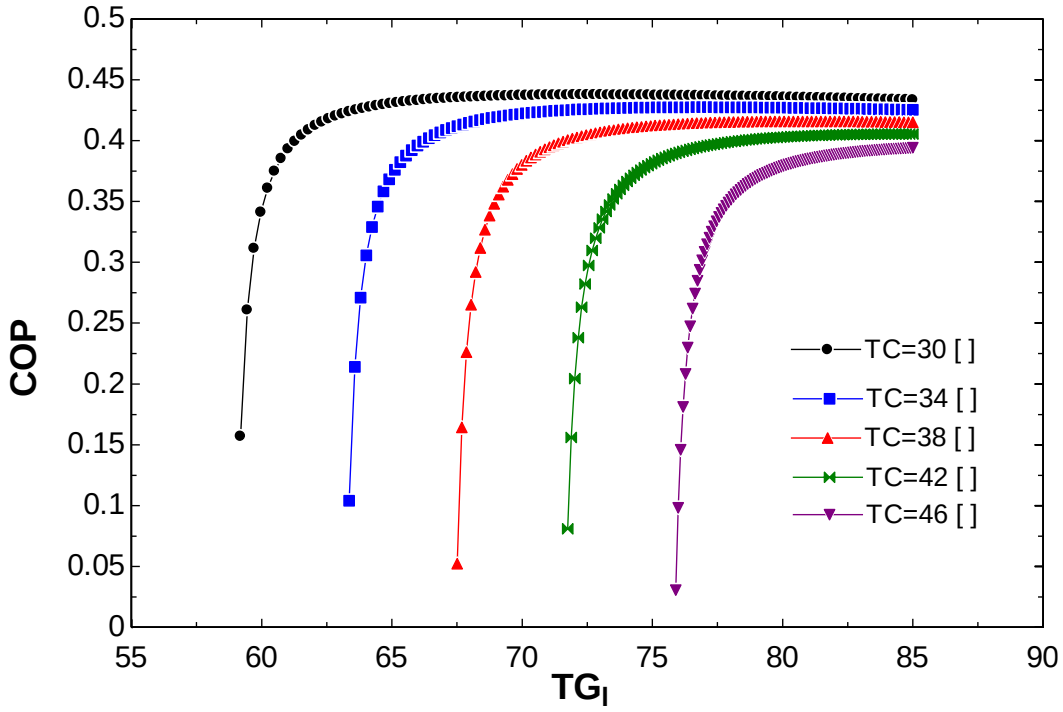

Figure 5.1-Coefficient of performance (COP) versus generator temperature (TG in °C) and condenser temperature (TC) at (TE = 7°C)

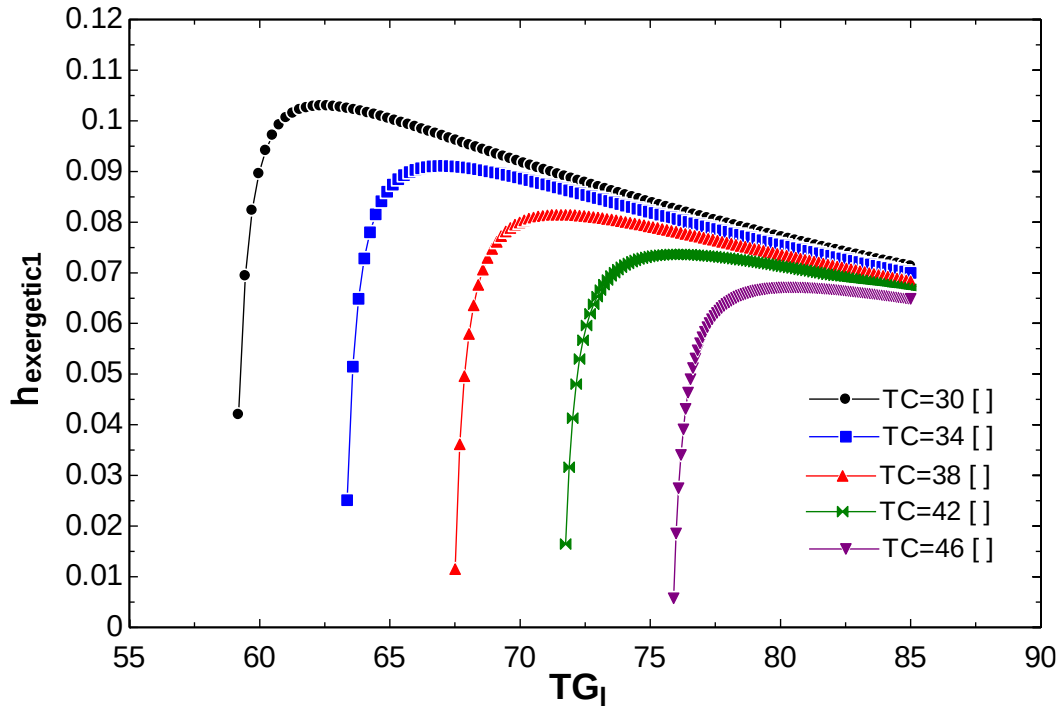

Figure 5.2-Exergetic Efficiency versus generator temperature (TG in °C) and condenser temperature (TC) at (TE = 7°C)

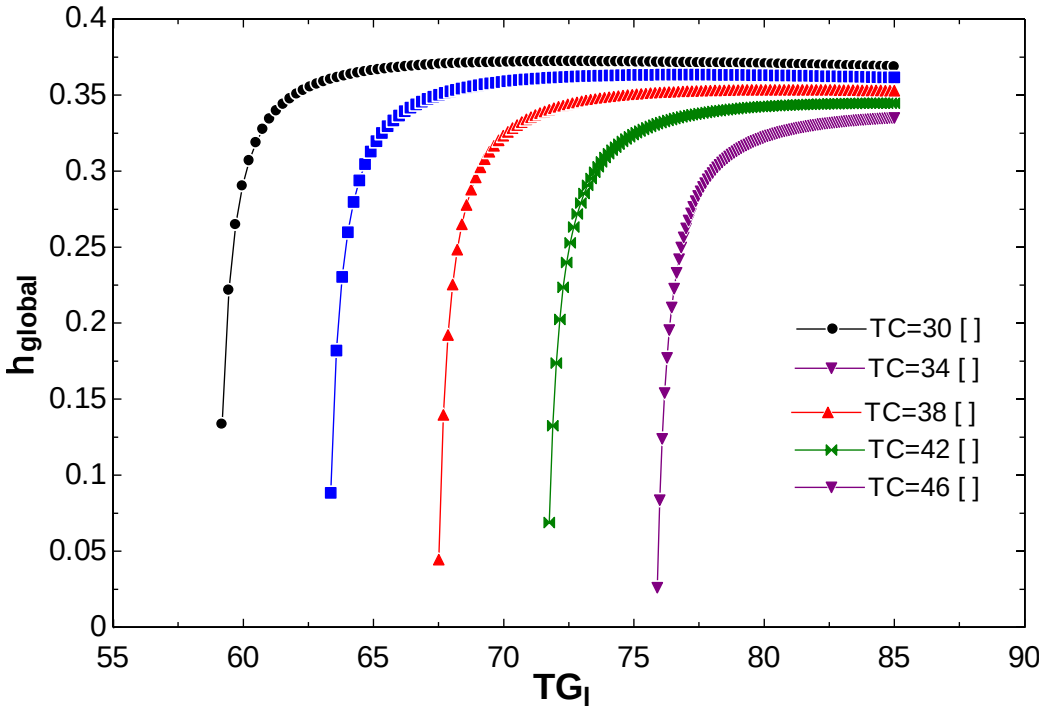

Figure 5.3-Overall Efficiency of the global system versus generator temperature (TG in °C) and condenser temperature (TC) at (TE = 7°C)

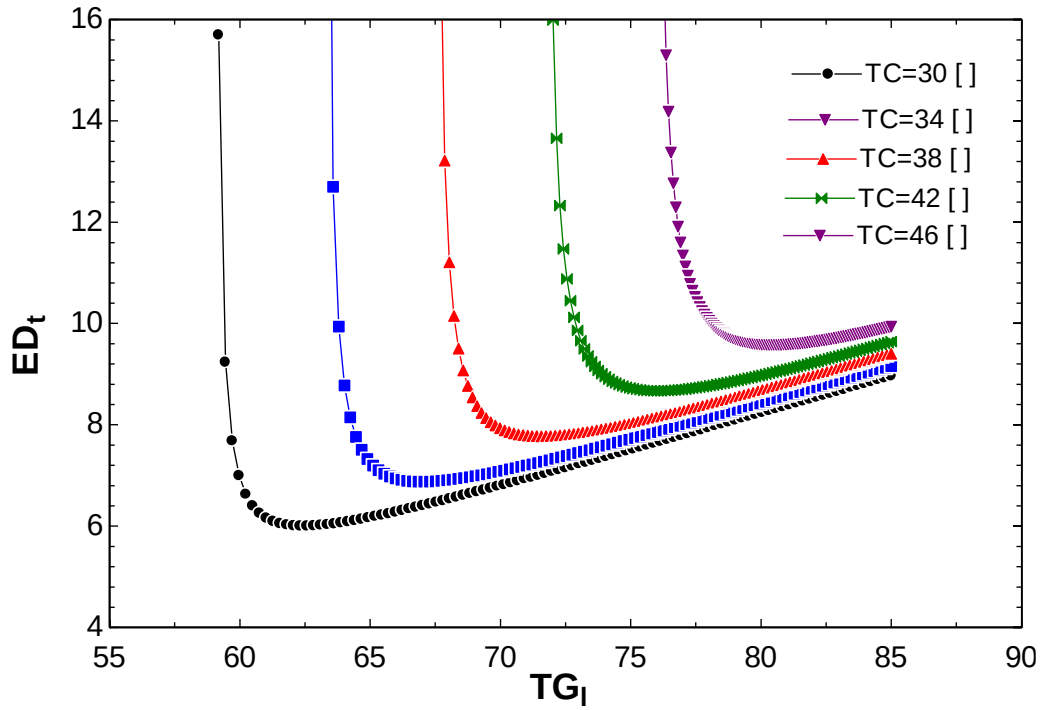

Figure 5.4-Total Exergy Destruction versus generator temperature (TG in °C) and condenser temperature (TC) at (TE = 7°C)

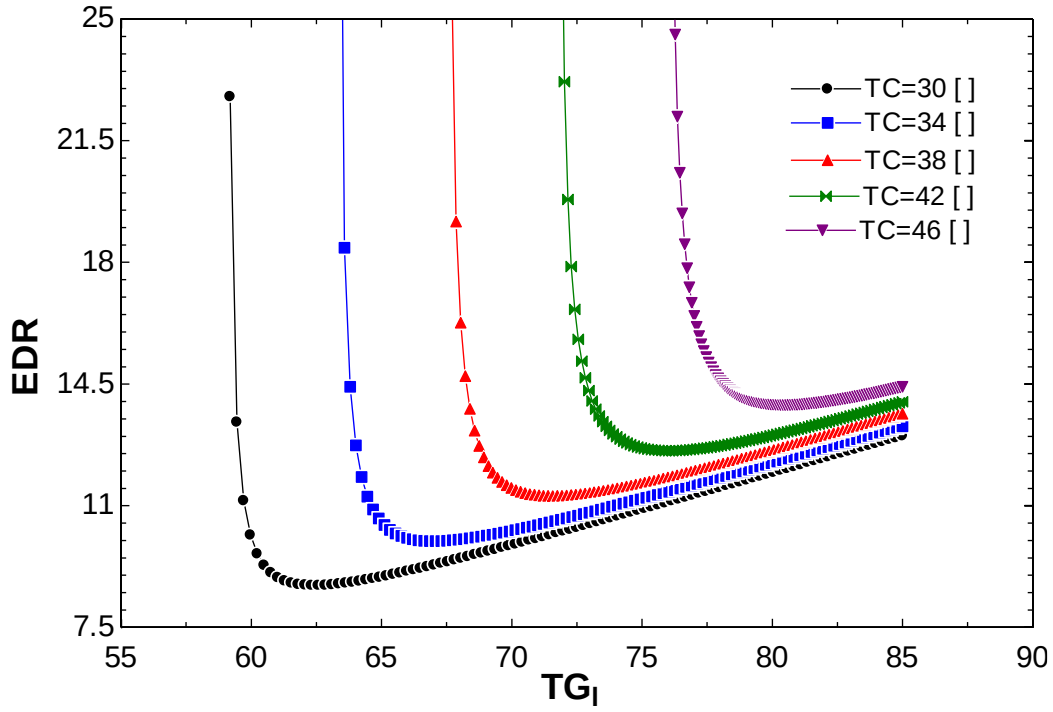

Figure 5.5-Exergy Destruction Ratio versus generator temperature (TG in °C) and condenser temperature (TC) at (TE = 7°C)

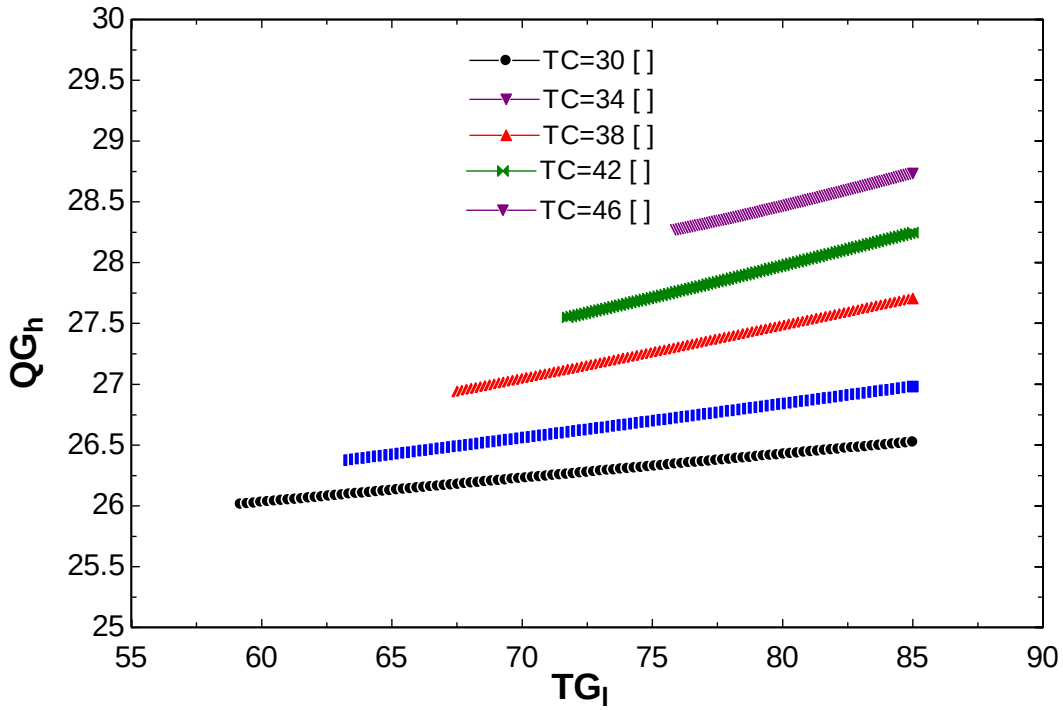

Figure 5.6-Heat supplied in High pressure Generator (Q_{gh} in kW) versus generator temperature (TG in °C) and condenser temperature (TC) at (TE = 7°C)

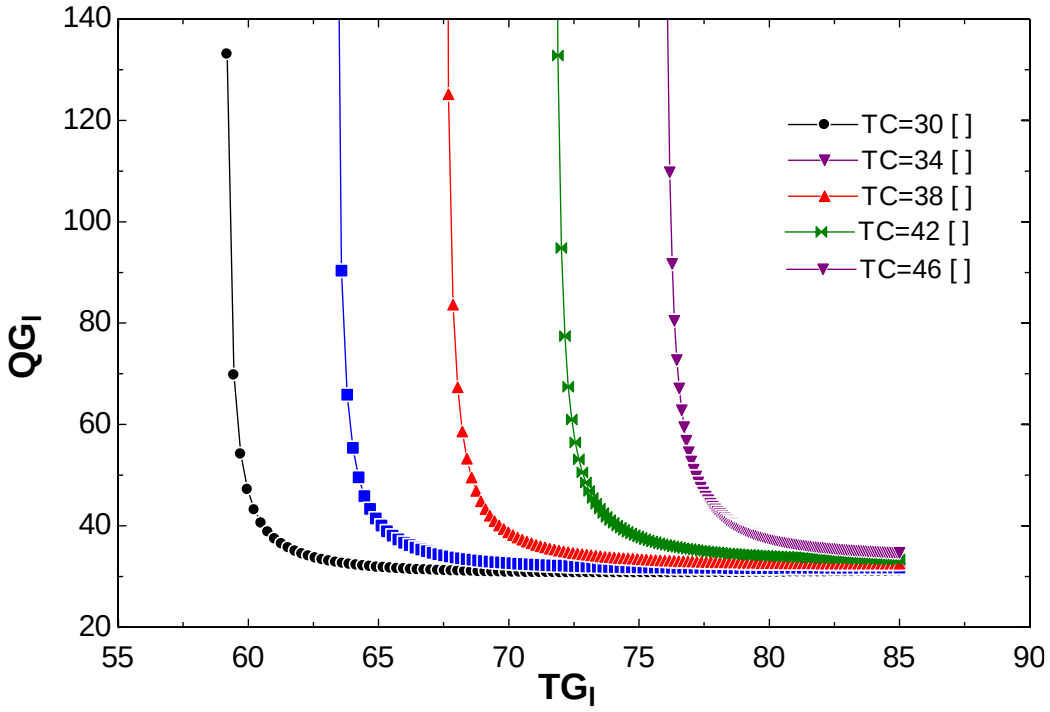

Figure 5.7-Heat supplied in High pressure Generator (Q_{gl} in kW) versus generator temperature (TG in °C) and condenser temperature (TC) at (TE = 7°C)

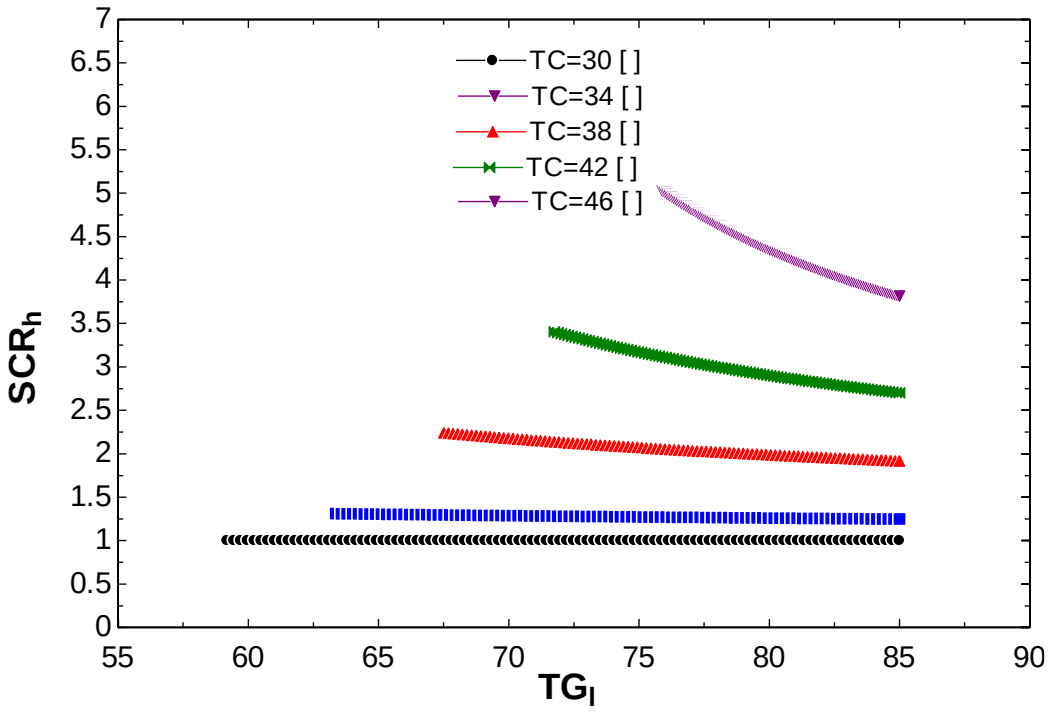

Figure 5.8-High Pressure side solution circulation ration (SCRh) versus generator temperature (TG in °C) and condenser temperature (TC) at (TE = 7°C)

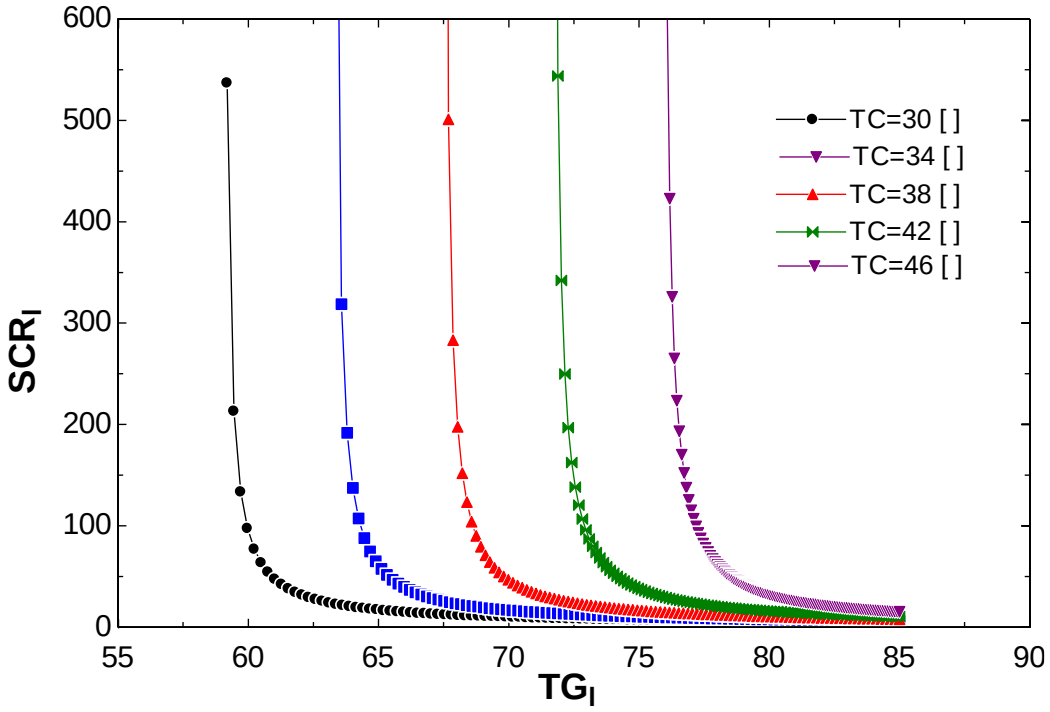

Figure 5.9-Low Pressure side solution circulation ration (SCRl) versus generator temperature (TG in °C) and condenser temperature (TC) at (TE = 7°C)

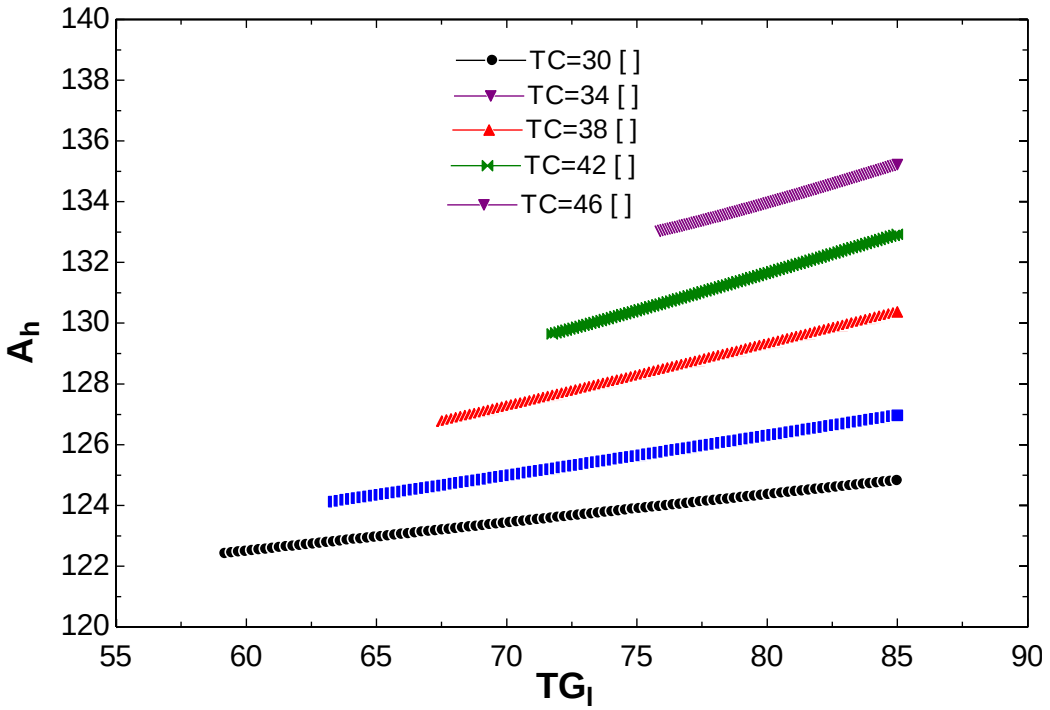

Figure 5.10-Area of flat plate collector on High Pressure side (Ah in m^2) versus generator temperature (TG in °C) and condenser temperature (TC) at (TE = 7°C)

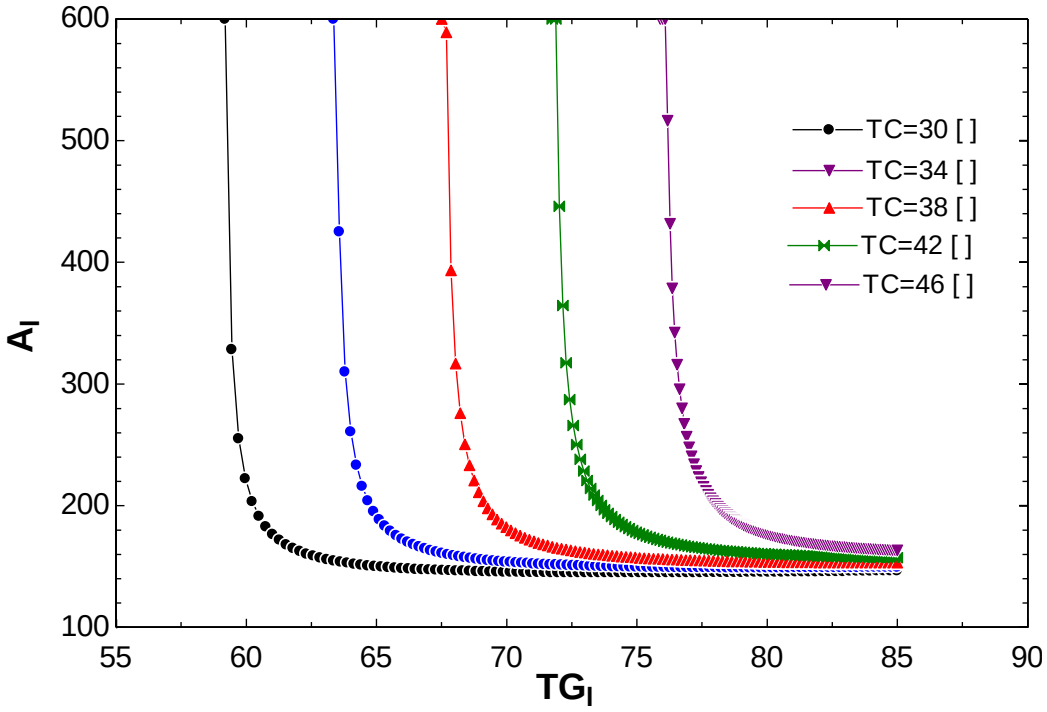

Figure 5.11-Area of flat plate collector on Low Pressure side (Al in m^2) versus generator temperature (TG in °C) and condenser temperature (TC) at (TE = 7°C)

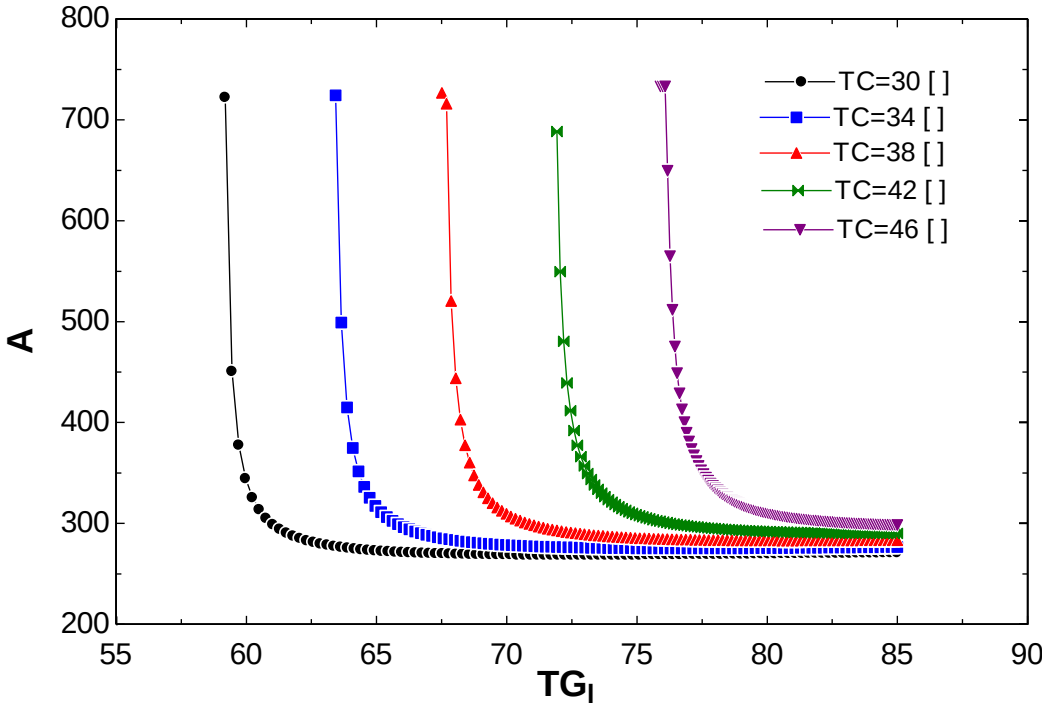

Figure 5.12-Total Area of flat plate collector (A in m^2) versus generator temperature (TG in °C) and condenser temperature (TC) at (TE = 7°C)

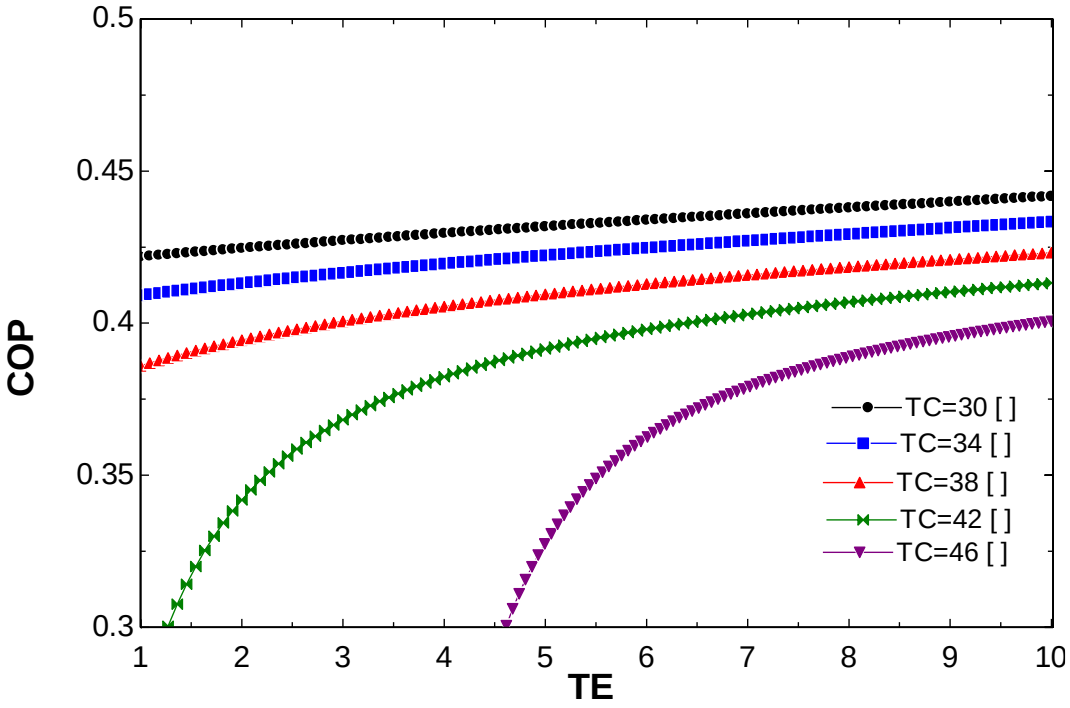

Figure 5.13-Coefficient of performance (COP) versus evaporator temperature (TE in °C) and condenser temperature (TC) at (TG = 80°C)

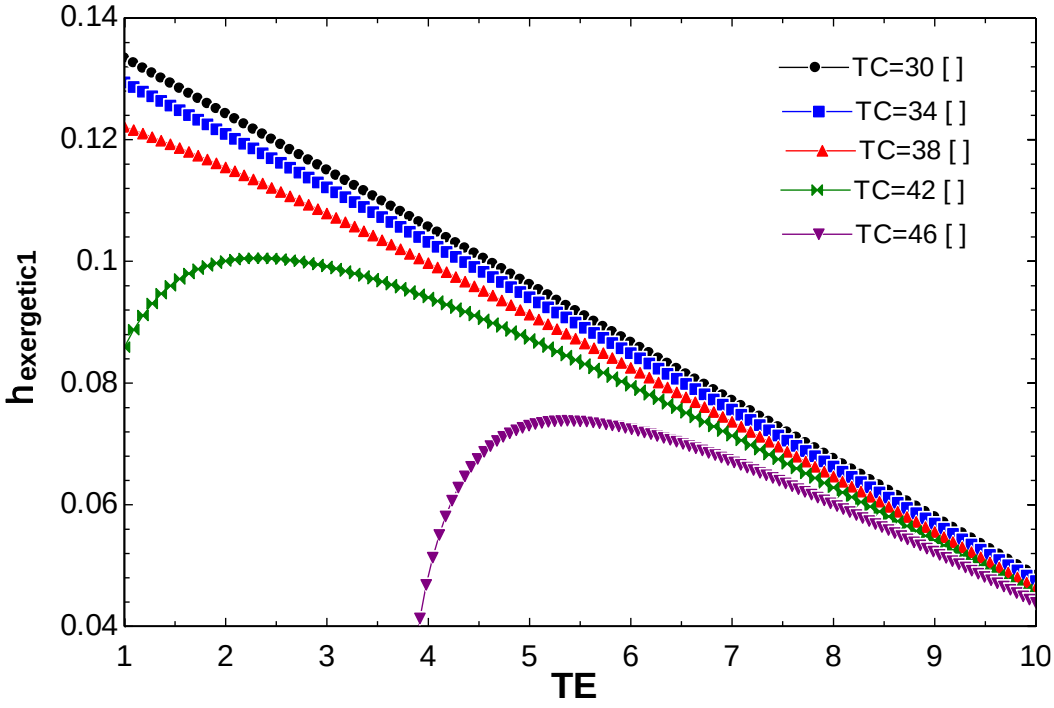

Figure 5.14-Exergetic Efficiency versus evaporator temperature (TE in °C) and condenser temperature (TC) at (TG = 80°C)

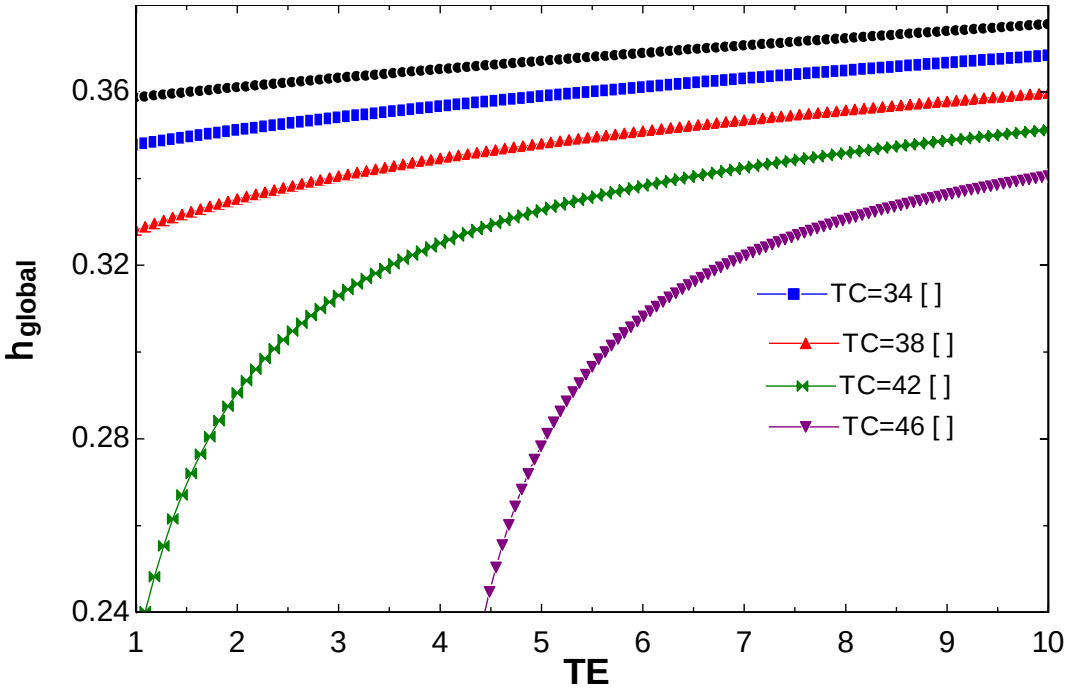

Figure 5.15-Overall Efficiency of the global system versus evaporator temperature (TE in °C) and condenser temperature (TC) at (TG = 80°C)

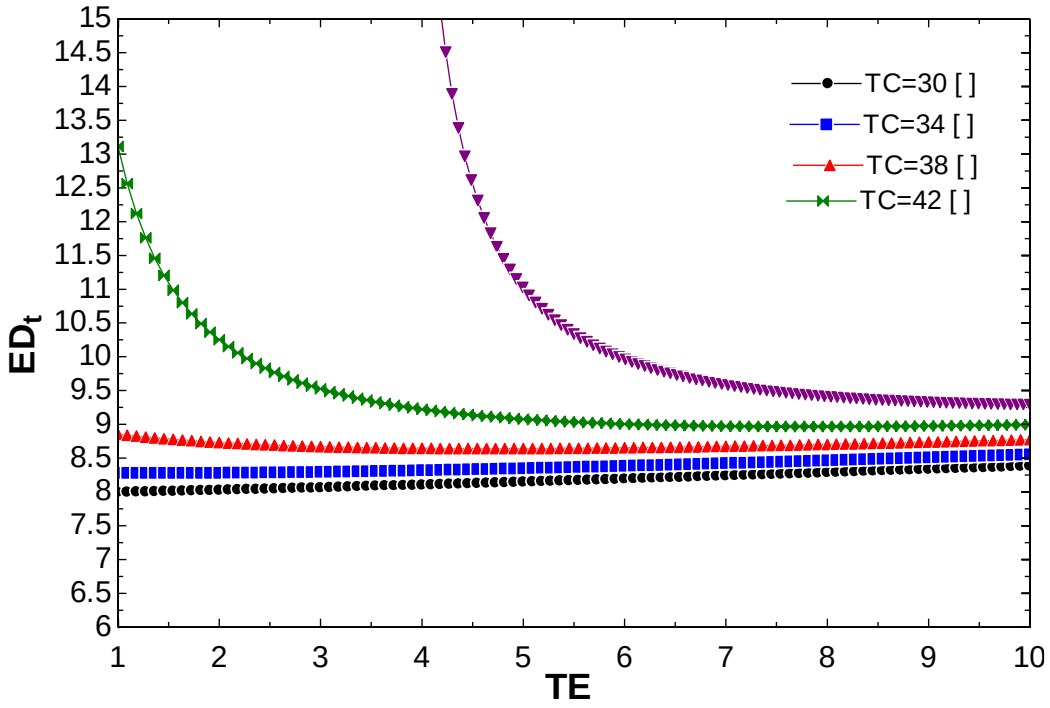

Figure 5.16-Total Exergy Destruction versus evaporator temperature (TE in °C) and condenser temperature (TC) at (TG = 80°C)

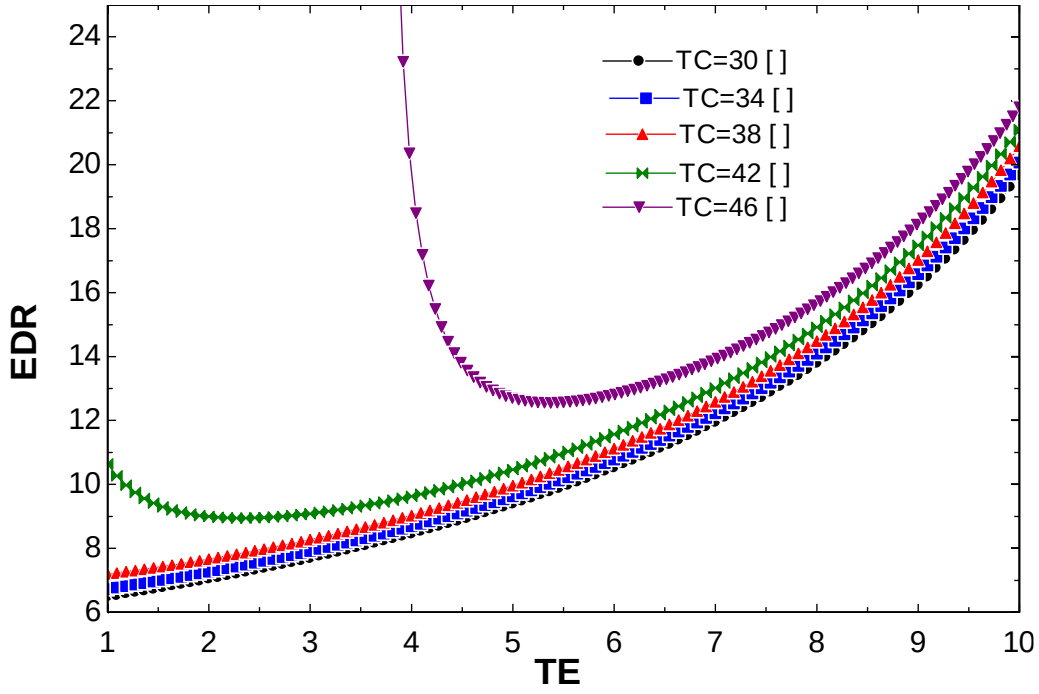

Figure 5.17-Exergy Destruction Ratio versus evaporator temperature (TE in °C) and condenser temperature (TC) at (TG = 80°C)

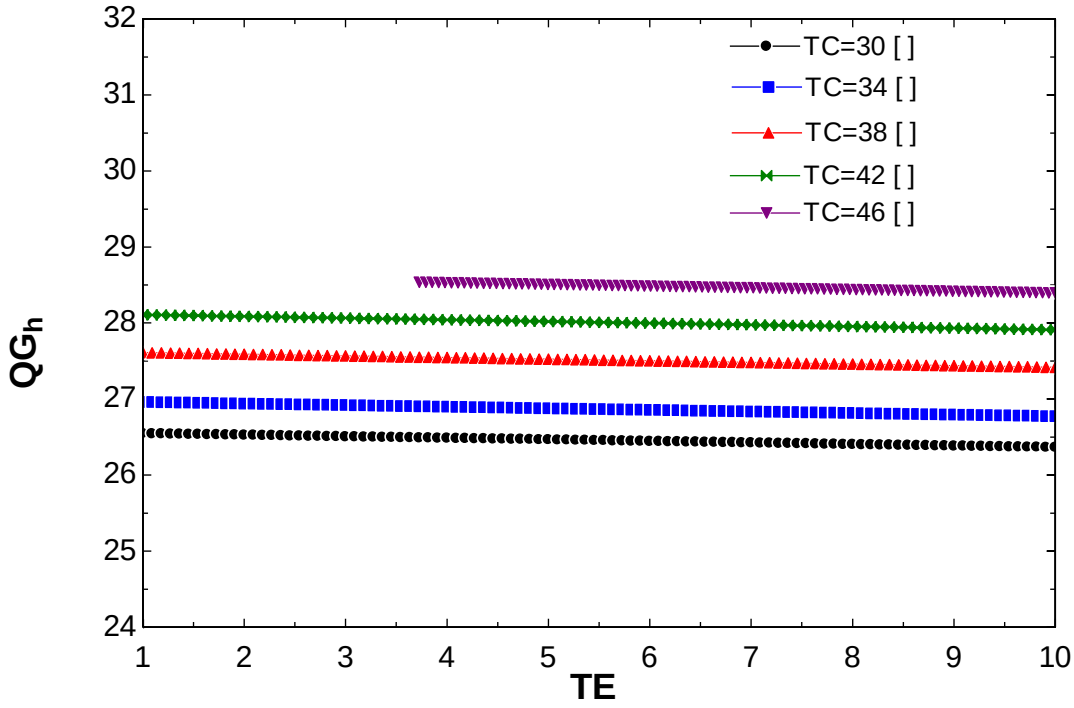

Figure 5.18-Heat supplied in High pressure Generator (Q_{gh} in kW) versus evaporator temperature (TE in °C) and condenser temperature (TC) at (TG = 80°C)

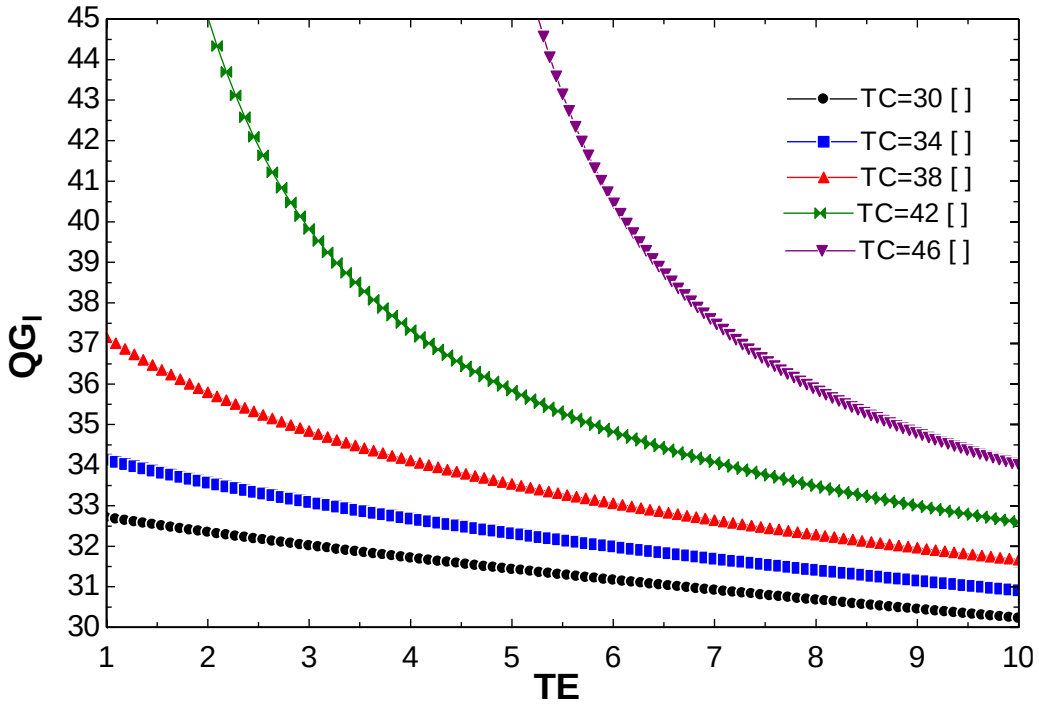

Figure 5.19-Heat supplied in High pressure Generator (Q_{gl} in kW) versus evaporator temperature (TE in °C) and condenser temperature (TC) at (TG = 80°C)

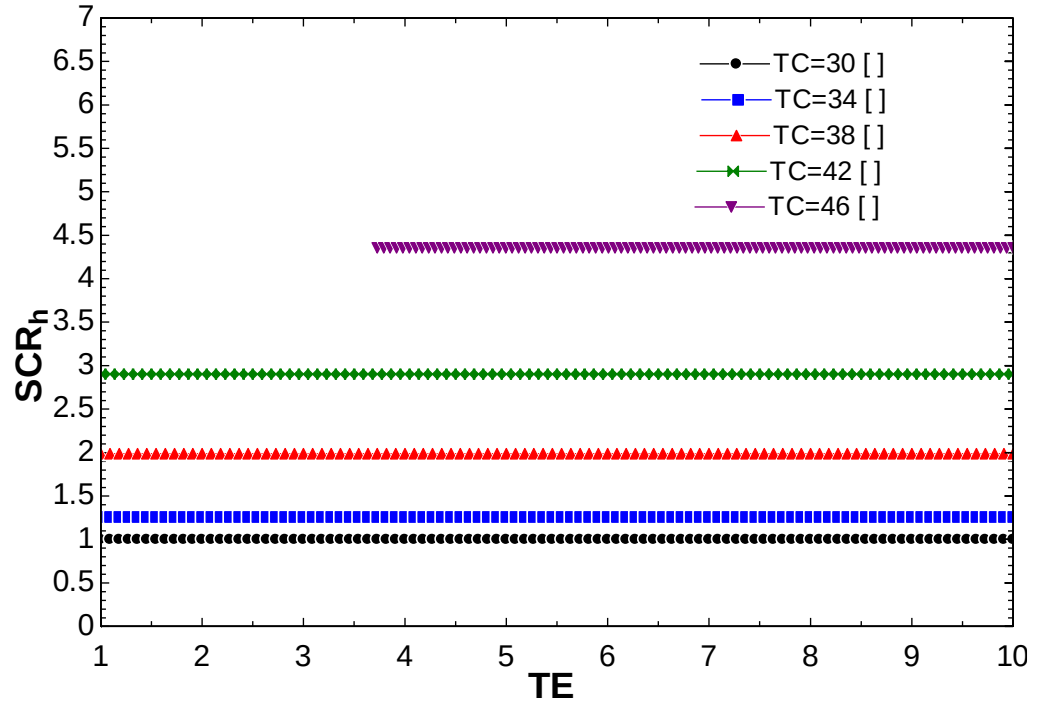

Figure 5.20-High Pressure side solution circulation ration (SCRh) versus evaporator temperature (TE in °C) and condenser temperature (TC) at (TG = 80°C)

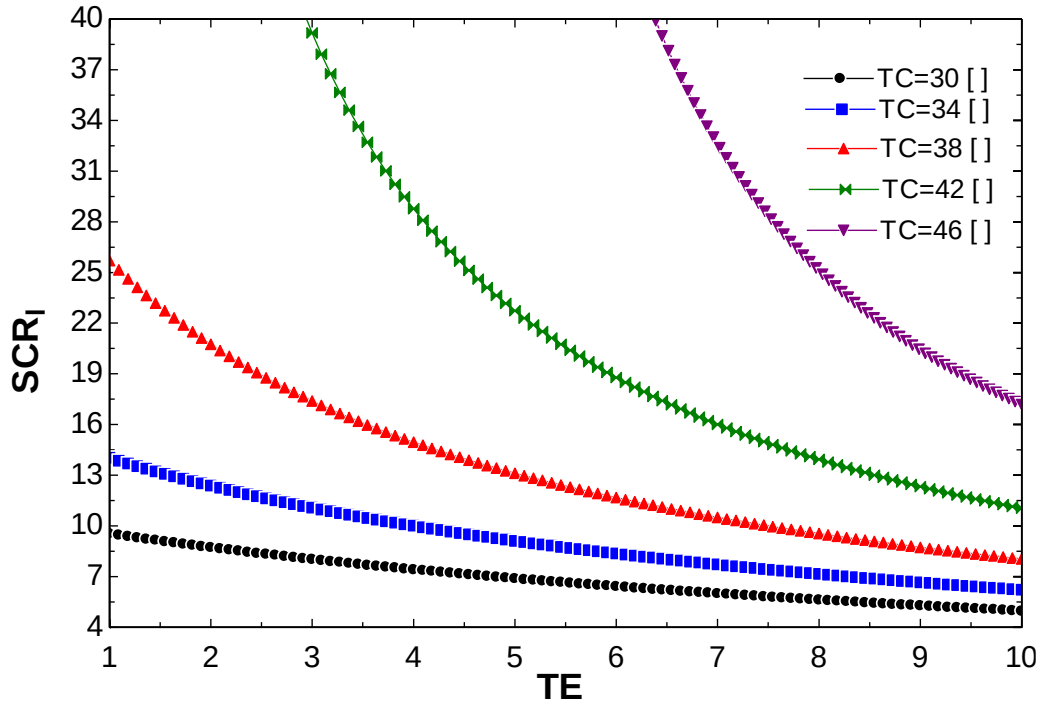

Figure 5.21-Low Pressure side solution circulation ration (SCRl) versus evaporator temperature (TE in °C) and condenser temperature (TC) at (TG = 80°C)

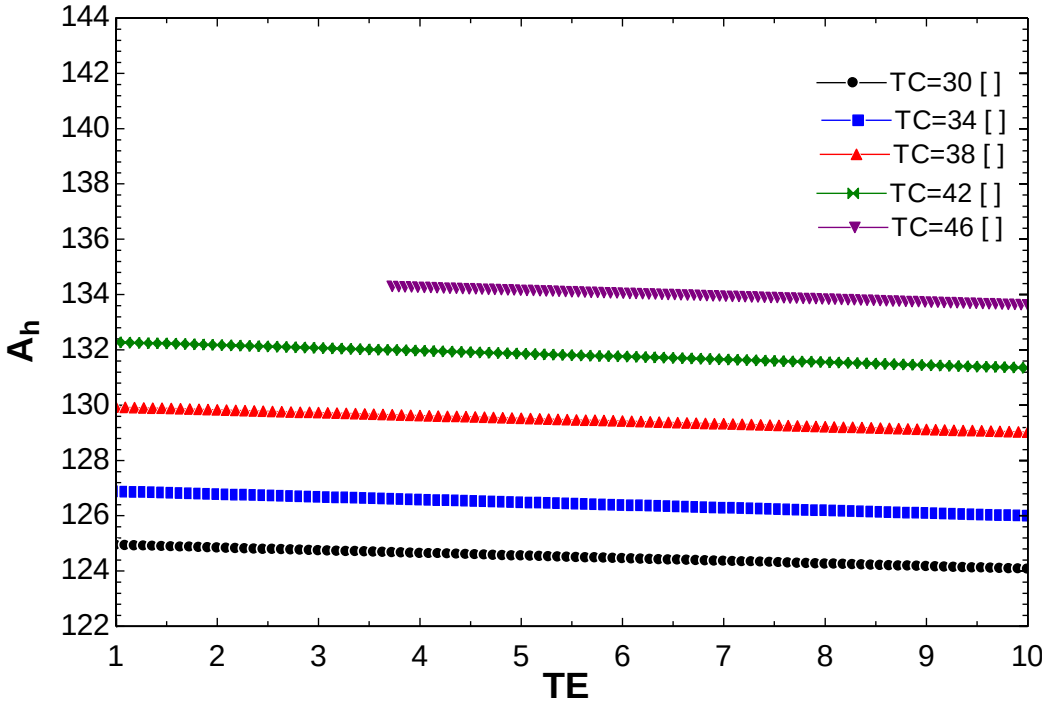

Figure 5.22-Area of flat plate collector on High Pressure side (Ah in m^2) versus generator temperature (TG in °C) and condenser temperature (TC) at (TE = 7°C)

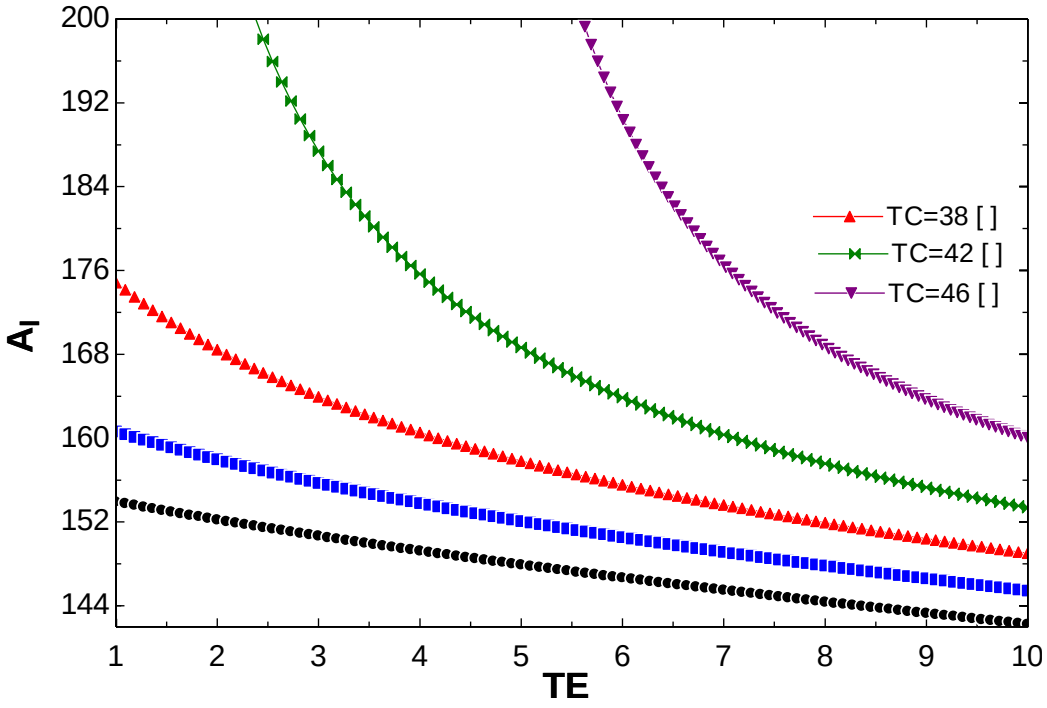

Figure 5.23-Area of flat plate collector on Low Pressure side (Al in m^2) versus generator temperature (TG in °C) and condenser temperature (TC) at (TE = 7°C)

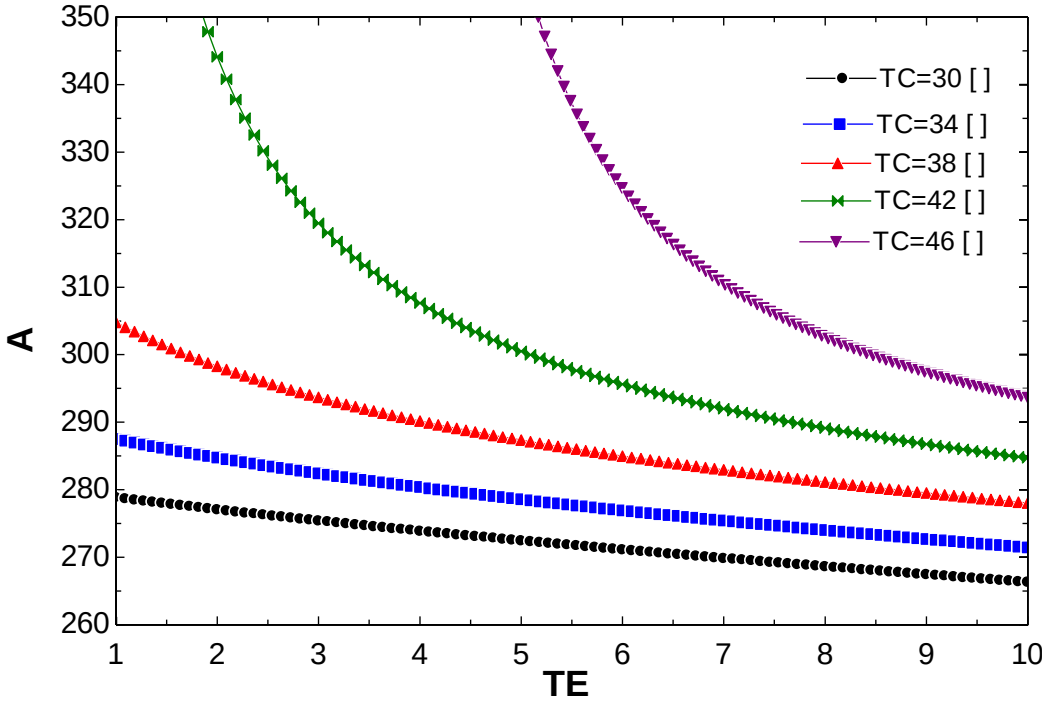

Figure 5.24-Total Area of flat plate collector (A in m^2) versus generator temperature (TG in °C) and condenser temperature (TC) at (TE = 7°C)

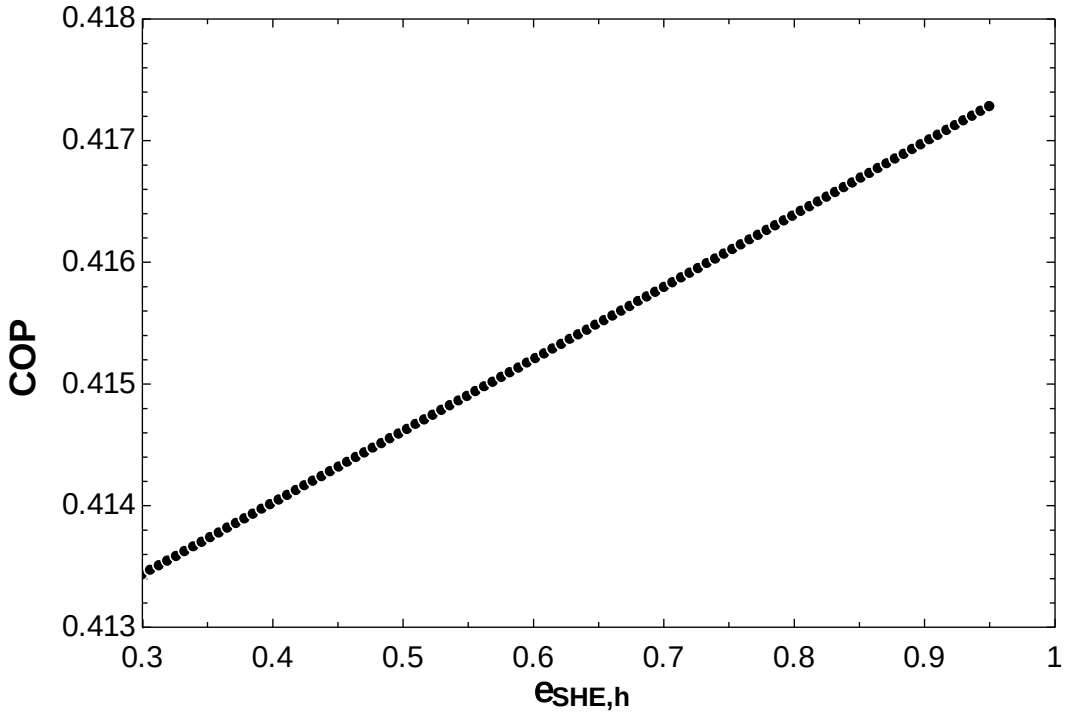

Figure 5.25-Coefficient of performance (COP) versus Effectiveness of high pressure side heat exchanger (EHXh) at (TC = 38°C, TG = 80°C, TE = 7°C)

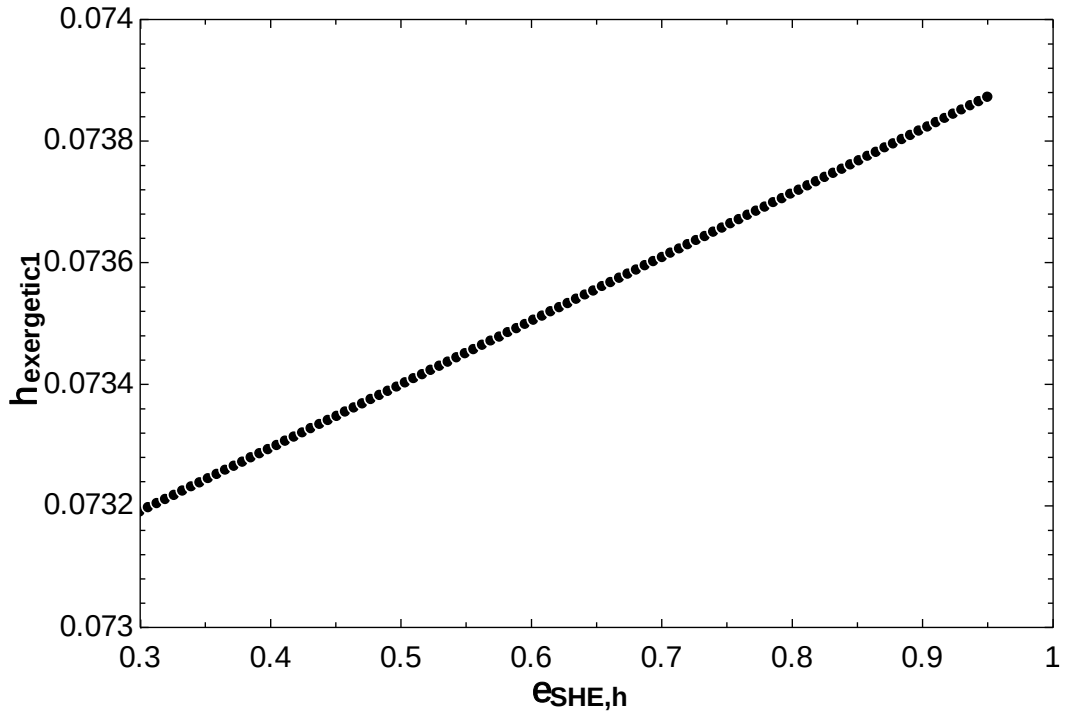

Figure 5.26-Exergetic Efficiency versus Effectiveness of high pressure side heat exchanger (EHXh) at (TC = 38°C, TG = 80°C, TE = 7°C)

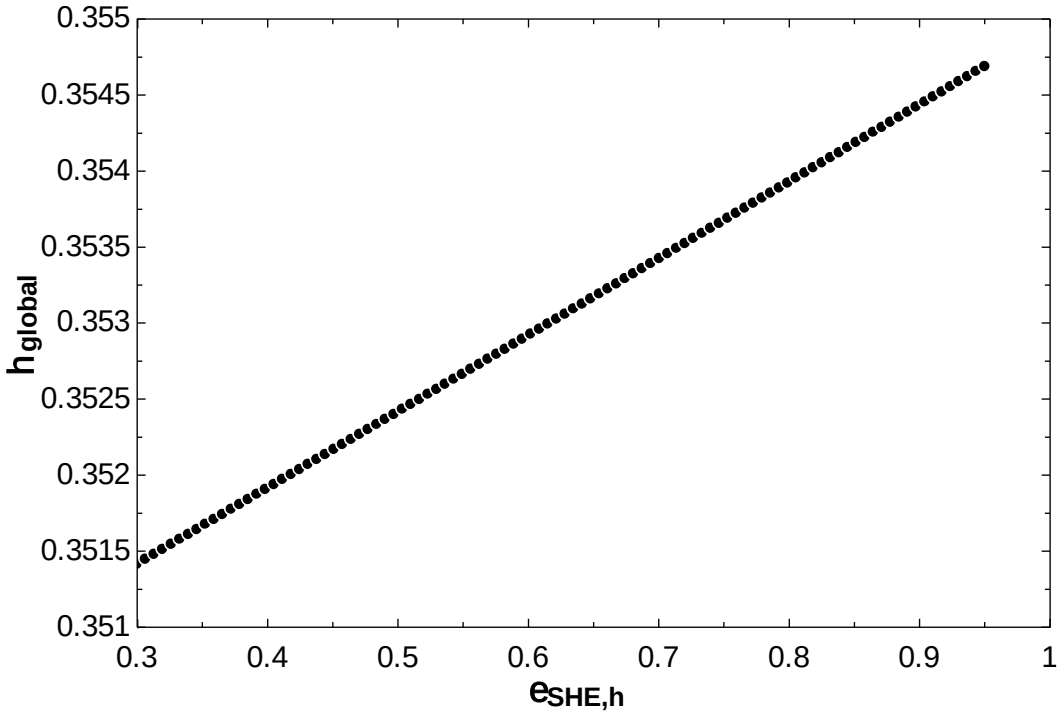

Figure 5.27-Overall Efficiency of the global system versus Effectiveness of high pressure side heat exchanger (EHXh) at (TC = 38°C, TG = 80°C, TE = 7°C)

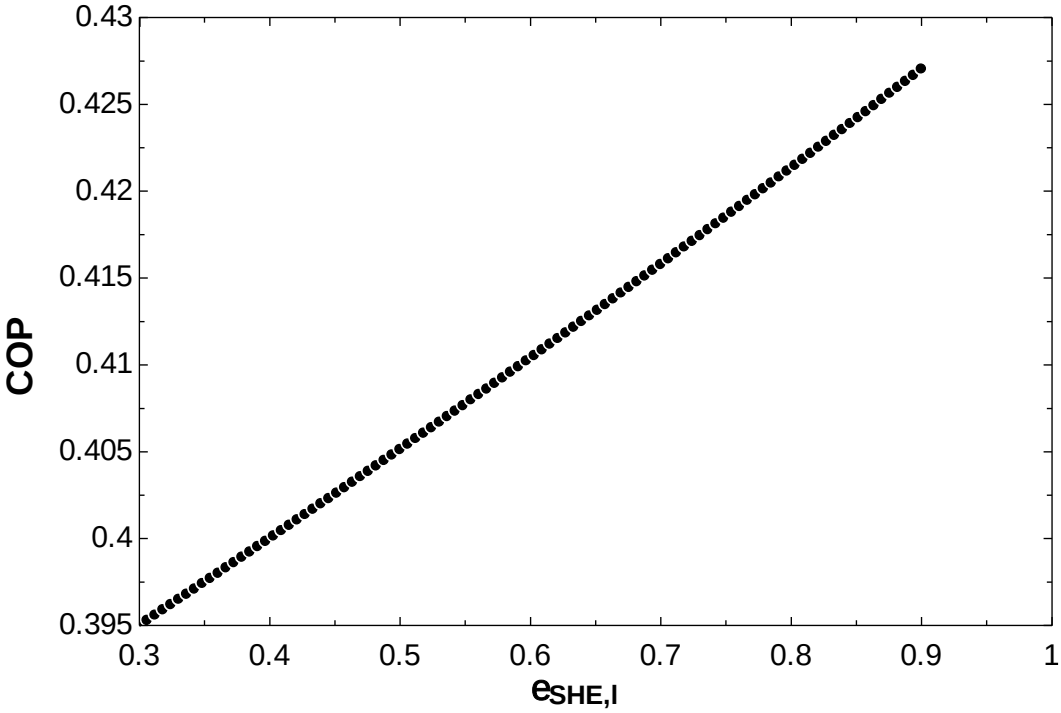

Figure 5.28-Coefficient of performance (COP) versus Effectiveness of low pressure side heat exchanger (EHXl) at (TC = 38°C, TG = 80°C, TE = 7°C)

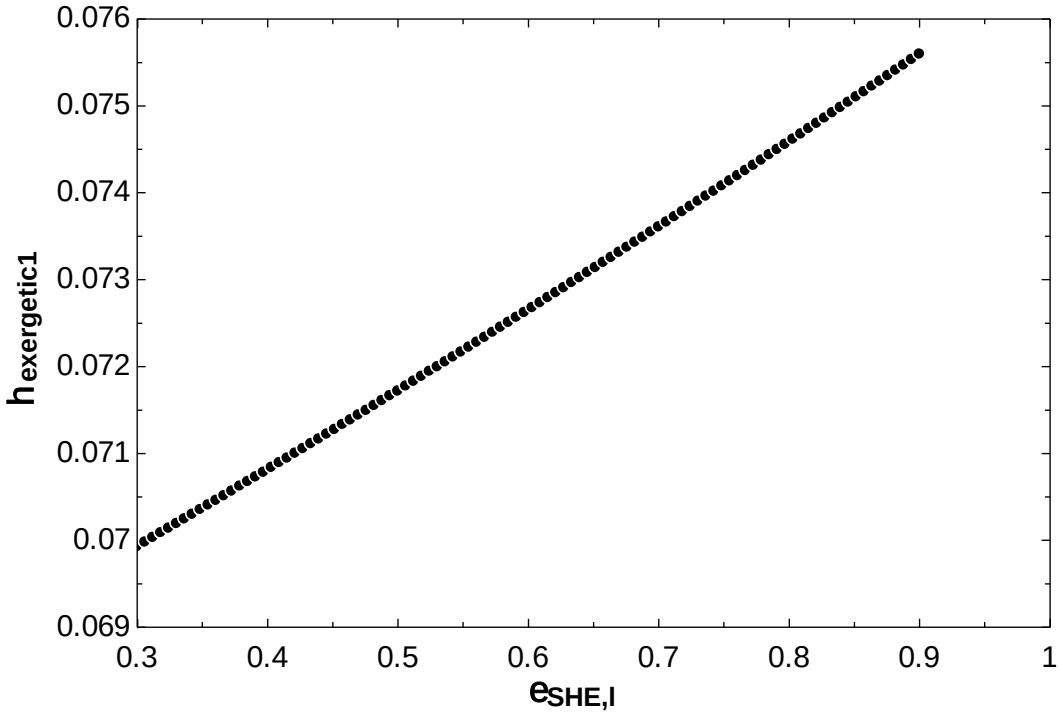

Figure 5.29-Exergetic Efficiency versus Effectiveness of low pressure side heat exchanger (EHXl) at (TC = 38°C, TG = 80°C, TE = 7°C)

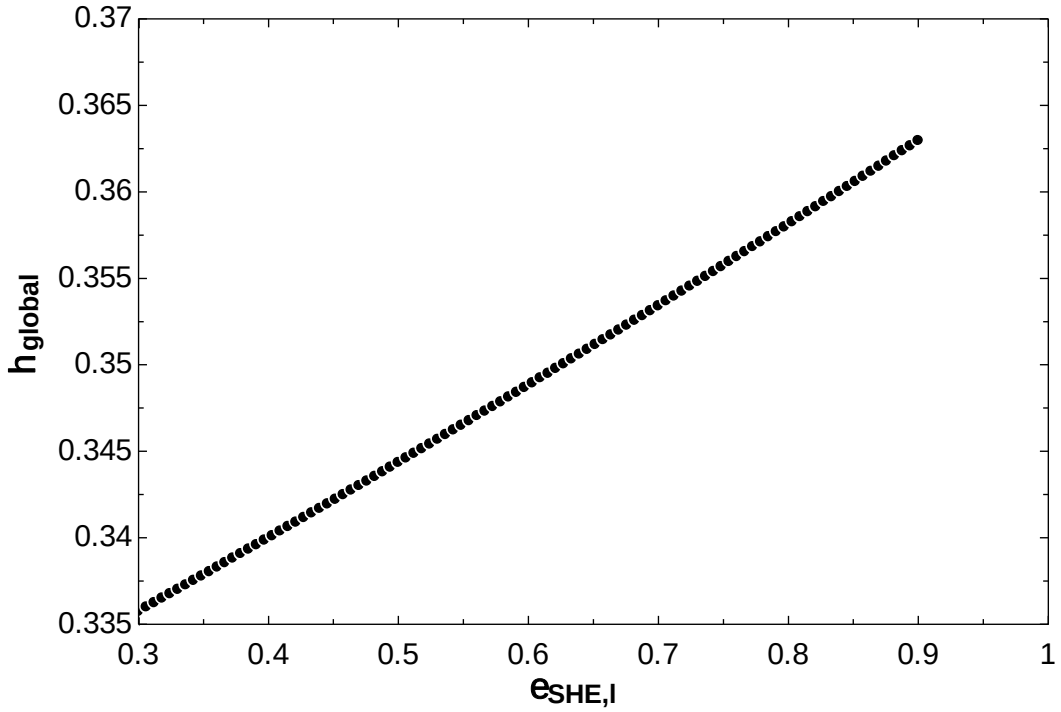

Figure 5.30-Overall Efficiency of the global system versus Effectiveness of low pressure side heat exchanger (EHXl) at (TC = 38°C, TG = 80°C, TE = 7°C)

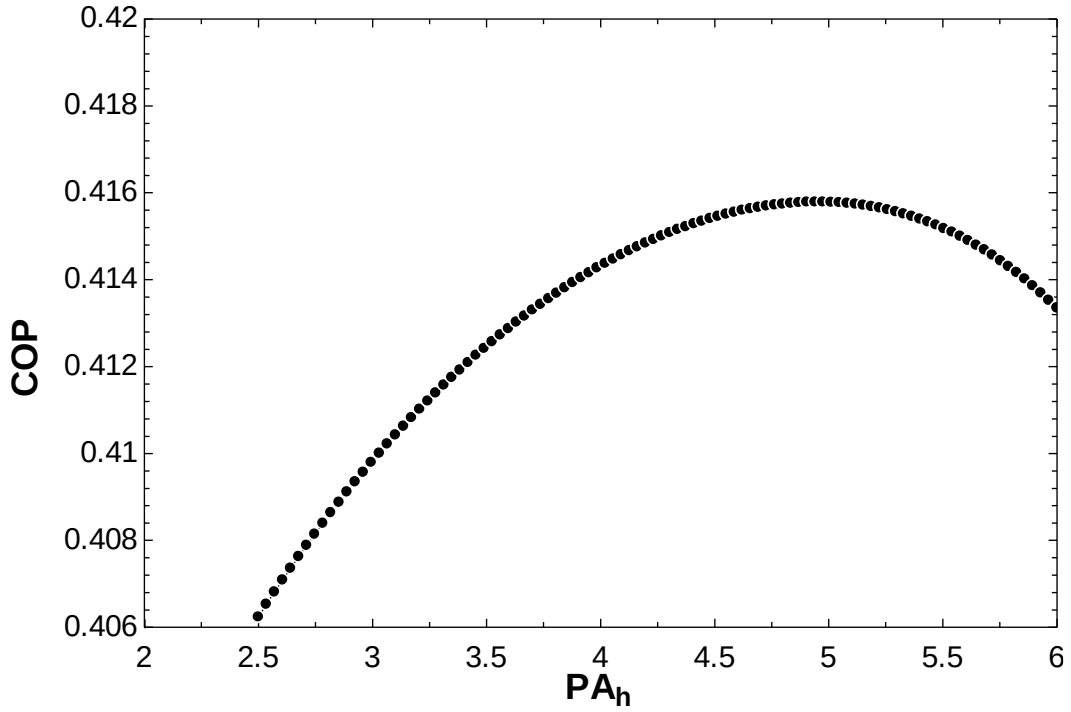

Figure 5.31-Coefficient of performance (COP) versus Intermediate Pressure (PAh in kPa) at (TC = 38°C, TG = 80°C, TE = 7°C)

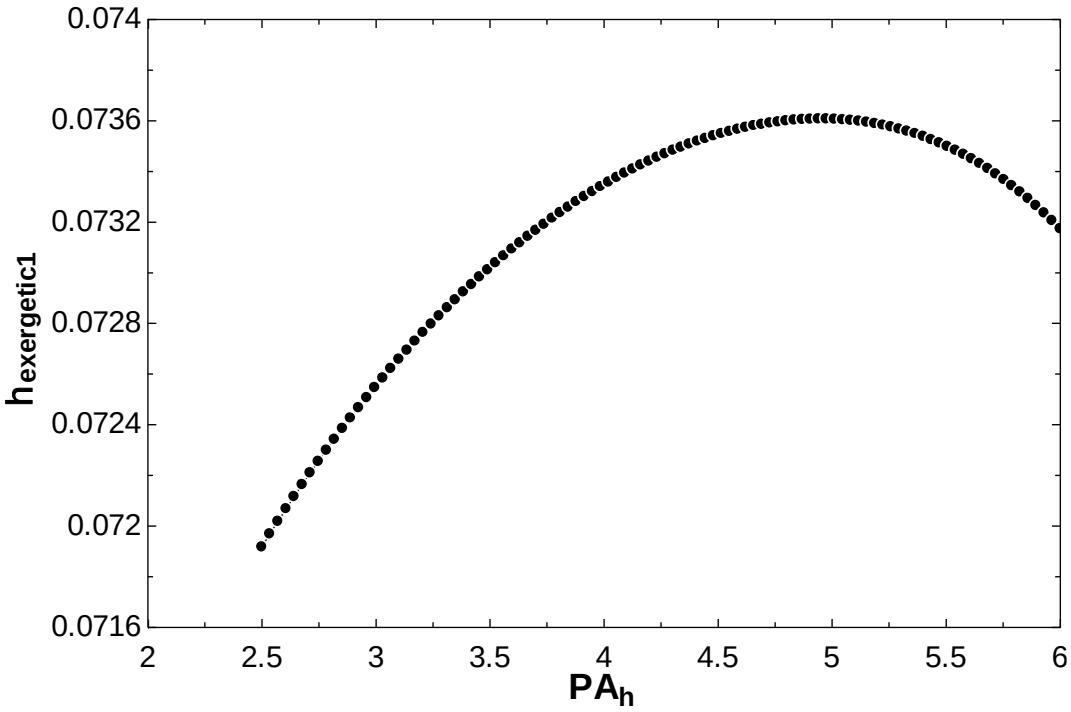

Figure 5.32-Exergetic Efficiency versus Intermediate Pressure (PAh in kPa) at (TC = 38°C, TG = 80°C, TE = 7°C)

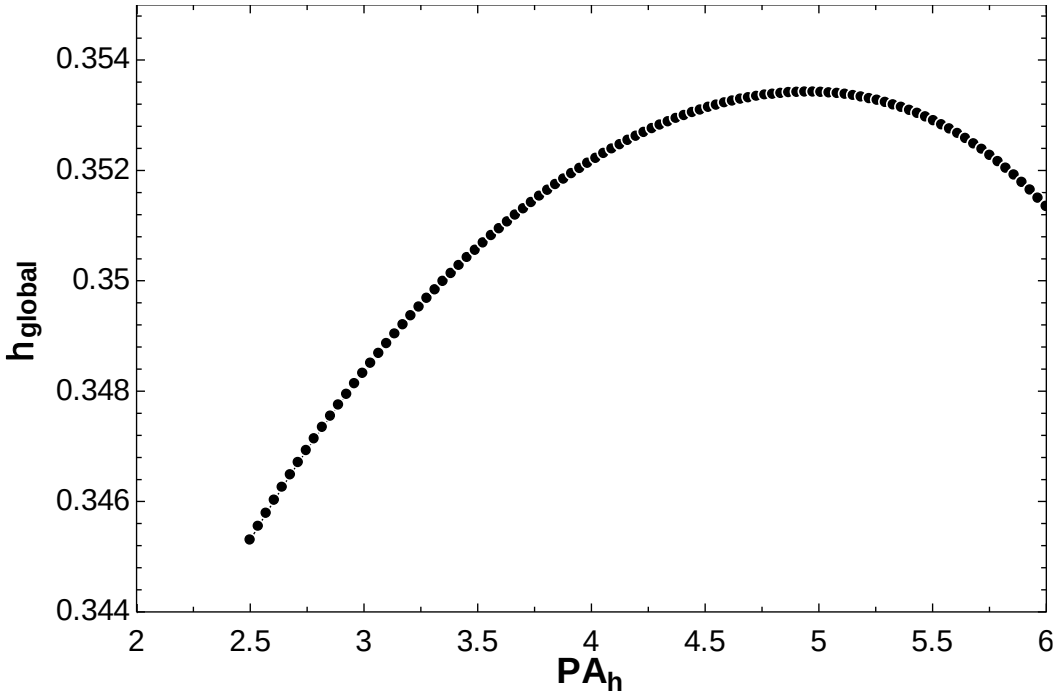

Figure 5.33-Overall Efficiency of the global system versus Intermediate Pressure (PAh in kPa) at (TC = 38°C, TG = 80°C, TE = 7°C)

Table 5.1 Thermodynamic state at each point of HVARS.

State Points	.h (kJ/kg)	T (^{o}C)	.s (kJ/kg K)	P (kPa)	.m (kg/s)	X (%)
1	92.75	35	0.2255	1.002	0.1116	55.64
2	92.75	35	0.2255	4.953	0.1116	55.64
3	142.4	62.47	0.3523	4.953	0.1116	55.64
4	202	50	0.4427	4.953	0.101	61.5
5	147.2	50.74	0.2505	4.953	0.101	61.5
6	147.2	50.74	0.2505	1.002	0.101	61.5
7	96.22	35	0.4426	4.953	0.0211	29.15
5	96.23	35	0.4426	6.63	0.0211	29.15
9	124.7	47.91	0.5325	6.63	0.0211	29.15
10	155.5	50	0.4617	6.63	0.01045	55.69
11	131.4	50.76	0.2922	6.63	0.01045	55.69
12	131.4	50.76	0.2922	4.953	0.01045	55.69
13	2649	50	5.533	6.63	0.01062	0
14	159.1	35	0.5455	6.63	0.01062	0
15	159.1	7	0.5694	1.002	0.01062	0
16	2513	7	5.973	1.002	0.01062	0
17	2650	50	5.665	4.953	0.01062	0

5.3 Results from Flat plate collector calculation:

The following results are deduced from the calculation of flat plate collector:

Area of Flat Plate collector used in high pressure side

A 1 = 130 m^2

Area of Flat Plate collector used in Low pressure side

A 2 = 154 m^2

Total Area of Flat Plate Collector

A = 284 m^2

Number of Flat Plate Collectors required in High Pressure Side (N1)

N1 = 44 Plates

Number of Flat Plate Collectors required in Low Pressure Side (N2)

N1 = 52 Plates

Cost of Flat Plate Collectors required in High Pressure Side (C1)

C1 = Rs. 264000

Number of Flat Plate Collectors required in Low Pressure Side (N2)

C2 = N2 x 6000
C2 = Rs. 312000

Total Cost (C) = C1 + C2

C = Rs. 576000

Total cost of Flat Plate Collector required = Rs 5.76 Lakhs.

This is the only cost which is considered to cool the given space, thus it is considered to be the cost of cooling of HVARS and is given by C_{HVARS} .

C_{HVARS} = Rs. 576000.

5.4 Results from cost analysis and Payback period calculation :

The proposed solar driven half effect system is compared with the Vapour compression refrigeration system (VCRS) with the same input parameters.

The cost associated with the HVARS system is only the cost of flat plate collectors. ($\mathbf{C_{HVARS}}$) is calculated as **Rs. 576000**

The cost of VCRS system is due to the cost electricity, ($\mathbf{C_{VCRS}}$) and is calculated to as **Rs. 204675**

The payback period of Half-effect solar driven absorption unit (HVARS) is calculated to be

2.8 years.

CHAPTER 6

CONCLUSIONS AND SCOPE FOR FUTURE WORK

6.1 Conclusions:

The thermodynamic analysis and simulation of vapour absorption half effect cooling system using flat plate solar collectors as source of energy, for an office space has been done and the system performances were analyzed parametrically by using EES. The cooling load calculation of an office space was carried out on 21st of June located at Dehradoon, Uttarakhand India (Latitude 30°N). The estimated capacity of the office space (Q_e), comes out to be 25 kW (approx),

The main results obtained are concluded below:

- Higher temperature of evaporator and generator, results in higher COP of the system due to the fact that as generator temperature increases, the heat transfer to the solution in the generator increases, result in the increase of mass flow rate and so does the COP.

- Low condensing temperature results in higher COP due to the fact that as the condensing temperature increases it causes less heat transfer in the condenser, which results in an increase in temperature and enthalpy of the refrigerant at the condenser outlet. Hence, the cooling capacity decreases as does the COP.

- The thermal efficiency of the global system will decrease with an increase of the generator temperature and condenser temperature. The maximum COP and maximum exergetic efficiency are higher when LP generator temperature is higher in comparison to HP generator temperature.

- When the evaporator temperature is maintained constant at 7°C and condenser temperature is varied from 30°C and 46°C and generators temperatures are varied from 65 to 85 °C the maximum COP is 0.4158 and the maximum exergetic efficiency is about 7.36% .

- For a given condenser temperature there is an optimum generator temperature for which the total area flat plate collector is minimum. This optimum generator temperature comes out to be 80°C. This generator temperature gives the maximum COP and exergetic efficiency of the absorption cooling system.

- There exists a specific generator temperature below which a half effect system ceases to work. The COP and exergetic efficiency are zero corresponding to this value. In the present work, this value is found to be 67.51ºC, corresponding to an intermediate pressure of 4.953 kPa (for TC = Tal =Tah = 38°C, TE = 7°C and Tgh = Tgl = 80°C).

- There exists an optimum intermediate pressure corresponding to which COP and exergetic efficiency are maximum. The optimum intermediate pressure comes out to be 4.935 kPa. (for TC = Tal =Tah = 38°C, TE = 7°C and Tgh = Tgl = 80°C). This pressure increases with increase in LP or HP generator temperatures and evaporator temperature (at a particular absorber temperature) and decreases with increase in absorber temperature (at a particular generator temperature).

.

- This absorption air cooling system is alternative to conventional vapor compression cycle. The proposed solar driven half effect system is compared with the Vapour compression refrigeration system (VCRS) with the same input parameters. The ultimate goal in the long term would ideally be to reduce the consumption of electricity used for refrigeration and air conditioning. The payback period of Half-effect solar driven absorption unit (HVARS) is calculated to be 2.8 years.

6.2 Scope For Future Work

- Exergo-economics analysis of the half effect system can be performed.
- By the use of the present system carbon credits saved and its impact on global warming can be analyzed.
- Design of each component of the half effect system can be include for minimizing the cost.
- The flat plate collector unit can be utilized in winter for meeting the hot water demand.

CHAPTER 7

REFERENCES

[1] Abdulateef, J.M., 2008, Review on solar-driven ejector refrigeration technologies. Renew SustainEnergy Rev.

[2] Thermodynamics: An Engineering Approach, 5th edition, 2005 By Y.Cengel's M. Boles

[3] NPTEL, IIT Kharagpur Version 1 ME, IIT Kharagpur

[4] Absorption Chillers Guideline Southern California Gas Company, New Buildings Institute, Advanced Design Guideline Series pg 4 to 5.

[5] Rabah GOMRI , (2010). Solar Energy to Drive Half-Effect Absorption Cooling System, Int. J. of Thermal & Environmental Engineering, Volume 1, No. 1 , 1-8.

[6] Akhilesh Arora, Manoj Dixit, and S.C. Kaushik, 2016, Computation Of Optimum Parameters Of A Half Effect Water-Lithium Bromide Vapour Absorption Refrigeration System, Journal of Thermal Engineering, Vol. 2, No. 2, pp. 683-692, April.

[7] S. Arivazhagan , R. Saravanan , S. Renganarayanan, 2006, Experimental studies on HFC based two-stage half effect vapour absorption cooling system, Applied Thermal Engineering 26 pg1455–1462.

[8] S. Arivazhagan, S.N. Murugesan, R. Saravanan a, S. Renganarayanan, 2005, Simulation studies on R134a—DMAC based halfeffect absorption cold storage systems, Energy Conversion and Management Vol. 46 pg 1703–1713.

[9] Rabah GOMRI, 2011, Development of Intermediate Pressure Correlation for the Half-Effect Absorption Cooling Chiller, Int. J. of Thermal & Environmental Engineering Volume 2, No. 1 pg 35-40.

[10] Jianzhao Wang, Danxing Zheng,, 2009, Performance of one and a half-effect absorption cooling cycle of H2O/LiBr system, Energy Conversion and Management Vol. 50, pg 3087–3095.

[11] V.K.Bajpai, 2012, Design of Solar Powered Vapour Absorption System Proceedings of the World Congress on Engineering 2012 Vol III WCE 2012, July 4 – 6, London, U.K.

[12] L.A. Domínguez-Inzunza, J.A. Hernández-Magallanes, M. Sandoval-Reyes, W. Rivera , 2014, Comparison of the performance of single-effect, half-effect, double-effect in series

and inverse and triple-effect absorption cooling systems operating with the NH3eLiNO3 mixture, Applied Thermal Engineering Vol. 66 pg 612-620

[13] Saeed. Sedigh , Hamid. Saffari, 2011, Thermodynamic Analysis Of Single Effect And Half Effect Absorption Refrigeration Systems, International Journal of Energy & Technology Vol. 3 pg 1-9.

[14] Jhalak Raj Adhikari, Bivek Baral, Ram Lama, Badri Aryal, and Roshan Khadka , 2012, Design and analysis of solar absorption air cooling system for an office building Design and analysis of solar absorption air cooling system for an office building, Rentech Symposium Compendium, Volume 2, December.

[15] Neeraj Kumar Sharma Mr. Pradeep Singh Deepak Gaur, 2013, Design& Analysis Of Solar Vapour Absorption System Using Water And Lithium Bromide, International Journal of Engineering Research & Technology (IJERT) ISSN: 2278-0181 Vol. 2 Issue 6, June.

[16] K.R. Ullah , R.Saidur , H.W.Ping , R.K.Akikur , N.H.Shuvo , 2013, A review of solar thermal refrigeration and cooling methods, Renewable and Sustainable Energy Reviews, Vol. 24 pg 499–513.

[17] Berhane H. Gebreslassie , Eckhard A. Groll and Suresh V. Garimella ,2012, Multi-objective optimization of sustainable single-effect water/Lithium Bromide absorption cycle, Renewable Energy Vol. 46 pg 100-110.

[18] Berhane H. Gebreslassie, Marc Medrano and Dieter Boer, 2010, Exergy analysis of multi-effect water–LiBr absorption systems: From half to triple effect, Renewable Energy, Vol. 35 pg 1773–1782.

[19] Z.F. Li, K. Sumathy, 2000, Technology development in the solar absorption air-conditioning systems, Renewable and Sustainable Energy Reviews, Vol. 4 pg 267±293.

[20] V Mittal, K S Kasana and N S Thakur, 2006, Modelling and simulation of a solar absorption cooling system for India, Journal of Energy in Southern Africa • Vol 17 No 3 • August.

[21] K. Sumathy , Z. C. Huang And Z. F. Li , 2002, Solar Absorption Cooling With Low Grade Heat Source — A Strategy Of Development In South China, Solar Energy Vol. 72, No. 2, pp. 155–165.

[22] G.A. Florides, S.A. Kalogirou, S.A. Tassou and L.C. Wrobel, 2003, Design and construction of a LiBr–water absorption machine, Energy Conversion and Management, Vol. 44 pp 2483–2508.

[23] Anurag Kumar Singh, Ms Akanksha Mishra, and Mr. K. K. Dubey, (2016), Cooling Load Estimation for Library, International Journal of Emerging Technologies in Engineering Research (IJETER) Volume 4, Issue 2, February.

[24] Ma WB, Deng SM, 1996, Theoretical analysis of low temperature hot source driven two stage LiBr-H2O absorption refrigeration system. International Journal of refrigeration; Vol. 19(2): pp 141-146.

[25] Z. Crepinsek, D. Goricanec, J. Krope, 2009, Comparison Of The Performances Of Absorption Refrigeration Cycles, Wseas Transactions On Heat And Mass Transfer, Issn: 1790-5044 Issue 3, Volume 4, July.

[26] Hans-Martin Henning, and Jochen Döll, (2012), Solar systems for heating and cooling of buildings, Energy Procedia, Vol. 30 pp 633 – 653.

[27] Berhane H. Gebreslassiea, Mélanie Jimeneza, Gonzalo Guillén-Gosálbezb, Laureano Jiménezb and Dieter Boera, 2010, Multi-objective optimization of solar assisted absorption cooling system, 20th European Symposium on Computer Aided Process Engineering – ESCAPE20.

[28] GOMRI, 2010, Solar energy to drive absorption cooling systems suitable for small building applications, Proceedings of the Tenth International Conference Enhanced Building Operations, Kuwait, October 26-28.

[29] Absorption Chillers and Heat Pumps, Second Edition, By Keith E. Herold, Reinhard Radermacher, Sanford A. Klein, 1994.

[29] Refrigeration And Air Conditioning, Third Edition, published by Tata McGraw-Hill Education private Limited, 2012 By C.P. Arora.

[30] ASHRAE Handbook Fundamentals, 2001

[31] Kalogirou, S.A., 2004 Solar thermal collectors and applications. Progress in Energy and Combustion Science, pp.231-95.

[32] Tyagi,V.V.,2012, Advancement in solar photovoltaic/thermal (PV/T) hybrid collector technology. Renewable and Sustainable Energy Reviews, Vol. (16), pp.1383– 1398

[33] Solar Engineering of Thermal Processes, 3rd Edition, 2006 By John A. Duffie, William A. Beckman.

APPENDIX [A]

A.1 EES PROGRAM FOR HALF EFFECT SYSTEM

"In the analysis of this cycle the following assumption is considered
1. The pumping is isentropic
2. Across Solution expansion valve entropy change is negelcted and temperature is also constant."

```
TE = 7

Pg_l= 4.953
To= 298.15

TA_l = 38 "C"
TA_h=TA_l
TC = TA_l "C"

TG_l = 80

TG_h=TG_l
EPSILON_SHE_l= 0.7
EPSILON_SHE_h= 0.7

QE = 25

ms_l*Xs_l = mw_l*Xw_l

mr + mw_l = ms_l

PE = PRESSURE(Water,T=TE, X = 0)

PA_l = PE

PC = PRESSURE(Water,T=TC, X = 0)

PA_l=P_librjj(Xs_l,TA_l+273.15)

T[1] = TA_l

h[1]= enthalpy_librjj(Xs_l,(TA_l+273.15))

T[2]=TA_l
```

V2=V_LIBR('SI' ,TA_l,Xs_l)/1000

h[2]= h[1] + V2*(PG_l-PA_l)

Wp_l= ms_l*(h[2]-h[1])

h[5] =enthalpy_librjj(Xw_l,(T[5]+273.15))

PG_l=P_librjj(Xw_l,TG_l+273.15)

T[4] = TG_l

h[4]= enthalpy_librjj(XW_l,(TG_l+273.15))

EPSILON_SHE_l = (h[4] - h[5]) /(h[4] - h2_4)

ms_l*(h[3]-h[2]) = mw_l*(h[4]-h[5])

h[3] =enthalpy_librjj(Xs_l,(T[3]+273.15))

h2_4 =enthalpy_librjj(Xw_l,(T[2]+273.15))

h[6]=h[5]

ms_h*Xs_h = mw_h*Xw_h

PA_h = Pg_l

PA_h=P_librjj(Xs_h,TA_h+273.15)

T[7] = TA_h

PG_h=PC

h[7]= enthalpy_librjj(Xs_h,(TA_h+273.15))

T[8]=TA_h

V8=V_LIBR('SI' ,TA_h,Xs_h)/1000

h[8]= h[7] + V8*(PG_h-PA_h)

Wp_h= ms_h*(h[8]-h[7])

h[11] =enthalpy_librjj(Xw_h,(T[11]+273.15))

PG_h=P_librjj(Xw_h,TG_h+273.15)

T[10] = TG_h

h[10]= enthalpy_librjj(XW_h,(TG_h+273.15))

EPSILON_SHE_h = (h[10] - h[11]) /(h[10] - h8_10)

ms_h*(h[9]-h[8]) = mw_h*(h[10]-h[11])

h[9] =enthalpy_librjj(Xs_h,(T[9]+273.15))

h[11]=h[12]

h[13] =ENTHALPY(Steam,T=TG_h,P=PG_h)

mr+ mw_h = ms_h

h[14] =ENTHALPY(Water,T=TC,X=0)

h[15]=h[14]

h[16] = ENTHALPY(Steam,T=TE,X=1)

QG_l+ ms_l*h[3]= mr*h[17] + mw_l*h[4]

QG_h+ ms_h*h[9]= mr*h[13] + mw_h*h[10]

QA_l= ms_l*h[1]-(mw_l*h[6] + mr*h[16])

QA_h= ms_h*h[7]-(mw_h*h[12] + mr*h[17])

QC = mr*(h[14]-h[13])

QE = mr*(h[16]-h[15])

QSHE_l= ms_l*h[3]- ms_l*h[2]

QSHE_h= ms_h*h[9]- ms_h*h[8]

check1= QG_h +QG_l+ QE +Wp_h+wp_l

CHECK2 = QA_l +QA_h+ QC

COP= QE/(QG_h +QG_l+ Wp_h+wp_l)

```
S[1]=ENTROPY_librjj(Xs_l, TA_l+273.15)
S[2]=S[1]
S[3]=ENTROPY_librjj(Xs_l,T[3]+273.15)
S[4]=ENTROPY_librjj(Xw_l,TG_l+273.15)
S[5]=ENTROPY_librjj(Xw_l,T[5]+273.15)
S[17] = ENTROPY(Steam,T=TG_l,P=PG_l)
V5=V_LIBR('SI',T[5],Xw_l)/1000
S[6]=S[5] - V5*(PA_l-PG_l)/(T[5]+273.15)
S[7]=ENTROPY_librjj(Xs_h, TA_h+273.15)
S[8]=S[7]
S[9]=ENTROPY_librjj(Xs_h,T[9]+273.15)
S[10]=ENTROPY_librjj(Xw_h,TG_h+273.15)
S[11]=ENTROPY_librjj(Xw_h,T[11]+273.15)
S[13] = ENTROPY(Steam,T=TG_h,P=PG_h)
V11=V_LIBR('SI',T[11],Xw_h)/1000
S[12]=S[11] - V11*(PA_h-PG_h)/(T[11]+273.15)
S[14]=ENTROPY(Water,T=TC,X=0)
Hf_15=ENTHALPY(WATER,T=TE,X=0)
Hg_15 =ENTHALPY(WATER,T=TE,X=1)
H[15]=Hf_15+X_15*(Hg_15-Hf_15)
Sf_15=ENTROPY(WATER,T=TE,X=0)
Sg_15 =ENTROPY(STEAM,T=TE,X=1)
S[15]=Sf_15+X_15*(Sg_15-Sf_15)
```

S[16]=ENTROPY(WATER,T=TE,X=1)

T[16] =TE

P[1] = PE
P[6] = PE
P[8] = PC
P[9] = PC
P[10] = PC
P[11] = PC
P[13] = PC
P[14] = PC
P[15] = PE
P[16] = PE

P[2] = Pg_l
P[3] = Pg_l
P[4] = Pg_l
P[5] = Pg_l
P[7] =Pg_l
P[12] = Pg_l
P[17] = Pg_l

m[1] = m[2]
m[2] = m[3]

m[3] = ms_l

m[4] = m[5]
m[5] = m[6]

m[6] = mw_l

m[7] = m[8]
m[8] = m[9]

m[9] = ms_h

m[10] = m[11]
m[11] = m[12]

m[12] = mw_h

m[13] = m[14]
m[14] = m[15]

m[15] = m[16]
m[16] = m[17]

m[17] = mr

X[1] = X[2]
X[2] = X[3]

X[1] = Xs_l

X[4] = X[5]
X[5] = X[6]

X[4] = Xw_l

X[7] = X[8]
X[8] = X[9]

X[7] = Xs_h

X[10] = X[11]
X[11] = X[12]

X[10] = Xw_h

X[13] = X[14]
X[14] = X[15]

X[15] = X[16]
X[16] = X[17]

X[17] = 0

T[6] = T[5]
T[11] = T[12]

T[14] = TC

T[15] =T [16]

T[13] = TG_l
T[17] = TG_l

{Exergy Analysis}

ED_a_l= {(1-To/(TA_l+273.15))*QA_l +} mr*(h[16]-To*s[16])+mw_l*(h[6]-To*s[6])-ms_l*(h[1]-To*s[1])

P_ED_a_l=ED_a_l*100/ED_t

{{(1-To/(TA_l+273.15))*QA_l +} ,
{(1-To/(TA_h+273.15))*QA_h +}
and {(1-To/(TC+273.15))*QC +} this term should not be included
since we are assuming absorber and condenser boundary at ambient surrounding temperatures}

ED_a_h= {(1-To/(TA_h+273.15))*QA_h +} mr*(h[17]-To*s[17])+mw_h*(h[12]-To*s[12])-ms_h*(h[7]-To*s[7])

P_ED_a_h=ED_a_h*100/ED_t

ED_g_l= (1-To/(TG_l+273.15))*QG_l + ms_l*(h[3]-To*s[3])-mw_l*(h[4]-To*s[4])-mr*(h[17]-To*s[17])

P_ED_g_l=ED_g_l*100/ED_t

ED_g_h= (1-To/(TG_h+273.15))*QG_h + ms_h*(h[9]-To*s[9])-mw_h*(h[10]-To*s[10])-mr*(h[13]-To*s[13])

P_ED_g_h=ED_g_h*100/ED_t

ED_c= {(1-To/(TC+273.15))*QC +} mr*(h[13]-To*s[13])-mr*(h[14]-To*s[14])

P_ED_c=ED_c*100/ED_t

ED_e= (1-To/(Tr+273.15))*QE + mr*(h[15]-To*s[15])-mr*(h[16]-To*s[16])

P_ED_e=ED_e*100/ED_t

ED_she_l= ms_l*(h[2]-To*s[2])-ms_l*(h[3]-To*s[3]) +mw_l*(h[4]-To*s[4])-mw_l*(h[5]-To*s[5])

P_ED_she_l=ED_she_l*100/ED_t

ED_she_h= ms_h*(h[8]-To*s[8])-ms_h*(h[9]-To*s[9]) +mw_h*(h[10]-To*s[10])-mw_h*(h[11]-To*s[11])

P_ED_she_h=ED_she_h*100/ED_t

ED_stv_l= mw_l*(h[5]-To*s[5])-mw_L*(h[6]-To*s[6])

P_ED_stv_l=ED_stv_l*100/ED_t

ED_stv_h= mw_h*(h[11]-To*s[11])-mw_h*(h[12]-To*s[12])

P_ED_stv_h=ED_stv_h*100/ED_t

ED_rtv= mr*(h[14]-To*s[14])-mr*(h[15]-To*s[15])

P_ED_rtv=ED_rtv*100/ED_t

ED_t=
ED_a_l+ED_a_h+ED_g_l+ED_g_h+ED_c+ED_e+ED_she_l+ED_she_h+ED_stv_l+ED_stv_h+
ED_rtv

Exergy_input= Qg_h*(1-To/(TG_h+273.15))+Qg_l*(1-To/(TG_l+273.15))+wp_l+wp_h

exergy_product_E = -QE*(1-(To/(TR+273.15)))

EDR   = ED_t/exergy_product_E

ETA_exergetic1= exergy_product_E / exergy_input

eta_exergetic2= 1- ED_t /exergy_input

"Circulation Ratio SCR"

SCR_l = ms_l/mr

SCR_h = ms_h/mr

"Claculation of flat plate collector Area"

K= 0.85 "efficiency of collector plate (assume k=0.85)"
F = 250 " average solar heat falling on earth's surface=6 kwhr/m2/day= 250 W/m2"
QG_h = K*F*A_h/1000

QG_l = K*F*A_l/1000

A = A_h + A_l "Total Area of flat plate collector required"

ETA_global = COP * K

OUTPUT

Variables in Main

A=282.9

A_h=129.3

A_l=153.6

check1=85.126

CHECK2=-85.126

COP=0.415791 [kJ/kg-kPa]

EDR=12.59 [kg/kJ]

ED_a_h=1.91

ED_a_l=1.958

ED_c=1.155

ED_e=0.917

ED_g_h=1.906

ED_g_l=0.4892

ED_rtv=0.07563

ED_she_h=0.03808

ED_she_l=0.2255

ED_stv_h=0.000009816 [kPa]

ED_stv_l=0.0002156 [kPa]

ED_t=8.675

EPSILON_SHE_h=0.7

EPSILON_SHE_l=0.7

ETA_exergetic1=0.07361 [kJ/kg-kPa]

eta_exergetic2=0.07361

ETA_global=0.3534 [kJ/kg-kPa]

Exergy_input=9.364 [kPa]

exergy_product_E=0.6893 [kJ/kg]

F=250

h2_4=123.7 [kPa]

h8_10=106.8 [kPa]

Hf_15=29.42 [kJ/kg]

Hg_15=2513 [kJ/kg]

K=0.85

mr=0.01062

ms_h=0.0211

ms_l=0.1116

mw_h=0.01048

mw_l=0.101

PA_h=4.9530 [kPa]

PA_l=1.002 [kPa]

PC=6.63 [kPa]

PE=1.002 [kPa]

PG_h=6.63 [kPa]

Pg_l=4.9530 [kPa]

P_ED_a_h=22.02

P_ED_a_l=22.57

P_ED_c=13.31

P_ED_e=10.57

P_ED_g_h=21.98

P_ED_g_l=5.639

P_ED_rtv=0.8718

P_ED_she_h=0.439

P_ED_she_l=2.6

P_ED_stv_h=0.0001132 [kPa]

P_ED_stv_l=0.002485 [kPa]

QA_h=-27.48 [kPa]

QA_l=-31.2 [kPa]

QC=-26.44 [kJ/kg]

QE=25 [kJ/kg]

QG_h=27.48 [kPa]

QG_l=32.65 [kPa]

QSHE_h=0.6011 [kPa]

QSHE_l=5.537 [kPa]

SCR_h=1.987

SCR_l=10.51

Sf_15=0.1063 [kJ/kg-K]

Sg_15=8.973 [kJ/kg-K]

TA_h=38

TA_l=38

TC=38

TE=7

TG_h=80

TG_l=80

To=298.150

Tr=17

V11=0.000607

V2=0.0006262

V5=0.0005871

V8=0.0008145

Wp_h=0.00002881 [kPa]

Wp_l=0.0002761 [kPa]

Xs_h=29.15

Xs_l=55.64

Xw_h=58.69

Xw_l=61.5

X_15=0.05222.

Thermodynamic Properties at all points:

State Points	.h (kJ/kg)	T (ºC)	.s (kJ/kg K)	P (kPa)	.m (kg/s)	X (%)
1	92.75	35	0.2255	1.002	0.1116	55.64
2	92.75	35	0.2255	4.953	0.1116	55.64
3	142.4	62.47	0.3523	4.953	0.1116	55.64
4	202	50	0.4427	4.953	0.101	61.5
5	147.2	50.74	0.2505	4.953	0.101	61.5
6	147.2	50.74	0.2505	1.002	0.101	61.5
7	96.22	35	0.4426	4.953	0.0211	29.15
5	96.23	35	0.4426	6.63	0.0211	29.15
9	124.7	47.91	0.5325	6.63	0.0211	29.15
10	155.5	50	0.4617	6.63	0.01045	55.69
11	131.4	50.76	0.2922	6.63	0.01045	55.69
12	131.4	50.76	0.2922	4.953	0.01045	55.69
13	2649	50	5.533	6.63	0.01062	0
14	159.1	35	0.5455	6.63	0.01062	0
15	159.1	7	0.5694	1.002	0.01062	0
16	2513	7	5.973	1.002	0.01062	0
17	2650	50	5.665	4.953	0.01062	0

A.2 EES PROGRAM FOR VAPOUR COMPRESSION SYSTEM

```
"Condenser Temperature"
TC = 38
"Evaporator Temperature"
TE = 7
"Refregerating capacity "
Q_e = 47.25 [Kw]

h[1]=Enthalpy(R12,T=TE,x=1)
h[3]=Enthalpy(R12,T=TC,x=0)
h[4]=h[3]

s[1]=Entropy(R12,T=TE,x=1)
s[1]=s[2]

P[3]=Pressure(R12,T=TC,x=0)
P[1]=Pressure(R12,T=TE,x=1)

h[2]=Enthalpy(R12,s=s[2],P=P[3])

"Refrigeration effect "
R.E. = h[1] - h[4]

"Mass flow rate"
m= Q_e/R.E.

"Compressor work "
W_c = h[2]-h[1]

"Powe consumption by compressor "
P=m*W_c

"Theoretical Horse Power "
HP = 1000*P/746

HPTR = HP/15


v[1]=Volume(R12,T=TE,x=1)

"Theoretical Piston Displacement "
V = m*v[1]

"Piston displacement per ton "
V_t = V/15
```

"Heat Rejected in condenser "
Q = m* (h[2]-h[3])

"COP"
COP=R.E./W_c

OUTPUT

Variables in Main

COP=7.743

HP=8.18 [Kw]

HPTR=0.5453 [Kw]

m=0.4006 [Kw-kg/kJ]

P=6.102 [Kw]

Q=53.35 [Kw]

Q_e=47.25 [Kw]

R.E.=117.9 [kJ/kg]

TC=38

TE=7

V=0.01792 [Kw-m^3/kJ]

V_t=0.001195 [Kw-m^3/kJ]

W_c=15.23 [kJ/kg]

APPENDIX [B]

FLAT PLATE COLLECTOR SPECIFICATIONS (cost Rs. 6000 per unit)S

SUNSCAN™
Solar Energy Technologies

SPECIFICATIONS – SS-FP RANGE

Collector Type	SS-FP-3.0
General Information	
Standard Dimensions	2.005mm x 1.505mm
Gross Area	3.0
Aperture Area	2.94
Absorber Area	2.61 m2
Number of Covers	1
Cover Material	tempered glass
Cover Thickness	3mm
Cover Transmission	88%
Weight	48kg
Power output at 1000W/m2 (tm-ta) = 30 °C	1543.5 W
Casing	
Frame Material	Aluminium
Frame Colour	Bronze Brown
Back Plate Material	Aluminium
Sealing Gasket	Ethylene-Propylene Diene Monomer
Absorber	
Material	Aluminium
Thickness of Absorber Plate	0.5mm
Surface Treatment	Cu and Al complex
Volume of Absorber	2.49 L
Header Material	Copper
Header Tube Size	22mm
Riser Material	Copper
Riser Tube Size	12mm
Operature Pressure	1000kPa
Test Pressure	1500 kPa
Stagnation temperature	153 °C
Thermal Insulation	
Insulation Material	Glass Wool
Back Insulation Thickness	35mm
Side Insulation Thickness	25mm

APPENDIX [B]

TARRIF RATES IN UTTARAKHAND

UTTARAKHAND POWER CORPORATION LIMITED

PUBLIC-NOTICE

In terms of the provisions of section 45 of the Electricity Act, 2003, the consumers and the general public are hereby informed of the tariff and charges for different categories of consumers approved by the Uttarakhand Electricity Regulatory Commission and effective from 01-04-2012, as follows:

Rate Schedule	Descriptions		Fixed / Demand Charges (Per Month)	Energy Charges
RTS-1: Domestic	1.	Metered	Rs. 6/Connection	Rs 1.50/KWH
	1.1	Life Line Consumers Below Poverty line including Kutir Jyoti having load upto 1 KW and Consumption upto 30 units per Month		
	1.2	Other Domestic Consumers having load upto 4 KW	Rs. 30/Connection	For 1-100 Units p.m. Rs 2.30/KWH For 101-200 Units p.m. Rs 2.60/ KWH For remaining Units p.m. Rs 3.10/KWH
	1.3	Other Domestic Consumers having load above 4 KW	Rs. 80/Connection	
	2.	Single Point Bulk Supply above 50 kW	Rs. 30/ kW	Rs 2.80/KWH
	3.1	Un-metered in Rural (Hilly) Areas (See Note 1(ii) below)	Rs 130/Connection	Nil
	3.2	Un-metered in Rural (Other) Areas	Rs 285/Connection	Nil
RTS-1A: Snowbound	1. Domestic		Rs. 6/Connection	Rs 1.50/KWH
	2. Non-Domestic upto 1 kW		Rs. 6/Connection	Rs 1.50/KWH
	3. Non-Domestic above 1 kW & upto 4 kW		Rs. 6/Connection	Rs 2.05/KWH
	4. Non-Domestic above 4 kW		Rs. 12/Connection	Rs 3.10/KWH
RTS-2: Non-Domestic	1.	(i) Government / Municipal Hospitals (ii) Government / Government aided Educational Institutions (iii) Charitable Institutions registered under the Income Tax Act, 1961 and whose income is exempted from tax under this Act.		
	1.1	Upto 25 KW	Rs 30/KW	Rs 3.70/KWH
	1.2	Above 25 KW	Rs 30/KW	Rs 3.30/KVAH
	2.	Other Non-Domestic / Commercial Users		
	2.1	Upto 25 kW	Rs 30/KW	Rs 4.40/KWH
	2.2	Above 25 kW	Rs 30/KW	Rs 4.40/KVAH
	3.	Single point bulk supply above 50 KW for shopping complexes / multiplex / malls	Rs 30/KW	Rs 4.30/KVAH
RTS-3: Public Lamps	1.	Metered	Rs 25/KW	Rs 3.95/KWH
	2.	Un-metered (Rural)	-Rs. 155 Per 100 W Lamp or part thereof -For every 50 W or part thereof increase over and above 100 W Lamps additional Rs. 60	-
	3.	Maintenance Charge	For 1 and 2 above Rs. 10/Light point	-
RTS-4: Private Tube-wells / Pumping sets	1.	Metered	Nil	Rs 1.00/KWH
	2.	Un-metered	Rs.165/BHP (Plus Rs. 20 for light load not more than 2 lamps)	Nil